# Redox regulation and reversible methionine oxidation in the mitochondria

By

Stefan Geldon, BSc (Hons)

Submitted in fulfilment of the requirements for the degree of

**MSc (Research) Biochemistry and Biotechnology**

Institute of Molecular Cell and Systems Biology

College of Medical Veterinary and Life Sciences

University of Glasgow

October 2021

# Abstract

Mitochondria are double membrane bound organelles required for cellular respiration via the oxidative phosphorylation system (OXPHOS) that results in the generation of ATP. The OXPHOS system involves the use of an electron transport chain (ETC) comprised of several mitochondrial inner membrane embedded enzyme complexes (termed complexes I-V in mammals). The mitochondria contains its own genome, the mitochondrial DNA (mtDNA) that encodes the essential subunits of these complexes while the accompanying structural and assembly factors are cytosolically translated and imported into the mitochondria.

Reactive oxygen species (ROS) are generated inside the mitochondria at the ETC due to electron leakage at the complexes which results in the partial reduction of oxygen. An accumulation of ROS results in oxidative stress (OS) which can result in damage to nucleic acids, lipids, and proteins. Methionine residues in proteins are particularly susceptible to ROS modifications leading to the generation of methionine sulfoxidated groups which are harmful to proteins causing them to unfold and rendering them dysfunctional. Therefore, the reduction of these adducts by enzymes termed methionine sulfoxide reductases (Mxr) is essential to maintaining proteins in their native functional conformation.

In this thesis the mitochondrial targeted yeast methionine sulfoxide reductase enzyme (Mxr2) was studied. We discovered using radiolabelled protein import experiments that Mxr2 is targeted to the mitochondria and becomes dually localised to both the intermembrane space (IMS) and matrix compartments. In addition, we found that the presence of the Tom20 import receptor and the major IMS oxidative folding protein, Mia40, were required for efficient import. Studies involving knockout Mxr2 yeast cells revealed that the absence of Mxr2 resulted in a growth defect when cells were oxidatively stressed alongside alterations in respiratory capacity and metabolic substrate utilisation. Lastly the import and complex assembly of the small Tim chaperone Tim10 was demonstrated to be altered in the absence of Mxr2 using BN PAGE analysis as was the formation of respiratory supercomplexes.

The second part of the thesis focused on the complex IV assembly factor 8 (COA8). Mutations in this protein have been implicated with complex IV deficiencies and mitochondrial encephalopathy phenotypes. Here we investigated how COA8 can be oxidatively regulated at several conserved cysteines residues to alter the import capacity of this matrix targeted protein.

# Table of Contents

# List of Figures

# List of Tables

# Acknowledgements

First, I would like to thank my supervisor Professor Kostas Tokatlidis for giving me the opportunity to work and study in his lab and for all his expertise, advice, and support both inside and outside the lab.

Next, I would like to thank all members of the Tokatlidis lab group for all their advice and for creating a friendly and welcoming atmosphere inside the lab. I would like to thank Dr Ross Eaglesfield, for investing lots of his time to train me and answering all my many questions in the initial months, Dr Erika Fernandez-Vizarra for introducing me to the COA8 project and collaborating with me on a review paper and Dr Ruairidh Edwards for his unwavering support, enthusiastic outlook, and depth of knowledge.

Lastly, I would like to thank both Eleanor-Dickson Murray and Roza Dimogkioka for their constant support, buffer calculation help, music playlists and friendship. Without you (and the many ice cream trips) the year would never have been the same.

# Authors Declaration

I declare that except where explicit reference is made to the contribution of others, that this thesis is the result of my own work and has not been submitted for any other degree at the University of Glasgow or any other institution.

# List of Abbreviations

**·OH** Hydroxyl Radical

**Δψ** Inner Mitochondrial Membrane Potential

**AAC** ADP/ATP Carrier

**Ab** Antibody

**ADP** Adenosine Diphosphate

**AMS 4**-acetamido-4'-malemidylstilbene-2-,2' disulfonic acid

**Ape1** Apurinic/ apyrimindic endonuclease 1

**ATP** Adenosine Triphosphate

**BER** Base Excision Repair

**BN** Blue Native

**BSA** Bovine Serum Albumin

**CCCP** Carbonyl cyanide m-chlorophenyl hydrazine

**CE** Carbonate Extraction

**CHCH** Coiled-Helix-Coiled-Helix

**COA8** Cytochrome C Oxidase Assembly Factor 8

**CoQ** Coenzyme Q

**COX** Cytochrome C Oxidase

**Cys** Cysteine

**Cyt C** Cytochrome C

**DHFR** Dihydrofolate reductase

**DTT** Dithiothreitol

**ETC** Electron Transport Chain

**GPDH** Glycerol-3-Phosphate Dehydrogenase

**$H_2O_2$** Hydrogen Peroxide

**$H_2S$** Hydrogen Sulfide

**HEK** Human Embryonic Kidney

**HEPES** 4-(2-hydroxyethyl)piperazine-1-ethanesulfonic acid

**Hsp** Heat Shock Protein

**IgG** Immunoglobulin G

**IM** Inner Membrane

**IMP1** IMS Localised Protease 1

**IMS** Intermembrane Space

**ITS** Internal Targeting Signal

**LB** Luria-Bertani

**MC** tetrazolium redox dye

**Met** Methionine

**Met-O** Methionine Oxidation

**Met-R-O** Methionine-R-Sulfoxide

**Met-S-O** Methionine-S-Sulfoxide

**MG** Malate Glutamate

**MIA** Mitochondrial Import and Assembly

**MICOS** Mitochondrial Contact Site and Cristae Organisation System

**MIM** Mitochondrial Import Machinery

**MP** Mitoplasts

**MPP** Mitochondrial Processing Peptidase

**MRI** Magnetic Resonance Imaging

**Msr/ Mxr** Methionine Sulfoxide Reductase

**MW** Molecular Weight

**NADH** Nicotinamide Adenine Dinucleotide

**NO** Nitric Oxide

**$O_2^{\cdot-}$** Superoxide

**OCR** Oxygen Consumption Rate

**OD** Optical Density

**OM** Outer Membrane

**OXA** Oxidase Assembly Insertase Complex

**OXPHOS** Oxidative Phosphorylation

**PAGE** Polyacrylamide gel electrophoresis

**PBS** Phosphate Saline Buffer

**PCR** Polymerase Chain Reaction

**Pel** Pellet

**PI3K** Phosphoinositide 3-Kinase Pathway

**PK** Proteinase K

**PMF** Proton Motive Force

**PMSF** Phenylmethylsulphonyl Fluoride

**Prx1** Peroxiredoxin 1

**RNS** Reactive Nitrogen Species

**ROS** Reactive Oxygen Species

**SAM** Sorting and Assembly Complex

**SBTI** Soybean Trypsin Inhibitor

**SDS** Sodium Dodecyl Sulphate

**Sup** Supernatant

**TCA** Trichloroacetic acid

**TIM** Translocase of the Inner Membrane

**TMD** Transmembrane Domain

**TNT** Coupled Transcription and Translation System

**TOM** Translocase of the Outer Membrane

**Trx** Thioredoxin

**Try** Trypsin

**Tx** Triton-X100

**UPS** Unfolded Protein Response

**WT** Wild Type

**YPD** Yeast Extract, Peptone, Dextrose

**YPLac** Yeast extract, Peptone, Lactic Acid

# Chapter 1: Introduction

Aspects of this introduction form part of a recently accepted review paper submitted to Frontiers in Cell and Developmental Biology that was written as part of the MScR degree (Geldon, Fernández-Vizarra and Tokatlidis, 2021).

## 1.1 Introduction

Mitochondrial biogenesis is essential for cell fitness and viability. Mitochondria are double membrane bound organelles composed of an outer membrane (OM), intermembrane space (IMS), inner membrane (IM) and matrix that harbours its own mitochondrial genome, the mtDNA. This genome encodes only 13 polypeptides in humans or 8 polypeptides in yeast cells that are subsequently translated into many key components of the respiratory chain complexes found embedded in the IM. Assembly of the respiratory chain complexes relies on the import of nuclear encoded proteins into the mitochondria through several well-defined mitochondrial import pathways.

A large proportion of proteins imported into the intermembrane space (IMS) are rich in conserved cysteine residues and are imported via the mitochondrial import and assembly pathway (MIA). Import via this pathway involves the oxidation of cysteine residues and subsequent folding of the protein into its native conformation thereby trapping it in this compartment. Many substrates for this pathway are involved in the biogenesis and maturation of the respiratory chain complexes, functioning as key assembly factors. The presence of these cysteines results in these proteins becoming redox regulated in the IMS which can alter the import capacity and function of these assembly factors to regulate biogenesis of the respiratory chain complexes.

The presence of these complexes in mitochondria allows energy production in this organelle through the oxidative phosphorylation (OXPHOS) systems. Production of reactive oxygen species (ROS) as a by-product of electron transport through the respiratory complexes can oxidatively challenge cells resulting in modifications to lipids, nucleic acids, and proteins. Proteins can become modified through oxidation of methionine residues which causes them

to misfold and renders them dysfunctional. Reduction of these adducts occurs through the action of methionine sulfoxide reductase (Mxr) enzymes and is essential to maintain proteins in their native conformation.

This thesis will investigate how oxidative stress can regulate the import of proteins involved in the assembly of the respiratory chain complexes and aim to characterise the action of Mxr enzymes inside the mitochondria to reduce methionine sulfoxidated proteins as a consequence of ROS production inside this organelle.

## 1.2 Overview of Mitochondrial Protein Import Pathways

The mitochondrial proteome consists of 1,000-1,500 proteins (Sickmann *et al.*, 2003; Reinders *et al.*, 2006; Pagliarini *et al.*, 2008; Rath *et al.*, 2021) but only eight in the yeast *S. cerevisiae* and thirteen in humans, and other mammalian species, are encoded in the mitochondrial genome and translated inside the organelle. This implies that the remaining 99% of all mitochondrial proteins (1163 polypeptides in human mitochondria according to the last collection of MitoCarta 3.0 (Rath *et al.*, 2021) are nuclear encoded, translated on cytosolic ribosomes and guided to the mitochondria by a variety of cytosolic chaperones. From here they can be sorted within the organelle through numerous import pathways that direct the protein to the correct sub compartment **(Fig 1.1)**.

### 1.2.1 Protein Entry into the Mitochondria

The translocase of the outer membrane (TOM) complex forms the entry gate for >90% of mitochondrial proteins into the mitochondria. It is composed of seven different functional and receptor subunits. Outside the mitochondria, precursor proteins possessing a cleavable N-terminal presequence are recognised by the Tom20 receptor while the Tom70 receptor is involved in recognition of precursor proteins that lack this presequence but instead contain an internal targeting signal (ITS)
(Brix, Dietmeier and Pfanner, 1997; Backes *et al.*, 2018; Yamamoto *et al.*, 2009). Tom22 is the central receptor of the complex that helps recruit both Tom20 and Tom70 to the TOM core

complex and is involved in the transfer of preproteins from the aforementioned receptor subunits to the main Tom40 translocation pore (Van Wilpe *et al.*, 1999; Yamano *et al.*, 2008).

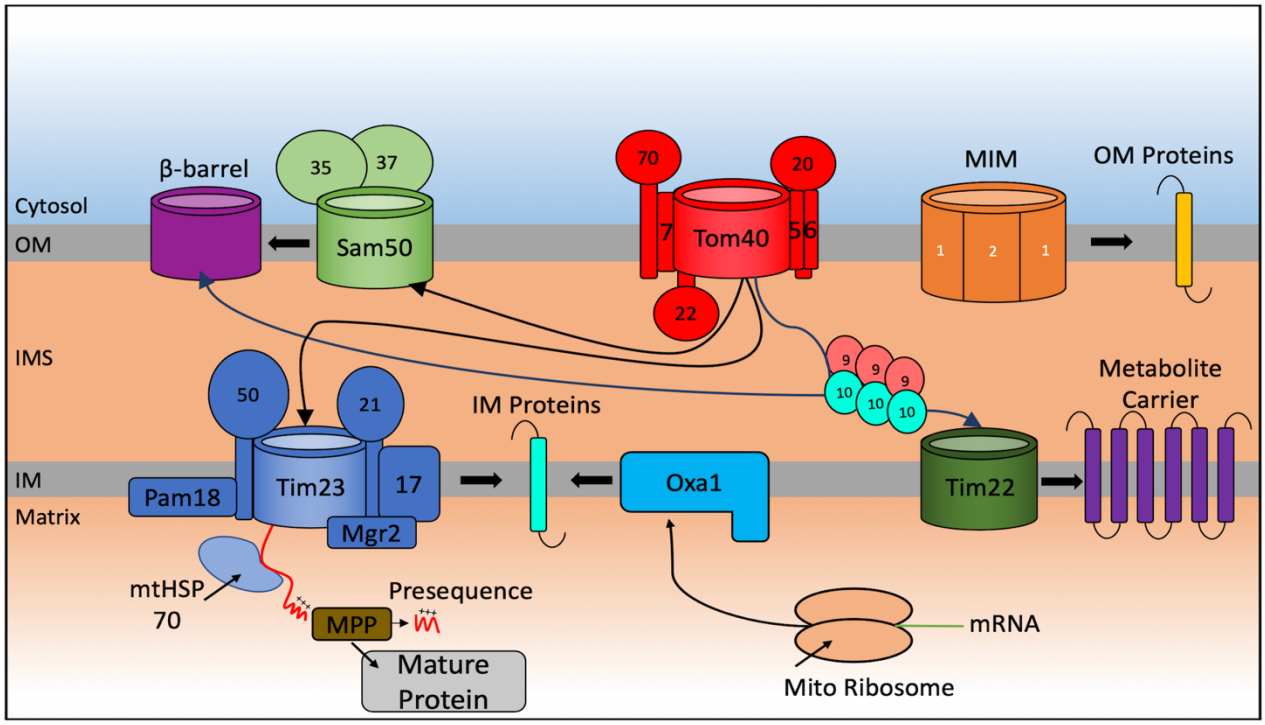


**Figure 1.1 General Import Pathways for Proteins into the Mitochondria**. Nuclear encoded proteins destined for the mitochondria are translated in the cytosol. The translocase of the outer membrane (TOM) complex represents the major import pore for protein entry into the mitochondrial intermembrane space (IMS). The sorting and assembly (SAM) complex integrates β-barrel proteins into outer membrane (OM) lipid bilayer, while the mitochondrial import machinery (MIM) complex integrates α-helical containing proteins. The small Tim9-Tim10 chaperone complex escorts proteins to the translocase of the inner membrane (TIM22) complex for insertion into the inner membrane (IM) or aids insertion of β-barrel proteins. Preproteins imported into the IMS can be translocated into the matrix through the TIM23 translocase with the aid of mitochondrial Hsp70 (mtHSP70). Once in the matrix the presequence is cleaved by the matrix processing peptidase (MPP) enzyme. Proteins passing through the TIM23 complex can also be integrated into the lipid bilayer of the IM. Mitochondrial encoded proteins are translated on mitochondrial ribosomes in the matrix and integrated into the IM by the oxidase assembly (OXA) complex.

The structure of the *S. cerevisiae* TOM complex was recently solved using cryo-electron microscopy to a 3.8Å resolution (Araiso *et al.*, 2019). This highly detailed structure revealed that the translocation pore is formed from two main β-barrels that are contributed by two Tom40 subunits (Yamano, Tanaka-Yamano and Endo, 2010). These are anchored to the outer membrane by six α-helical integrated transmembrane regions that are supplied by accompanying subunits (Ahting *et al.*, 2001; Esaki *et al.*, 2003; Becker *et al.*, 2005). These subunits include the N-terminal transmembrane domains (TMDs) of Tom20 and Tom70

alongside the C-terminal TMDs of Tom5, Tom6, Tom7 and Tom22 (Makki *et al.*, 2019). A three-channel trimeric conformation of the yeast TOM complex has also been observed, this time formed from three Tom40 pores (Shiota *et al.*, 2015). The transmembrane domains of Tom22 play a role in linking the Tom40 pores together thus stabilizing either the dimeric or the trimeric pore complex (Bausewein *et al.*, 2017).

The small TOM proteins such as Tom5, Tom6 and Tom7 are involved in the maturation of the TOM complex. Tom5 first associates with the Tom40 precursor protein aiding the formation of the mature β-barrel complex (Becker *et al.*, 2010; Qiu *et al.*, 2013). Tom5 also functions to aid the assembly of Tom6 with Tom40, with Tom7 regulating the assembly of Mdm10-mediated assembly of Tom40 (Dembowski *et al.*, 2001). Following passage of preproteins through the translocation pore they are then sorted into the different mitochondrial sub compartments through specific domains of the Tom22, Tom7 and Tom40 proteins (Court *et al.*, 1996; Gabriel, Egan and Lithgow, 2003; Esaki *et al.*, 2004).

### 1.2.2 Protein Sorting in the Inner Mitochondrial Compartments

Once preproteins are translocated through the TOM complex in the OM, they are subsequently sorted through a number of different import pathways depending on their final localisation into either the matrix, the IM and the IMS (Jensen and Johnson, 2001; Grevel, Pfanner and Becker, 2019; Hansen and Herrmann, 2019). Most precursor proteins that are targeted to the matrix are synthesised with an N-terminal positively charged cleavable presequence (Vögtle *et al.*, 2009) and follow the matrix targeting pathway, which accounts for nearly two thirds of all mitochondrial proteins. The presequence translocase of the inner membrane (TIM23 complex) is the key translocon that allows passage of these matrix-targeted precursor proteins through the inner membrane. The positively charged region of the presequence is recognised by the Tom20 and Tom22 receptors as part of the TOM complex and facilitates the translocation across the OM. The Tim50 subunit of TIM23 feeds the positively charged region into the Tim23 channel (Dayan *et al.*, 2019). The translocation of these precursors through the central pore of the TIM23 complex is dependent on the membrane potential ($\Delta\psi$) across the IM generated from the activity of the respiratory chain complexes.

Additionally, the TIM23 complex is also involved in releasing proteins that possess a strong hydrophobic transmembrane segment adjacent to the matrix-targeting presequence, laterally into the inner membrane. These proteins begin to engage with the Tim23 channel guided by the presequence but become stalled because of their strong hydrophobic 'stop-transfer' signal inside the translocation pore of the Tim23 channel. This prevents their complete import into the matrix until a specific cleavage of the 'stop-transfer' signal by the IMS localised protease 1 (IMP1) releases the mature protein into the IMS. The translocation-arrest mechanism of these bipartite presequence containing preproteins requires a specific conformation of the TIM23 complex that contains Tim17, Tim21 and Tim23, termed the $TIM23^{SORT}$ translocase (Chacinska *et al.*, 2010). The TIM23 complex can also associate with the Pam18 subunit which blocks the lateral release of TM segments into the lipid bilayer and instead promotes their translocation into the matrix. The Pam18 containing form of this complex is referred to as the $TIM23^{PAM}$ translocase (Schendzielorz *et al.*, 2018).

The ATP-dependent activity of the mitochondrial heat shock protein 70 (mtHsp70) is also required for protein transport into the matrix, alongside the energy provided by the electrochemical potential of the IM (Pais, Schilke and Craig, 2011). Mgr2 is the newest identified component of the TIM23 complex. It fulfils a quality control function by delaying the lateral release of preproteins into the inner membrane (Lee *et al.*, 2020; Matta, Kumar and D'Silva, 2020). Once the protein reaches the matrix, the presequence region is cleaved by the activity of the mitochondrial processing peptidase (MPP), which gives rise to the mature mitochondrial protein.

The mitochondrial metabolite inner membrane carrier proteins (at least 35 proteins in *S. cerevisiae* and more than 50 in mammalian cells) are critical for the trafficking of small metabolites across the IM. These IM localised carrier proteins are synthesised without a cleavable presequence and interact with the Tom70 receptor, engage with the TOM channel, and are guided to the inner membrane TIM22 complex. The small TIM chaperones localised in the IMS escort the carrier proteins in this aqueous environment preventing their aggregation during import. This import and insertion process constitutes the carrier pathway, and while membrane potential-dependent occurs independent of adenosine triphosphate (ATP) hydrolysis in the matrix (Sirrenberg *et al.*, 1996). Recent data has revealed that the

human TIM22 complex associates with the mitochondrial contact site and cristae organisation system (MICOS) complex, which is required for the efficient import of carrier proteins into the IM. However, this association is not conserved in yeast mitochondria and is specific to higher eukaryotes (Callegari *et al.*, 2019).

Proteins that are encoded by the mtDNA in the mitochondrial matrix, are all IM proteins. These are synthesised on mitochondrial ribosomes in the matrix and are inserted co-translationally by the oxidase assembly (OXA) insertase assembly complex ((Hell, Neupert and Stuart, 2001).

### 1.2.3 Protein Insertion into the Mitochondrial Outer Membrane

The mitochondrial outer membrane contains either β-barrel membrane proteins (which are absent from the inner membrane) or α-helical transmembrane proteins. Precursors of the β-barrel proteins are first recognised by the TOM complex, which allows transport across the OM, and are then transferred to the sorting and assembly (SAM) complex from the IMS side of the OM. A recent cryo-electron microscopy structure of the SAM complex revealed that it is composed of two copies of the central subunit Sam50, that forms a β-barrel channel (Takeda *et al.*, 2021) to allows the lateral release of the precursor proteins into the outer membrane (Paschen *et al.*, 2003; Klein *et al.*, 2012). The SAM complex also contains the Sam35 and Sam37 subunit proteins found on the cytosolic side of the outer membrane. Sam35 is thought to stabilise the precursor-Sam50 interaction, while Sam37 is involved in the release of substrate proteins from the SAM complex (Chan and Lithgow, 2008; Kutik *et al.*, 2008). It is thought that the TOM and SAM complexes form super complexes to ensure the efficiency of protein insertion into the OM. The small Tim chaperones complexes also play a critical role in this process as they transiently bind to precursors in transit through the IMS and before final insertion into the IMS. Presumably binding to exposed hydrophobic regions preventing their aggregation (Wenz *et al.*, 2015; Weinhäupl *et al.*, 2018).

Proteins destined for the OM that contain a single or multiple TM α-helical regions are first recognised by the Tom70 receptor but do not pass through the TOM complex translocation pore (Otera *et al.*, 2007; Mårtensson *et al.*, 2019). Instead the mitochondrial import machinery (MIM) complex inserts these precursors into the OM (Becker *et al.*, 2011; Dimmer

*et al.*, 2012). The MIM complex is composed of multiple copies of the Mim1 subunit which can spontaneously form a channel when reconstituted into a lipid bilayer alongside one or two copies of the Mim2 subunit (Dimmer *et al.*, 2012). The formation of this channel is thought to be involved in the integration of these precursor proteins into the OM (Krüger *et al.*, 2017). Recently the single-helix spanning proteins Atg32 and Msp1 were identified as new substrates of the MIM complex, demonstrating that this complex is not limited to integrating multi-spanning transmembrane proteins as previously though (Vitali *et al.*, 2020).

### 1.2.4 Protein Import into the Intermembrane Space

A detailed proteomic analysis of the mitochondrial IMS for the yeast *S. cerevisiae* revealed that approximately 50 proteins were localised to this sub-compartment (Vögtle *et al.*, 2012). In humans, the IMS proteome accounts for about 5% of the total mitochondrial proteome (53 proteins) (Rath *et al.*, 2021). Most of these IMS-located proteins lack a typical mitochondrial targeting sequence and are instead characterised by conserved cysteine residues that are organised into twin $CX_nC$ (typically either $CX_3C$ or $CX_9C$) motifs that are necessary for the import, correct folding, and maturation of these proteins into the mitochondria. The oxidative folding or mitochondrial protein import and assembly (MIA) pathway relies on the function of Mia40, in yeast, and CHCHD4 (also known as MIA40), in humans, as the key protein that facilitates the introduction disulfide bonds in these proteins thereby trapping them in the IMS (Mesecke *et al.*, 2005) **(Fig 1.2)**.

Many of the classical MIA substrates are vital for the biogenesis and function of mitochondria. Examples include the members of the small Tim protein family, including Tim 8, Tim 9, Tim 10, and Tim13 (Sideris and Tokatlidis, 2007). These proteins form the Tim9-Tim10 and Tim8-Tim13 chaperone complexes that are essential to deliver hydrophobic proteins to the TIM22 complex for insertion into the IM. Other examples of MIA substrates are proteins necessary for the biogenesis of the electron transport chain ETC complexes detailed in subsequent section and include proteins with a dual $CX_9C$ motif that are involved mostly in the assembly and maintenance of cytochrome *c* oxidase (COX), also known as complex IV (CIV) (Gabriel *et al.*, 2007; Koch and Schmid, 2014a; Habich *et al.*, 2019; Gladyck *et al.*, 2021). Recent studies in the literature demonstrate that MIA can recognise proteins with non-classical $CX_nC$ motifs,

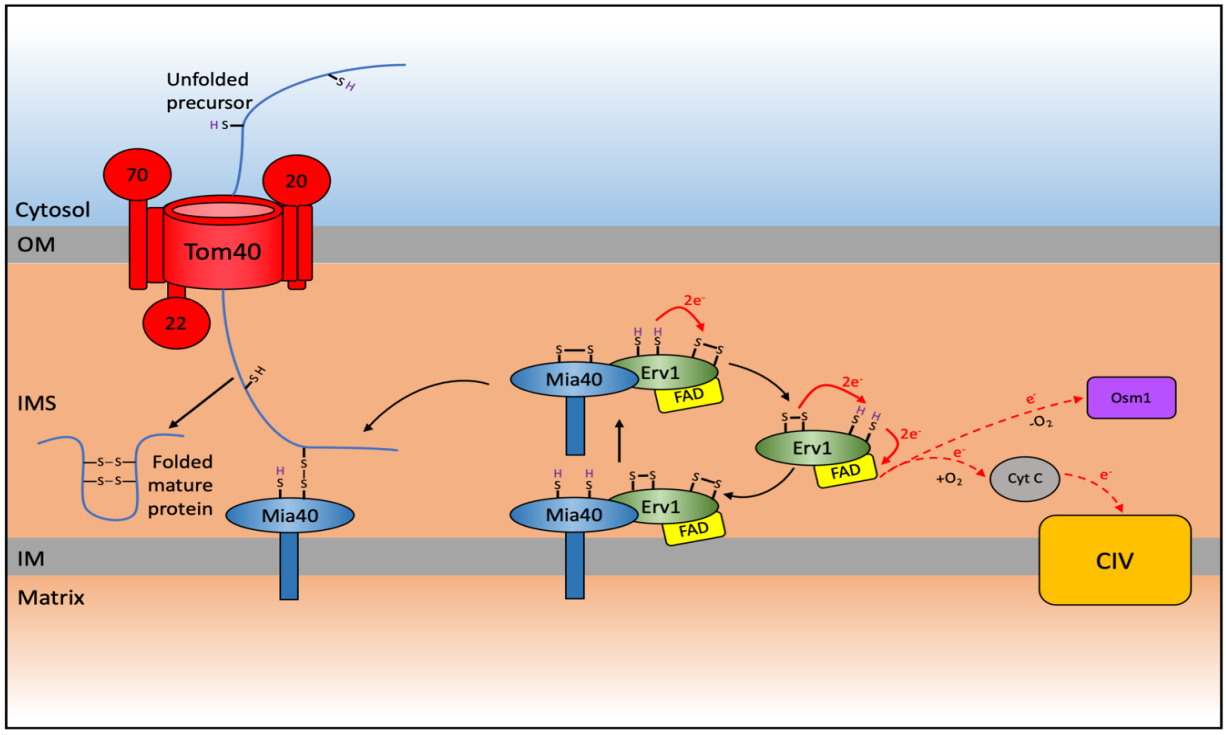


**Figure 1.2 The components and electron flow of the mitochondrial import and assembly (MIA) pathway (yeast).** A subset of nuclear-encoded proteins destined for the intermembrane space (IMS) are imported via the MIA pathway to oxidatively fold the substrates and trap them in this compartment. These proteins are encoded with a $CX_nC$ motif and are first translocated through the translocase of the outer membrane (TOM) complex. Substrates of this pathway possess an IMS-targeting signal (ITS) that facilitates interaction with Mia40. This interaction leads to oxidation of the substrate, resulting in its folding and trapping it in the IMS. Mia40 is left in a reduced state that must be reoxidised to allow oxidation of newly imported substrates. This reoxidation is facilitated by the interaction with Erv1. Electrons are subsequently transported to cytochrome C (Cyt C) and complex IV (CIV) under aerobic conditions or via Osm1 in anaerobic conditions.

like the yeast Erv1 protein (with a $CX_{15}C$ motif) (Terziyska *et al.*, 2007; Kallergi *et al.*, 2012), yeast Atp23 (10 cysteine residues not organised in any specific cysteine motif, (Weckbecker *et al.*, 2012)), yeast Mix23 (with an unusual twin cysteine $CX_{13}C/CX_{14}C$ motif, (Vögtle *et al.*, 2012; Zöller *et al.*, 2020)) or human COA7 that contains thirteen Cys residues (Mohanraj *et al.*, 2019). Other proteins without classical $CX_nC$ motifs that have been described as substrates of CHCHD4/MIA40 also include p53, AK2 and MICU1 (Zhuang *et al.*, 2013; Petrungaro *et al.*, 2015). It is also of note that Ccs1, the copper chaperone for Cu, Zn superoxide dismutase (Sod1), is a Mia40 substrate in yeast but the import of the human ortholog (CCS1) into the IMS occurs independent of CHCHD4/MIA40 (Groß *et al.*, 2011; Suzuki *et al.*, 2013).

The other main component of the yeast MIA pathway is the FAD-dependant sulfhydryl oxidase Erv1 (Chacinska *et al.*, 2004; Mesecke *et al.*, 2005). known as ERV1, ALR or GFER in humans ((Lange *et al.*, 2001; Di Fonzo *et al.*, 2009) **(Fig 1.3)**. Mia40 and Erv1 function in a disulfide relay system to catalyse the protein import into the IMS through an oxidative folding process. This ultimately results in the introduction of disulfide bonds into the imported proteins. This in turn promotes their folding into their native conformation thereby trapping them in the IMS. Substrates of the MIA pathway are translated cytosolically and pass through the TOM complex in a reduced and unfolded state (Lu *et al.*, 2004; Sideris and Tokatlidis, 2007). During translocation these substrates can interact with Mia40, which acts as a trans site receptor to drive protein import into the IMS (Milenkovic *et al.*, 2007; Sideris and Tokatlidis, 2007; Peleh, Cordat and Herrmann, 2016).

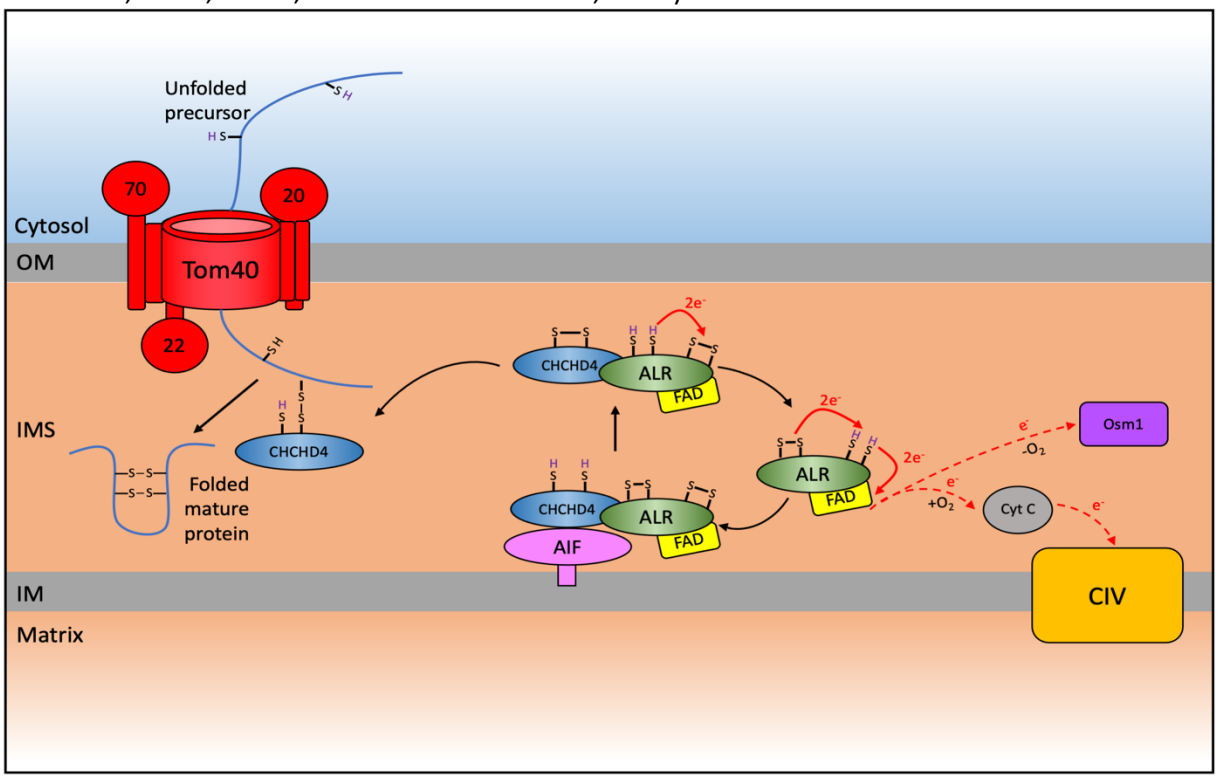


**Figure 1.3 The components and electron flow of the mitochondrial import and assembly (MIA) pathway in mammals.** A subset of nuclear encoded proteins destined for the intermembrane space (IMS) are imported via the MIA pathway to oxidatively fold the substrates and trap them in this compartment. These proteins are encoded with a $CX_nC$ motif and are first translocated through the translocase of the outer membrane (TOM) complex. Substrates possess an IMS-targeting signal (ITS) that facilitates interaction with CHCHD4 to result in oxidation of the substrate, resulting in its folding and trapping it in the IMS. CHCHD4 is a soluble IMS protein in mammals and interacts with the inner membrane (IM) embedded apoptosis-inducing factor (AIF). This oxidation reaction leaves CHCHD4 in a reduced state that must be reoxidised to allow oxidation of newly imported substrates. This reoxidation is facilitated by the interaction with ALR. Electrons are subsequently transported to cytochrome C (Cyt C) and complex IV (CIV) under aerobic conditions or via Osm1 in anaerobic conditions.

This N-terminal domain and instead is found as a soluble protein of around 15 kDa in the mitochondrial IMS (Hofmann *et al.*, 2005) **(Fig 1.3)** where it interacts with AIFM1 that is found anchored in the IM. This interaction facilitates the import of MIA40 into the IMS (Hangen *et al.*, 2015). The C-terminal region was recently established to be important in maintaining the stability of the protein in the cytosol. MIA40 can often reside for extended periods cytosolically as a consequence of slow import kinetics during AIFM1-mediated import (Murschall *et al.*, 2020).

However, all Mia40 homologs contain a highly conserved core domain of around 8 kDa that harbours six conserved cysteine residues that are folded into a coiled-helix-coiled-helix (CHCH) domain (Banci *et al.*, 2009). NMR and X-ray crystallography were used to solve the human and the yeast structures respectively (Banci *et al.*, 2009; Kawano *et al.*, 2009). Invariant cysteine residues in this domain form a redox-active CPC motif that readily switches between an oxidised and reduced state, followed by a twin $CX_9C$ motif that can form two structural disulfide bonds. The CHCH domain itself folds to form a characteristic hydrophobic cleft allowing substrates to bind and interact with Mia40 (Banci *et al.*, 2009; Sideris *et al.*, 2009).

Most Mia40 substrates therefore contain a hydrophobic sequence, also known as an IMS-targeting signal (ITS, ((Sideris *et al.*, 2009) or alternatively termed the mitochondrial IMS-sorting signal (MISS, (Milenkovic *et al.*, 2009)) to bind within this hydrophobic cleft. The signal is a 9 amino acid internal peptide sequence that is necessary and sufficient for IMS targeting of proteins to Mia40. Deletion of the ITS results in a complete loss of import (Sideris *et al.*, 2009). This sequence aids the first interaction with Mia40 via hydrophobic stacking (Milenkovic *et al.*, 2009; Sideris *et al.*, 2009) by orientating the substrate towards Mia40 to allow the formation of a transient intermolecular disulfide bond between the second cysteine of the redox active CPC motif of Mia40 and the docking cysteine of the ITS in the imported substrate (Banci *et al.*, 2009; Koch and Schmid, 2014b). This transient disulfide bond is subject to a nucleophilic attack by another cysteine in the substrate resulting in the formation of an intramolecular disulfide bond. This in turn promotes the release of Mia40 and the correct folding of the protein, thereby trapping it in the IMS and completing its import process.

The introduction of a disulfide into a substrate by Mia40 leaves it in a reduced state and unable to oxidise any further imported proteins. Thus, to maintain a functional MIA pathway, Mia40 needs to continually be re-oxidised through interaction with the other main component of the MIA pathway, Erv1, which contains three pairs of highly conserved cysteine residues (Mesecke *et al.*, 2005). The FAD-binding catalytic core domain has a CXXC redox-active disulfide (Cys130 – Cys133) and a C-terminal $CX_{16}C$ structural disulfide (Cys156 and 179). A third disulfide bond (Cys30 – Cys33) is present within the flexible N-terminal of the protein, which is natively disordered and is the disulphide that is involved in the interaction with reduced Mia40 and the transfer of electrons towards the redox active-site disulfide (Lionaki *et al.*, 2010; Banci *et al.*, 2011, 2013). From here electrons are transferred to a final electron acceptor via the FAD cofactor (Banci *et al.*, 2012). Under aerobic conditions Erv1 can either transfer electrons directly onto molecular oxygen ($O_2$) which results in the production of hydrogen peroxide ($H_2O_2$) within the IMS, or onto cytochrome *c* (Cyt C) *,* the mobile electron transfer protein that donates electrons to CIV (Allen *et al.*, 2005; Dabir *et al.*, 2007; Daithankar, Farrell and Thorpe, 2009; Banci *et al.*, 2012; Peker *et al.*, 2021). Alternatively, under anaerobic conditions the Osm1, a fumarate reductase can be used as an electron acceptor (Neal *et al.*, 2017).

Interestingly, Mia40 is in itself a substrate of the MIA pathway and requires interaction with endogenous Mia40 to facilitate its own import, which follows three steps. First, Mia40 is inserted through the Tim23 translocon in the inner mitochondrial membrane. Next, the core domain of the protein is folded through interactions with endogenous Mia40. Lastly, Mia40 interacts with Erv1 to oxidise the CPC motif to produce functional Mia40 that can oxidise incoming substrates of the MIA pathway (Chatzi *et al.*, 2013). Yeast Mia40 has an N-terminal insertion domain which is dependent on Tim23 for insertion. Therefore, it is likely that the first molecules of Mia40 are probably inserted via the TIM23 complex and then start to catalyse their own folding via the core domain of Mia40 (containing the CX9C motif). It is hypothesised that insertion of Mia40 in the IM is not lost as presumably the whole molecule is anchored in the membrane to maintain stability. Contrastingly human Mia40 which does not have an N-terminal anchored domain is probably maintained in the membrane via interactions with other human proteins such as AIF which are themselves anchored in the IM.

### 1.2.5 The Small Tim Chaperones as Substrates of the MIA Pathway

The essential small Tim proteins that function as chaperones in the IMS were the first discovered substrates of the MIA pathway, that interact with Mia40 to control their redox-regulated import (Chacinska *et al.*, 2004). These small Tims possess non-cleavable internal targeting signals (ITS) that harbour conserved cysteine motifs involved in targeting them to the mitochondria (Milenkovic *et al.*, 2009; Sideris *et al.*, 2009). The cysteines are arranged in a $CX_3C$ motif, a classical substrate motif for Mia40 (Koehler, 2004). The ITS signal directs the small Tims to the IMS where they are imported by the MIA pathway through direct interaction with Mia40 (Chacinska *et al.*, 2004; Sideris *et al.*, 2009). This interaction results in the oxidation of the small Tims, leading to the formation of intramolecular disulfide bonds thereby trapping the proteins in the IMS.

The small Tims can form hexameric protein complexes consisting of either Tim9 – Tim10 or Tim8 – Tim13 with three subunits of each Tim protein. Structural analysis of the complexes revealed the subunits take on the form of an α-propellor with two helical blades that radiate from a narrow central pore (Webb *et al.*, 2006; Beverly *et al.*, 2008). The subunits are stabilised by the formation of intramolecular and structural disulfide bonds. Within the IMS these complexes act as chaperones to transport incoming hydrophobic precursors across this compartment to the TIM22 complex for their insertion into the IMM. The helper of Tims 13 (Hot13p) was also shown to be involved in maintaining the small Tims in their active conformation (Curran *et al.*, 2004).

## 1.3 Respiratory Chain Complex Assembly and Regulation in the Mitochondria

The mitochondria are the powerhouse of the cell. These organelles generate most of the chemical energy used by the cell and store it in the form of adenosine triphosphate (ATP) through the oxidative phosphorylation (OXPHOS) system. The OXPHOS system is comprised of four respiratory complexes that form the electron transport chain (ETC). Electron flow through the ETC is coupled to the generation of a proton gradient across the IM from which the energy derived is used by ATP synthase (complex V) to produce ATP. The mtDNA encodes

many of the main complexes involved in the OXPHOS system while many assembly factors involved with the biogenesis and maturation of these complexes are imported through the aforementioned mitochondrial import pathways.

### 1.3.1 Oxidative Phosphorylation in the Mitochondria

The ETC is physically located in the mitochondrial IM (therefore in contact to the IMS on the one side) and is composed of the four transmembrane protein complexes (complexes I-IV). The ETC is involved with the transfer of reducing equivalents from NADH or $FADH_2$ to oxygen, thereby reducing it to water, using the two mobile electron carriers: coenzyme Q (CoQ) and Cyt C. Electron transfer through complexes I, III and IV is coupled with proton pumping across the IM from the matrix to the IMS. This electrochemical gradient generates the proton motive force (PMF) employed by the ATP synthase (or complex V) for the synthesis of the majority of the cellular ATP in aerobic eukaryotes (Wikström *et al.*, 2015).

Complexes I, III, IV and V are large multimeric enzymes whose structures span across the IM, with subunits that protrude either into the matrix, the IMS or a combination of both (Letts and Sazanov, 2017). The processes of assembly and maturation of these complexes require the involvement of a significant number of proteins, generically termed assembly factors, that while not part of the mature respiratory complex are still necessary for ETC biogenesis. The structure and assembly of the respiratory complexes is conserved for the most part between yeast and humans, except for the absence of a multimeric and proton pumping complex I in *S. cerevisiae* (Signes and Fernandez-Vizarra, 2018). In yeast complex I is replaced by the monomeric NADH-dehydrogenases in yeast (Ndi and Nde).

There is an additional level of complexity in the organization of the ETC, which is the formation of supercomplex structures. In yeast, all of CIV is associated with the invariantly dimeric CIII ($CIII_2$) in $III_2IV_{1-2}$ stoichiometries (Hartley *et al.*, 2019; Rathore *et al.*, 2019). In mammalian mitochondria however, CI, $CIII_2$ and CIV have been shown to associate with different stoichiometries into super complexes, in which $CIII_2$ is always present, that are found alongside the individual non-associated complexes (Letts and Sazanov, 2017; Lobo-Jarne and Ugalde, 2018).

Many of the structural subunits and assembly factors directly involved in OXPHOS biogenesis are Cys-containing proteins located in the IMS and, therefore, may be subject to redox regulation within this sub-compartment (Habich, Salscheider and Riemer, 2019; Reinhardt *et al.*, 2020). Many of these are also substrates of Mia40 and are imported via the MIA pathway detailed prior. The Cys residues in these assembly factors and not just important for their biogenesis in terms of their import and stability in the IMS, but also play a functional role in some instances (Gladyck *et al.*, 2021). Most members of this group of proteins are also interesting from a medical point of view, as pathological variants in several genes encoding them have been found associated with respiratory chain deficiency and mitochondrial disease, making them attractive targets to study (Fernandez-Vizarra and Zeviani, 2021) Interestingly, the majority of IMS-located assembly factors appear to be involved in the maturation of CIV (Khalimonchuk and Winge, 2008; Longen *et al.*, 2009; Bourens *et al.*, 2013; Timón-Gómez *et al.*, 2018; Gladyck *et al.*, 2021).

### 1.3.2 Assembly and Maturation of Cytochrome C Oxidase

Complex IV, Cytochrome C Oxidase (COX) is the terminal component of the electron transport chain involved in catalysing the oxidation of cytochrome c and the reduction of $O_2$ into $H_2O$. Energy release from this redox reaction is used to pump two protons and four positive charges across the IM to maintain the electrochemical gradient that used by the ATP synthase. There are 14 structural CIV subunits. Three of these are encoded by the mtDNA termed MT-CO1, MT-CO2 and MT-CO3 and mutations in each of these subunits has been associated with COX deficiency (Rak *et al.*, 2016).

One of the most common biochemical characteristics in patients suffering from mitochondrial diseases is COX deficiency. Deficit of this complex is associated with a diverse array of clinical presentations aided by the identification of mutations within over twenty individual genes associated with COX and its accompanying assembly factors. Mutations have also been discovered in the other 11 remaining nuclear encoded subunits of COX alongside the three mt-encoded subunits. Many of these encode structural COX subunits though disease causing mutations in these genes appear to be much less common (Massa *et al.*, 2008; Baertling *et*

*al.*, 2015) and instead are found in the nuclear encoded proteins involved in COX biogenesis (Rak *et al.*, 2016; Timón-Gómez *et al.*, 2018). The absence of assembly factors results in an impaired formation of the fully assembled COX and subsequent COX deficiency. Despite this the exact molecular role of each of these assembly proteins is often unknown. Interestingly many of the proteins and assembly factors involved in biogenesis and maturation of COX are Cys-rich proteins, and substrates of the MIA pathway implying a role for redox regulation of these assembly factors in the IMS.

### 1.3.3 Cytochrome C Oxidase Assembly Factor 8 (COA8) and Mitochondrial Encephalopathies

Loss of functions in the *APOPT1* gene, which encodes the protein now referred to as Cytochrome C oxidase assembly factor 8 (COA8) have been linked to mitochondrial encephalopathies with associated COX deficiency (Rak *et al.*, 2016). This condition has been characterised by cavitating leukodystrophy with a unique magnetic resonance imaging (MRI) pattern found in seven different patients from six families (Melchionda *et al.*, 2014; Sharma *et al.*, 2018). In addition to the abnormal MRI patterns, patients were found to demonstrate neurometabolic failure and possess cystic lesions predominantly in the posterior region of the cerebrum (Hedberg-Oldfors *et al.*, 2020).

Although a genetic link has been established between pathogenic variants of *APOPT1* and COX deficiency there is no clear biochemical link demonstrated in terms of how the mutations alter assembly and maturation of COX. It is unknown if the mutations result in a failure of import of COA8 into the mitochondria or hinder the ability to associate with COX itself once inside the organelle. A range of COA8 mutations in patients have been demonstrated including but not limited to a nonsense mutation (p.Arg79*), a missense mutation (p.Phe118Ser) and a frameshift mutation (p.Glu121Valfs*4) (Melchionda *et al.*, 2014; Sharma *et al.*, 2018).

The *APOPT1* gene is only found in metazoans and encodes a 206 amino acid protein that is targeted to the mitochondria in mammalian cells (Melchionda *et al.*, 2014; Signes *et al.*, 2019). COA8 was experimentally determined to be associated with the IM, with the C-

terminal region exposed to the matrix. The protein was recently demonstrated to be oppositely regulated by the unfolded-protein response (UPS) and reactive oxygen species (ROS) (Signes *et al.*, 2019). Despite this the regulation of import of COA8 into the mitochondria and the link with CIV deficiency disorders are both still poorly understood and uncharacterised.

## 1.4 Oxidative Stress in the Mitochondria

Elevate levels of reactive oxygen species (ROS) can induce oxidative damage to cellular components such as proteins, lipids, and nucleic acids. Therefore, the levels of ROS in cells needs to be tightly balanced to prevent these detrimental modifications. Due to the presence of the electron transport chain (ETC) and the subsequent electron leakage in mitochondria this organelle is a large source of ROS production in the cell.

### 1.4.1 Generation of Reactive Oxygen Species

The production of reactive oxygen species (ROS) is ingrained to the aerobic metabolic pathways located in mitochondria (Murphy, 2009; Brand, 2016). ROS produced in this organelle mainly consists of superoxide ($O_2^{\cdot-}$), the majority of which is produced at complexes I and III (Brand, 2010, 2016), and is subsequently dismutated to hydrogen peroxide ($H_2O_2$), alongside the highly reactive and unstable hydroxyl radical (·OH), produced through the Fenton reaction (Lambert and Brand, 2009). Mitochondria also produce other redox active compounds such as reactive nitrogen species (RNS), primarily nitric oxide (NO) (Ghafourifar and Cadenas, 2005), or $H_2S$ (Kimura, Goto and Kimura, 2010; Paul, Snyder and Kashfi, 2021), which induce modifications of Cys in proteins, regulating their activities (Habich et al., 2019b). However, these are not the ROS directly produced by the ETC which are formed due to electrons slipping off from the chain and escaping from the redox active centres to partially reduce oxygen.

The consensus that ROS are mainly harmful molecules leading to detrimental effects for the cell and contributing different diseases and ageing, is readily being challenged (Scialò, Fernández-Ayala and Sanz, 2017; Ji and Yeo, 2021). Current literature presents ROS as signalling molecules mediating countless cellular responses (Holmström and Finkel, 2014;

Reczek and Chandel, 2015). Despite this cells have had to develop antioxidant defence systems to protect themselves from ROS overaccumulation and subsequent oxidative damage (Holmström and Finkel, 2014; Reczek and Chandel, 2015). As a result a correct balance between ROS production and scavenging is important to ensure the appropriate mediation of cellular responses while in turn preventing oxidative stress and associate damage (Ji and Yeo, 2021). In fact, a moderate production of ROS is the crux of the phenomenon called 'mitohormesis' leading to a stress adaptive response that results in improved mitochondrial function and life extension (Schulz *et al.*, 2007; Palmeira *et al.*, 2019).

In addition, it is becoming clear that ROS produced in the mitochondria play a key role in mediating mitochondrial biogenesis to compensate for dysfunction of the ETC(Dogan *et al.*, 2018). Superoxide radicals are produced by $CIII_2$ and glycerol-3-phosphate dehydrogenase (GPDH) and are generated in both sides of the IM, whereas all the other sites that produce ROS occur in the matrix (Brand, 2010). ALR (Erv1) has also been demonstrated to be a key contributor of $O_2^{\cdot-}$ radicals within the IMS (Daithankar *et al.*, 2012). $O_2^{\cdot-}$ produced in the matrix side is dismutated to $H_2O_2$ by the action of the mitochondrial manganese (Mn) superoxide dismutase (SOD2) which can subsequently diffuse to the cytosol (Boveris *et al.*, 2006; Murphy, 2009) or be released into the IMS and transported through voltage-dependent ion channels into the cytosol (Han *et al.*, 2003; Muller, Liu and Van Remmen, 2004). Once in there SOD1 converts it to $H_2O_2$. SOD1 is dually localized in the cytosol and the IMS in both mammals and yeast. In basal conditions the IMS pool of this enzyme seems to be inactive and is activated by modulation of its redox state (Iñarrea *et al.*, 2005, 2007). $H_2O_2$ in the cytosol is able to alter the redox state of target proteins through modification of key Cys residues. This has the effect of modulating the function regulatory kinases, phosphatases or transcription factors (Holmström and Finkel, 2014; Reczek and Chandel, 2015).

### 1.4.2 Methionine Oxidation as a Protein Modification

As discussed, the presence of ROS in cells can lead to the modification of proteins through oxidation of specific amino acid residues. While much of the literature focuses on the modification of Cys residues, methionine (Met) is one of the most oxidative prone amino acids. Methionine contains a sulphur atom in its side chain which has a prochiral centre.

Oxidation of this Sulphur atom by ROS leads to a mixture of two diastereomers termed Methionine-S-Sulfoxide (Met-S-SO) and Methionine-R-Sulfoxide (Met-R-SO) **(Fig 1.4)**. Methionione oxidation (Met-O) is a harmful protein modification that results in unfolding and subsequent dysfunction of the modified protein. As a result, reduction of these adducts is essential to maintaining the normal function and conformation of proteins in response to oxidative stress condition. Cells have evolved enzymes termed Methionine Sulfoxide Reductases (Mxr) that reduce Met-SO back into Met to maintain the stability and native function of these modified proteins (Stadtman and Levine, 2003; Weissbach, Resnick and Brot, 2005).

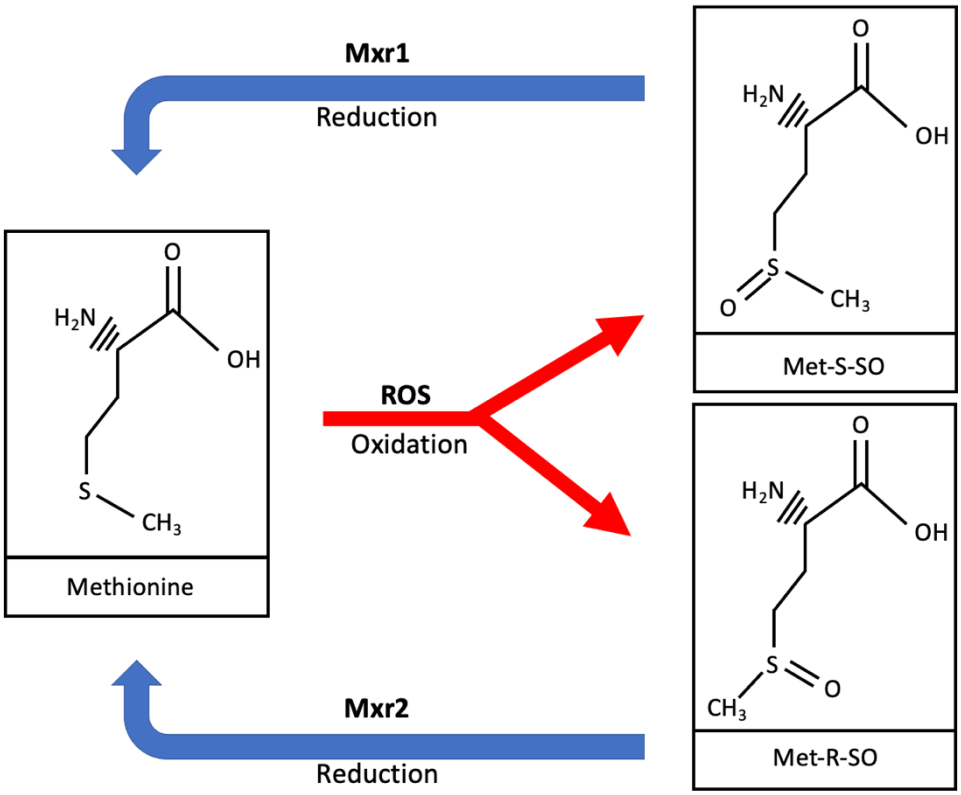


**Figure 1.4 Reversible oxidation and reduction of methionine residues.** Methionine residues have a sulphur atom in their side chain that is susceptible to oxidation in the presence of reactive oxygen species (ROS). As this sulphur is a prochiral atom oxidation gives rise to the formation of two enantiomers termed methionine-R-sulfoxide (Met-R-SO) and methionine-S-sulfoxide (Met-S-SO). These sulfoxidated residues can be reduced back into Methionine by the action of methionine sulfoxide reductase (Mxr) enzymes. In yeast the enzymes Mxr1 and Mxr2 are involved in catalysing the reduction of the Met-S-SO and Met-R-SO stereoisomers respectively.

### 1.4.3 The Role of Methionione Sulfoxide Reductase (Mxr) Enzymes

Yeast cells translate three different Mxr enzymes. As Met-O generates two stereoisomers two classes of enzymes are required to catalyse the complete reduction of this mixture. The first enzyme Mxr1 is encoded by the *MXR1* gene and is involved in reduction of Methionine-S-sulfoxide into Met. Mxr2 encoded by the *MXR2* gene is involved in reduction of the other stereoisomer Methionine-R-Sulfoxide **(Fig 1.4)**. Mxr1 and Mxr2 were demonstrated to localise to the cytoplasm and the mitochondria respectively through the use of GFP-fusion constructs (Kaya *et al.*, 2010a). The presence of only one form of these reductase enzymes in mitochondria suggest that only half of the oxidatively modified Met residues can be reduced in this organelle and there is no mechanism to reduce Met-S-SO groups here. The last enzyme, fRMxr reduces free methionine-R-sulfoxide groups (Le *et al.*, 2009). Mxr enzymes are conserved across species and humans encode several enzymes including MsrA (homolog of Mxr1) and three isoforms of the R-type reductase MsrB1, MsrB2, and MsrB3 (homologs of Mxr2) (Kim and Kim, 2008; Aachmann *et al.*, 2011). Each of these three isoforms is targeted to a different cellular compartment. Interestingly MsrB3 has recently been demonstrated to display oxidase activity towards protein substrates alongside its previously characterised reductase activity (Cao *et al.*, 2018). This novel mechanism allows the enzyme to reversibly regulate proteins through modification of methionine oxidation state. MsrB3 is also unique as it can be translated as two splice variants. While the mature protein stays the same the protein can be translated with either an ER or mitochondrial N-terminal targeting signal that targets the protein to the respective organelle (Kim and Gladyshev, 2004).

The mammalian MsrA enzyme has also been implicated in several human disorders including cancer and neurodegenerative disorders such as Alzheimer's and Parkinson's disease. In a number of breast cancer tumours MsrA has been reported to be downregulated, resulting in increased cell proliferation and degradation of the extracellular matrix, two of the key hallmarks of cancerous cells (De Luca *et al.*, 2010). The downregulation of MsrA in the tumours was found to result in upregulation of the phosphoinositide 3-kinase (PI3K) pathway and VEGF protein. In addition MsrA protein levels has also been demonstrated to be decreased in the brains of Alzheimer's patients, and the lack of MsrA has been linked to

increased stability of α-synuclein proteins implicated in the pathogenesis of Parkinson's disease (Gabbita *et al.*, 1999; Oien *et al.*, 2009; Oien, Carrasco and Moskovitz, 2011). The links to clinical disorders associated with these Mxr enzymes makes them attractive targets for study.

The mechanism of reducing oxidised methionine groups involves several conserved cysteine residues through a three-step mechanism. The first step involves the catalytic Cys residue in the Mxr enzyme nucleophilically attacking the oxidised methionine to release methionine and leading to the formation of a sulfenic acid intermediate. Next the catalytic Cys forms an intramolecular disulphide bond that gets resolved through a thiol-disulphide exchange with a third cysteine residue. This Mxr disulphide bond is subsequently reduced by thioredoxin (Trx) leading to regeneration of the reduced Mxr ($Mxr_{red}$) and oxidised Trx ($Trx_{ox}$) (Boschi-Muller *et al.*, 2005; Boschi-Muller, Gand and Branlant, 2008).

## 1.5 Aims

**Chapter 3** – *Elucidating the protein import pathway and localisation of yeast methionine sulfoxide reductase 2 (Mxr2) into the Mitochondria*

The main aim of this chapter was to determine the localisation of the yeast Mxr2 enzyme within the mitochondria and determine if the protein was solely localised to the matrix as previously determined or if it could also be found in the IMS. In addition, components of the protein import machinery essential for translocation of Mxr2 to the mitochondria were determined from sequence analysis of Mxr2 and through the use of mitochondria isolated from knockout strains.

**Chapter 4 –** *Investigating the effects of absence of Mxr2 in the mitochondria on respiratory capacity, tolerance to oxidative stress and assembly of small Tim complexes*

While the general reductase function of Mxr2 is well established little is understood of the main substrates for this enzyme or how control of methionine sulfoxidation is beneficial to mitochondrial biogenesis and fitness. Using a ΔMxr2 strain this chapter aimed to investigate how loss of this reductase enzyme influenced cell growth, tolerance to oxidative stress and respiratory capacity. Towards the end of the project research focused on how loss of Mxr2 resulted in a defect in the steady state levels of the small Tim chaperones of the mitochondria.

**Chapter 5 –** *Characterising the import pathway and redox regulation of the mitochondrial localised Cytochrome C Oxidase Assembly Factor 8 (COA8)*

In vivo studies determined that COA8 is a mitochondrial localised protein presumably destined for the matrix and demonstrated that several conserved cysteines may be oxidatively regulated to control the import of COA8. This chapter aimed to elucidate the role

of these individual cysteines in the import capacity of COA8 and how import was regulated under conditions of oxidative stress.

# Chapter 2: Materials and Methods

## 2.1 Materials

### 2.1.1 Plasmids

| Gene | Plasmid | Use | Sourced From |
|---|---|---|---|
| COA8 | pCR2.1 | Radiolabelled *in vitro* translation | Cloned in the Tokatlidis Lab during project |
| COA8 (C37A) | pCR2.1 | Radiolabelled *in vitro* translation | Cloned in the Tokatlidis Lab during project |
| COA8 (C59A) | pCR2.1 | Radiolabelled *in vitro* translation | Cloned in the Tokatlidis Lab during project |
| Mxr1 | pSP64-Mxr1 | Radiolabelled *in vitro* translation | Provided by Dr Ruairidh Edwards, Tokatlidis Lab |
| Mxr2 | pSP64-Mxr2 | Radiolabelled *in vitro* translation | Provided by Dr Ruairidh Edwards, Tokatlidis Lab |
| Su9-DHFR | pSP65-Su9DHFR | Radiolabelled *in vitro* translation | (Pfanner *et al.*, 1987) |
| Tim9 | pSP64-Tim9 | Radiolabelled *in vitro* translation | Tokatlidis Lab |
| Tim10 | pSP64-Tim10 | Radiolabelled *in vitro* translation | Tokatlidis Lab |
| AAC | pSP64-AAC | Radiolabelled *in vitro* translation | Tokatlidis Lab |

**Table 2.1** List of plasmids used in the study

### 2.1.2 Primers

All primers were obtained and purchased from Sigma-Aldrich. Primers were diluted in dd$H_2O$ at 100µM concentration and stored at -20$^oC$.

| Primer Name | Sequence 5'-3' | Use |
|---|---|---|

| | | |
|---|---|---|
| COA8-001-Pst1-Fw | CTGCAGCATGCTGCCGTGCGCCGCG | Forward primer to clone COA8 into pCR2.1-TOPO vector |
| COA8-Term-Rv | CTAGTTGCTCCTCTTCTTTTGTTTC | Reverse primer to clone COA8 into pCR2.1-TOPO vector |
| COA8-001-Pme1-Fw | GTTTAAACCATGCTGCCGTGCGCCGCG | Forward protein for cloning COA8 gene |
| COA8-HA-Rv2 | TCAAGCGTAATCTGGAACATCGTATGGGTAGTTGCTCCTCTTCTTTTGTTTC | Reverse primer to clone the COA8 HA tagged protein |
| C37A_COA8_Fw | CGCCTGCCGCGGCGCTCAACTCGCTCCG | Forward primer to introduce C37A point mutation into COA8 |
| C37A_COA8_Rev | GCTCCGGAGCGAGTTGAGCGCCGCGG | Reverse primer to introduce C37A point mutation into COA8 |
| C59A_COA8_Fw | GCGGGGTCTCAAGATTCGCCCCTCCAAGAAAGTCTT | Forward primer to introduce C59A point mutation into COA8 |
| C59A_COA8_Rev | AAGACTTTCTTGGAGGGGCGAATCTTGAGACCCCGC | Reverse primer to introduce C59A point mutation into COA8 |
| Mxr2_Fwd_pET24 | CATGCATATGAATAAGTGGAGCAGGCT | Forward primer to clone Mxr2 from pSP64 into pET34 vector for bacterial protein expression |
| Mxr2_Rev_pET24 | CATGCTCGAGATCCTTCTTGAGGTTTAAAGACGC | Forward primer to clone Mxr2 from pSP64 into pET34 vector for bacterial protein expression |
| Mxr2_Fwd_pRS361 | CATGCGATCCATGAATAAGTGGAGCAGGCTG | Forward primer to clone Mxr2 from pSP64 to pRS361 for yeast protein expression |
| Mxr2_Fwd_Met34Gly | ACGTCATTCGATTCGTCACTCCCTTTCTTGCTCTTATTCCAGTAC | Forward primer to mutagenize |

| | | |
|---|---|---|
| | | Met34 residue to Gly34 of Mxr2 |
| Mxr2_Rev_Met34Gly | GTACTGGAATAAGAGCAAGAAAGG GAGTGACGAATCGAATGACGT | Reverse primer to mutagenize Met34 residue to Gly34 of Mxr2 |
| Mxr2_Fwd_Met34Start | CATGTCTAGAATGAGTGACGAATCG AATGACGTG | Forward primer to mutagenize Δ1-33 residues of Mxr2 |
| Mxr2_Rev_Met34Start | CATGCCCGGGATCCTTCTTGAGGTT TAAAGACGC | Reverse primer to mutagenize Δ1-33 residues of Mxr2 |

**Table 2.2** List of primers used in the study and description of use.

### 2.1.3 Antibodies

| Name of Antibody | Species Origin | Species Raised in | Concentration | Company | Source |
|---|---|---|---|---|---|
| α-AAC | Yeast | Rabbit polyclonal | 1:1000 in 5% Milk in TSBT | Davids Biotechnology | Tokatlidis Lab |
| α-Aconitase | Yeast | Rabbit polyclonal | 1:10000 in 5% Milk in TSBT | Davids Biotechnology | Tokatlidis Lab |
| α-Cyt C | Yeast | Rabbit polyclonal | 1:1000 in 5% Milk in TSBT | Davids Biotechnology | Gifted by Professor Nikolaus. Pfanner |
| α-Erv1 | Yeast | Rabbit polyclonal | 1:1000 in 5% Milk in TSBT | Davids Biotechnology | (Lionaki *et al.*, 2010) |
| α-Gpx3 | Yeast | Rabbit polyclonal | 1:10000 in 5% Milk in TSBT | Davids Biotechnology | (Kritsiligkou *et al.*, 2017) |
| α-Hsp70 | Yeast | Rabbit polyclonal | 1:10000 in 5% Milk in TSBT | Davids Biotechnology | Gifted by Professor Nikolaus. Pfanner |
| α-Mia40 | Yeast | Rabbit polyclonal | 1:1000 in 5% Milk in TSBT | Davids Biotechnology | (Sideris *et al.*, 2009) |
| α-Porin | Yeast | Rabbit polyclonal | 1:10000 in 5% Milk in TSBT | Davids Biotechnology | Gifted by Professor Nikolaus. Pfanner |
| α-TFAM | Human | Mouse polyclonal | 1:2000 in 5% Milk in TSBT | Abnova | Abnova Product #BO1P |
| α-Tim10 | Yeast | Rabbit polyclonal | 1:1000 in 5% Milk in TSBT | Davids Biotechnology | Tokatlidis Lab |
| α-Tim8 | Yeast | Rabbit polyclonal | 1:1000 in 5% Milk in TSBT | Davids Biotechnology | Tokatlidis Lab |
| α-Tim9 | Yeast | Rabbit polyclonal | 1:1000 in 5% Milk in TSBT | Davids Biotechnology | Tokatlidis Lab |
| α-Tom40 | Yeast | Rabbit polyclonal | 1:1000 in 5% Milk in TSBT | Davids Biotechnology | Tokatlidis Lab |

| | | | | | |
|---|---|---|---|---|---|
| α-Tom70 | Yeast | Rabbit polyclonal | 1:1000 in 5% Milk in TSBT | Davids Biotechnology | Gifted by Professor Nikolaus. Pfanner |
| α-Rabbit IgG DyLight 680 | Rabbit | Goat | 1:10000 in TBST | Invitrogen | Invitrogen Product #35518 |
| α-Rabbit IgG HRP | Rabbit | Goat | 1:10000 in 5% Milk in TBST | Sigma Aldrich | Sigma Aldrich Product #AP307P |
| α-Mouse IgG DyLight 800 | Mouse | Goat | 1:10000 in TBST | Invitrogen | Invitrogen Product #A32730 |

**Table 2.3** List of antibodies used in the study.

### 2.1.4 Yeast Strains

| Yeast | Genotype | Description | Source |
|---|---|---|---|
| BY4741 | *MATα* his3Δ1, leu2Δ0, met15Δ0, ura3Δ0 | Wild-type strain used for comparison with ΔMxr1 and ΔMxr2 yeast strains | (Sherman, 1964) |
| D273-10B | *MATα mal* | Wild-type strain used for mitochondrial isolation | (Brachmann *et al.*, 1998) |
| ΔMxr1 (BY4741) | *MATα* his3Δ1, leu2Δ0, met15Δ0, ura3Δ0, Mxr1Δ0 | Deletion of Mxr1 in the BY4741 background | Dharmacon GE Healthcare |
| ΔMxr2 (BY4741) | *MATα* his3Δ1, leu2Δ0, met15Δ0, ura3Δ0, Mxr2Δ0 | Deletion of Mxr2 in the BY4741 background | Dharmacon GE Healthcare |
| ΔTom20 (BY4741) | *MATα* his3Δ1, leu2Δ0, met15Δ0, ura3Δ0, Tom20Δ0 | Deletion of Tom20 in the BY4741 background | Tokatlidis Lab |
| Gal Mia40 (FT5) | *MATα* ura3-52, trp1-Δ63, his3-Δ200, leu2::PET56, kanMX-GAL1-10-Mia40 | Conditional knock-out with Mia40 under the control of the Gal1-10 promoter | (Banci *et al.*, 2009) |
| Tim9TS | *MATα* ura3-52, trp1-Δ63, his3-Δ200, leu2::PET56, Tim9-M4 | Conditional knock-down of Tim9 sensitive to elevated temperature, induced by growth at 37°C for 12 hours. | Gifted by Professor Nikolaus Pfanner |

**Table 2.4** List of yeast strains used in this study.

### 2.1.5 Bacterial Strains

For cloning and transformation of plasmids DH5α cells were used and grown in Luria-Bertani (LB) medium (1% bacto-tryptone, 1% NaCl, 0.5% yeast extract in dd$H_2O$). For plate production 2% agar was added to the above medium. The media and plates were all autoclaved at 121$^oC$ for 15 minutes before use.

## 2.2 Molecular Biology

### 2.2.1 Plasmid DNA Purification and Sequencing

To isolate plasmid DNA, the QiaPrep Spin Miniprep kit (Qiagen) was used as per the manufacturers protocol. The isolated plasmid DNA and/or PCR fragments were sent for Sanger sequencing using Eurofins Genomics and the results analysed using Snapgene.

### 2.2.2 PCR

The primers detailed in **Table 2.2** were used to amplify the respective genes as described. Plasmids or yeast genomic DNA were used as template strands for the PCR reactions. The PCR reactions contained 1X polymerase buffer, 2mM $MgCl_2$, 2mM dNTPs, 0.2µM forward & reverse primer, 1ng/µl template DNA, and 1u/ µl DNA polymerase. Taq polymerase (NEB) was used for all PCR reactions. One PCR cycle consisted of the following stages: denaturation at 95$^oC$ for 1min, followed by annealing stage for 45 secs at 50-60$^oC$, and finally an extension stage at 72$^oC$ for 30secs for every kb of DNA to be amplified. DNA was amplified for 30-35 cycles with a final extension time of 5mins at 72$^oC$.

PCR amplified products were separated using agarose gel electrophoresis (0.8-1.25% w/v Agarose, 1X TAE buffer, 1X SYBRsafe) for 1 hour at 90V. A 1kb DNA ladder (Promega) was used for estimation of fragment size. PCR clean-up was performed using the QiaQuick PCR cleanup-kit (Qiagen) according to the manufacturer's instructions and DNA concentrations were measured on a Nanodrop Spectrophotometer (Thermo).

### 2.2.3 Ligation and Digestion Reactions

DNA inserts were generated using PCR amplification as detailed in section 2.2.2. PCR products were subsequently digested using appropriate restriction enzymes (NEB) for 2 hours at 37$^{o}$C. Digested products were separated by agarose gel electrophoresis at 90v for 1 hour. Ligated products were extracted using the QiaQuick gel extraction kit (Qiagen) as per the manufacturer's instructions. Ligation of inserts with the appropriate vector was carried out using the T4 DNA Ligase (NEB) at 16$^{o}$C overnight using a 1:3 vector: insert ratio. Ligated material was subsequently transformed into cell DH5α cells. The ligated product was presented to the competent DH5α cells and incubated on ice for 30 minutes, followed by a 45 second heat shock at 42$^{o}$C and a recovery for 1 hour at 37$^{o}$C shaking in 1ml of LB media. Transformed cells were pelleted via centrifugation at 8,000g for 5 minutes and resuspended in 200ml LB. This was subsequently plated on LB agar plates containing the correct antibiotic selection factor and grown at 37$^{O}$C overnight.

### 2.2.4 Site-directed Mutagenesis

1ng/ µl of plasmids containing the gene of interest was used as template DNA for PCR amplification to generate a mutant sequence using forward and reverse primers containing the mutation and the surrounding complementary DNA. Following amplification, the template DNA was digested using the restriction enzyme DPN1 (Promega) for 1 hour at 37$^{o}$C. A second digestion was carried out under the same conditions. PCR products were transformed into DH5α cells. Transformants were then plated on LB agar plates containing the correct antibiotic selection factor and grown at 37$^{O}$C overnight.

## 2.3 Biochemical Assays

### 2.3.1 SDS-PAGE and Western Blotting

Tris-Tricine SDS-PAGE was used to separate proteins depending on their molecular weight. 8-16% acrylamide gels were used depending on the molecular weight of the protein of interest. Samples were resuspended in 2X Laemmli buffer (375mM Tris-HCl pH6.8, 9% SDS, 40% glycerol, 0.03% bromophenol blue) prior to loading in the SDS-PAGE well. The gels were run

for 10 minutes at 120V to allow the proteins to pass through to the resolving gel before increasing the voltage to 150V and running until the dye front escaped from the gel. Lower tank buffer consisted of 200mM Tris-HCl pH 8.9, while the upper buffer comprised 100mM Tris-HCl, 100mM Tricine, 0.1% SDS adjusted to pH 8.25. Gels were then transferred onto nitrocellulose membrane for western blotting. A table containing the components and respective volumes for each Tris-Tricine SDS-PAGE gel is shown below **(Table 2.5)**.

| | **Stacking** | **Separating** | | | |
|---|---|---|---|---|---|
| | 5% Acrylamide | 8% | 12% | 14% | 16% |
| Acryl/ Bis Acryl (40%) | 0.375ml | 2ml | 3ml | 3.5ml | 4ml |
| Tricine Gel Buffer | 0.75ml | 3.3ml | 3.3ml | 3.3ml | 3.3ml |
| 87% Glycerol | N/A | 1.3ml | 1.3ml | 1.3ml | 1.3ml |
| dd$H_2O$ | 1.82ml | 3.29ml | 2.29ml | 1.79ml | 1.29ml |
| APS | 50µl | 100µl | 100µl | 100µl | 100µl |
| TEMED | 5µl | 10µl | 10µl | 10µl | 10µl |
| **TOTAL** | 3ml | 10ml | 10ml | 10ml | 10ml |

**Table 2.5** Recipes for casting Tris-Tricine SDS PAGE gels in 1.5ml plates

SDS-PAGE gels were transferred onto nitrocellulose system using a semi-dry transfer system (Bio-Rad) at 25V for 25 minutes. Three pieces of pre-soaked Whatmann paper in transfer buffer (25mM Tris, 190mM glycine, 20% methanol, 0.1% SDS) were placed either side of the nitrocellulose membrane and SDS-gel. After the transfer the membrane was blocked for 1 hour shaking at room temperature in 5% skimmed milk powder in TBST (150mM NaCl, 100mM Tris-HCl pH7.4, 0.01% Tween-20). Primary antibody was prepared as per **Table 2.3** and incubated with the membrane for 1 hour at the same conditions. The membranes were washed for 10 minutes, three times in TBST. Secondary antibodies were prepared in TBST (fluorescent antibodies) or 5% Milk TBST (HRP antibodies) and incubated with the membrane for a further hour before repeating the three washes with TBST. Fluorescent antibodies were

visualised with the LI-COR odyssey CLX. HRP secondary antibodies were visualised using chemiluminescence solution (Pierce).

### 2.3.2 Blue-Native PAGE

Bio-Rad mini-gel casting system was used to cast all Blue-Native PAGE (BN-PAGE) gels. 6-16% gradient gels were cast using the gradient mixer that kept each solution constantly stirring on the stirrer plate. The recipe for casting each gel is shown below in **Table 2.6**. Gels were cast at 4$^{o}$C to prevent the setting of the acrylamide in the gradient mixing chamber.

| | **Stacking** | **Separating** | |
|---|---|---|---|
| | 4% Acrylamide | 6% | 16% |
| **Acrylamide Mix (49% Acrylamid: Bisacrylamide (48:1.5))** | 0.25ml | 0.732ml | 1.294ml |
| **1D Gel Buffer 3X (1.5M Aminocaproic acid, 150mM Bis-Tris pH7** | 1ml | 2ml | 1.33ml |
| **Glycerol** | N/A | N/A | 0.72ml |
| **dd$H_2O$** | 1.75ml | 3.22ml | 0.54ml |
| **APS** | 50µl | 50µl | 25µl |
| **TEMED** | 5µl | 5µl | 3µl |

**Table 2.6** Recipes for casting Blue-Native PAGE gels in 1.5ml plates

For running the gel, the lower (Anode) buffer consisted of 50mM bis-Tris-HCl pH7, while the upper (Cathode) buffer consisted of 50mM Tricine, 15mM bis-Tris-HCl pH7, 0.02% Serva blue G250. Initially the gel was run at 90V for 30 minutes and then 12mA constant until the dye front reached the bottom of the gel. Once the dye front approached the half-way mark on the gel the upper buffer was discarded and replaced with a diluted upper buffer (50mM Tricine, 15mM bis-Tris-HCl pH7, 0.002% Serva blue G250) for the rest of the run.

After running the gel, the gel was placed in destaining buffer (50% $H_2O$, 40% methanol, 10% acetic acid) for 30 minutes at RT, shaking gently to allow better visualisation of the NativeMark™ Unstained Protein Standard markers (Invitrogen) and respiratory complexes. For BN gels containing imported radioactive material, the gels were vacuum dried on a piece of Whatmann paper using a Bio-Rad gel drier.

### 2.3.3 In vitro Radiolabelled Protein Translation

Genes of interest to be expressed were cloned into pSP64 vectors containing a SP6 promoter region to initiate transcription. The TNT® SP6 quick coupled transcription/ translation system (Promega) was used to synthesise proteins and incorporate $^{35}S$-labelled methionine residues as per the manufacturer's instructions, using a vector concentration of 20ng/ µl to ensure sufficient radiolabelled protein was synthesised. The TNT mix was incubated at 30°C for 90 minutes shielded form light. Ultracentrifugation was used to remove the ribosomes from the sample in a TLA-100 rotor at 131,400g at 4°C for 15 minutes.

### 2.3.4 Protein Precipitation and Denaturation

Following centrifugation of the TNT to pellet the ribosomes, the mix was precipitated using 3 volumes of $(NH_4)_2SO_4$ on ice for 30 minutes. Precipitated TNT mix was subsequently pelleted at 16,600g for 30 minutes at 4°C using a tabletop centrifuge. The pellet was then resuspended in the intended buffer for subsequent protein import assays: native import buffer (50mM HEPES-KOH pH7.4), native reducing buffer (50mM HEPES-KOH pH7.4, 20mM DTT) or denaturing buffer (8M urea, 50mM HEPES-KOH pH7.4, 20mM DTT).

### 2.3.5 Autoradiography

To visualise radioactive material within nitrocellulose membranes (section 2.3.1) or dried BN gels (section 2.3.2) they were incubated for 48 hours minimum exposed to autoradiographic film (Fujifilm). The film was subsequently visualised using a phosphoimager (Fujifilm FLA-7000). Intensity of the radioactive bands were normalised to a mitochondrial protein loading control, usually either a 5% or 10% control.

## 2.4 *In Organello* Assays

### 2.4.1 Isolation of Yeast Mitochondria

Mitochondria were isolated and purified from the yeast strains detailed in **Table 2.4**, following the protocol described in Glick et al, 1991 (Glick, 1991). Ten litres of YPLac media were inoculated with the yeast strain at an $OD_{600}$ of 0.1 and left to grow overnight at 30°C, shaking constantly (150rpm). Following overnight growth (~16hours) the yeast cells were pelleted via centrifugation at 3000g for 5mins at RT in a JLA8.1000. Pellets were washed in 300ml $H_2O$ and pelleted at 1850g for mins at 4°C in a JA14. The dry weight of the cell pellet was measured to estimate the yield of mitochondria.

The yeast cell wall was weakened by incubating with Tris-DTT buffer (Tris-$SO_4$ pH9.4, 10mM DTT) for 30 minutes at 30°C shaking at 150rpm. The cells were pelleted as before and resuspended in 80ml total sorbitol buffer (1.2M sorbitol, 20mM $KP_i$ pH7.4) to wash the cells before being pelleted again. To digest the cell wall, cells were resuspended in 5ml sorbitol buffer per gram of cells and accompanied with Zymolyase 20T (3.5mg/ g cells) (AMSBio). The resuspended cells were left at 30°C for 45mins at 150rpm for digestion of cell wall to occur and to generate spheroplasts.

Spheroplasts were gathered by centrifugation at 1480g and washed twice in sorbitol buffer, being kept at 4°C at all times now to protect the cells from environmental changes. The cells were cracked open using a type B pestle to dounce the cells 15 times in breaking buffer pH6 (0.6M sorbitol, 20mM MES-KOH pH6) with 2mM PMSF to inhibit any released proteases. Any unbroken cells were collected via centrifugation at 1480g, 5 mins, 4°C and the broken cells were saved in the supernatant. The douncing stage was repeated as above and the broken cells collected by centrifugation. The collected supernatants were pelleted at 12,000g for 10 minutes at 4°C to collect cellular organelles. This pellet was resuspended in breaking buffer pH6 minus PMSF and dounced using a PTFE dounce homogenizer. To remove any unbroken cells a low-speed spin at 1480g for 5 minutes was carried out, and the resulting supernatant was centrifuged at 12,000g for 20 minutes to pellet the crude mitochondrial fraction. The

concentration of crude mitochondrial was estimated using the conversion factor 0.21 $OD_{280}$ = 10mg/ ml mitochondrial proteins.

To further purify the mitochondrial fraction from the other organelles in the sample a nycodenz gradient ultracentrifugation was carried out. A 14.5% and 20% nycodenz solution were prepared in 1X breaking buffer pH6 and dd$H_2O$. Equal amounts of the 14.5% solution were overlayed slowly on top of the 20% solution to create a nycodenz gradient. The crude mitochondria fraction was overlayed on top of the gradient and centrifuged in a SW-40Ti rotor (Beckman Coulter) at 283,800g for 1 hour at 4°C. Following centrifugation, the pure mitochondrial fraction was harvested from the gradient using a 19-gauge needle and washed twice in breaking buffer pH7.4 (0.6M sorbitol, 20mM HEPES-KOH pH7.4) by centrifugation at 12,000g for 10 minutes at 4°C. The concentration of pure mitochondria was estimated spectrophotometrically using the conversion factor 0.12 $OD_{280}$ = 10mg/ ml mitochondrial proteins. Mitochondrial aliquots of 25mg/ml were prepared in breaking buffer pH7.4 supplemented with 10mg/ ml BSA as a cryoprotectant. Aliquots were flash frozen in liquid nitrogen and immediately stored at -80°C.

### 2.4.2 Protein Import into Yeast Mitochondria

Mitochondria were prepared as per the protocol in section 2.4.1. Mitochondria removed from -80°C storage were flash-thawed in a 30°C water bath and resuspended in breaking buffer pH7.4 to wash them. Mitochondria were pelleted at 16,000g for 5 mins at 4°C in a table-top centrifuge and the remaining breaking buffer aspirated. Pellets were resuspended in 25µl breaking buffer for approximately every 500µg mitochondria. Prior to imports the pure mitochondrial concentration was calculated as per section 2.4.1.

Mitochondria were suspended in import buffer (600mM sorbitol, $KH_2PO_4$, 50mM KCl, 50mM HEPES-KOH pH7.4, 10mM $MgCl_2$, 2.5mM EDTA, 5mM L-methionine, 1mg/ml fatty acid free BSA) and supplemented with 2mM ATP and 2.5mM NADH. In import reactions where the inner membrane potential ($\Delta\psi$) had been depleted the NADH was replaced by 25µM CCCP. Protein of interest was radiolabelled as described in section 2.3.3 and was added to the mitochondrial import mix (5µl of TNT reaction to 50µg of mitochondria) and the mix was incubated at 30°C in a water bath for the specified time-period. To terminate the import reaction the samples were placed on ice and centrifuged at 16,000g for 5 minutes at 4°C. The

pellets were then resuspended in the protease trypsin (0.1mg ml in breaking buffer pH7.4) to digest any unimported material in the samples and left for 30 minutes at 4$^{o}$C. As a control sample, the mitochondria were resuspended in 10% Triton-X100 in trypsin breaking buffer pH7.4 solution to solubilise the mitochondrial membranes and left for 30 minutes at 4$^{o}$C. Following trypsinisation the samples were centrifuged at 16,000g for 5 minutes at 4$^{o}$C and the pellets resuspended in the trypsin inhibitor SBTI (1mg/ ml in breaking buffer pH7.4) and left for 10 minutes at 4$^{o}$C. Mitochondria were again pelleted at 16,000 for 5 minutes, 4$^{o}$C and resuspended in 10µl 2X Laemmli buffer +/- β-mercaptoehanol for loading on Tris-Tricine SDS-gels as per section 2.3.1. For BN-PAGE analysis the mitochondria were instead solubilised in solubilisation buffer (20mM Tris-HCl pH7.4, 50mM NaCl, 10% glycerol, 0.5mM EDTA, 1% (w/v) digitonin (1mg/ ml) (Sigma)). Samples were solubilised for 10 minutes on ice followed by centrifugation at 16,000g for 5 minutes at 4$^{o}$C to remove and insoluble material. Supernatants were transferred to fresh tubes and 6X BN sample buffer (0.5% Coomassie G-250, 50mM aminocaproic acid, 10mM bis-Tris pH7) to a final concentration of 1X and loaded into the BN-PAGE gel as per section 2.3.2.

### 2.4.3 Mitoplasting

Mitoplasting was used to separate soluble IMS proteins from those of the matrix and embedded in the outer/ inner membranes. Following protease treatment of mitochondria as per section 2.4.2 the mitochondria were resuspended in 1X import buffer to a 5mg/ ml concentration and further diluted 8X in mitoplast buffer (20mM HEPES-KOH pH7.4) +/- proteinase K (0.1mg/ ml) and incubated on ice for 20 minutes. 1mM PMSF was added to inhibit the protease and left for a further 10 minutes on ice. The mitoplasts were pelleted at 16,000g for 5 minutes and the pellet (outer/ inner membrane and matrix proteins) resuspended in 2X Laemmli with 1mM PMSF. The supernatant was precipitated using 10% (w/v) final concentration trichloroacetic acid (TCA) by incubating on ice for 20 mins followed by centrifugation at 16,000g for 20 minutes at 4$^{o}$C. The pellet (soluble IMS proteins) was resuspended in 2X Laemmli buffer with 1mM PMSF.

### 2.4.4 Sodium Carbonate Extraction

Sodium carbonate extraction was used to separate insoluble integral membrane proteins from the soluble proteins of the IMS, matrix and any peripherally associated membrane proteins. 100mM $NaCO_3$ solution was incubated with 100µg of mitochondria for 30 minutes on ice and the sample pelleted via ultracentrifugation at 131,440g for 30 minutes at 4°C in a TLA-100 rotor. The supernatant was precipitated using TCA precipitation as detailed in section 2.4.3 and both supernatant and pellet fractions were resuspended in 2x Laemmli buffer.

### 2.4.5 Isolation of Mammalian Mitochondria

The protocol to isolate mammalian mitochondria was obtained from Kang et al., 2017 (Kang *et al.*, 2017). HEK293 cells were cultured in 7 to 10 T75cm$^2$ tissue culture flasks until 90% confluent and cells were harvested by scraping in 25ml phosphate buffer saline (PBS). Cells were pelleted through centrifugation at 800g for minutes at 4°C before resuspension in 24-32ml solution A (20mM HEPES-KOH pH7.6, 220mM mannitol, 70mM sucrose, 1mM EDTA, 0.5mM PMSF, 2mg/ml BSA) and incubated for 15 minutes on ice. Cells were homogenised using a drill-fitted pestle for 20-30 strokes and the solution centrifuged at 800g for 5 minutes at 4°C. Supernatant was collected and further centrifuged at 10,000g for 10minutes at 4°C to generate a crude mitochondrial pellet. This pellet was resuspended in solution B (solution A minus 2mg/ml BSA) and mitochondrial protein concentration estimated spectrophotometrically using the following equation.

$$\text{Mitochondrial protein} = \frac{\text{A280nm} - \text{A310nm}}{1.05} * \frac{600ul}{Xul} mg/ml$$

5ul of mitochondria was measured in 600µl of 50mM Tris, 0.1% SDS. Mitochondria were used fresh in import assays only as the inner membrane potential is lost upon freeze-thaw.

### 2.4.6 Protein Import into Mammalian Mitochondria

Isolated mitochondria from section 2.4.5 were pelleted at 10,000g for 5mins at 4°C and resuspended in cold import buffer (250mM sucrose, 5mM magnesium acetate, 80mM potassium acetate, 10mM sodium succinate, 20mM HEPES-KOH pH7.4) supplemented with 5mM ATP and 2.5mM NADH. 5µl of TNT translated product (section 2.3.3) was added to each

mitochondrial import mix containing 50µg of mitochondria and incubated for the desired length of import. For depletion of inner mitochondrial membrane, NADH was replaced with 10µM CCCP. Post imports the mitochondria were pelleted at 10,000g for 5 minutes at 4$^{o}$C and resuspended in trypsin (0.05mg/ml in import buffer). Samples were left for 20 minutes, and mitochondria pelleted as before. Pellets were resuspended in SBTI (0.5mg/ml in import buffer) to inhibit trypsin and left on ice for 10 minutes. Mitochondria were again pelleted at 10,000g for 5 minutes at 4$^{o}$C before final resuspension in 2X Laemmli buffer and SDS-PAGE performed to separate proteins.

### 2.4.7 Alkylation Shift Assay

4-acetamido-4'-malemidylstilbene-2-,2' disulfonic acid (AMS) (Thermofisher) was used to label free thiols in proteins to result in a 0.5kDa shift in molecular weight per free thiol labelled on SDS PAGE gel. 100µg of mitochondria were TCA precipitated as per section 2.3.4 and precipitated protein washed in acetone twice before suspension in 15mM AMS in ETS buffer (3mM EDTA, 50mM Tris-HCl pH8, 3% SDS). For controls samples were resuspended in ETS buffer alone, or 15mM AMS and 75mM DTT. Samples were wrapped in foil to protect the AMS from light and incubated for 30 minutes at 30$^{o}$C and a further 30minutes at 37$^{o}$C. 4X Laemlli buffer was added to each reaction and SDS-PAGE performed to separate proteins.

### 2.4.8 Oxygen Consumption Measurements of Yeast Mitochondria

Clark electrode was used to measure the oxygen consumption of isolated mitochondria in response to varying treatments. The oxygen in the chamber diffuses across a Teflon membrane into the compartment containing the electrode and fluctuations in oxygen consumption change the flux of the electrical circuit proportionally to the oxygen consumed. Change in amps was converted to change in voltage via Watts Law (volts * amps = watts), and thus the voltage was proportional to the amount of oxygen in the system.

3M KCl was added to the silver and platinum electrodes which were then covered with a 1cm$^2$ piece of tissue paper and PTFE membrane. The O ring was placed over the electrode to hold the membrane in place. The plastic base and incubation chamber were clamped to prevent oxygen entering the system.

2ml of 1X import buffer was added to the chamber and the voltage was measured until constant. The stopper was added to the system and allowed to equilibrate. 300µg of mitochondria in breaking buffer pH7.4 were added to the system to measure basal respiration rates. Next 1M each malate glutamate, 1M sodium pyruvate and 0.1M ADP were added in turn until a change in rate of voltage was observed. 1mM oligomycin was added to inhibit complex V followed by addition of 0.25mM CCCP as an uncoupler. Lastly 5mM sodium azide was added to inhibit the electron transport chain. With the addition of each treatment the electrode was left for 1-3 minutes until a change in rate was observed.

All data was collected using the PicoLog6 data recorder and results analysed in excel. Three repeats were carried out for each mitochondrial strain and the average oxygen consumption rate for each treatment calculated. Statistical significance was calculated using an unpaired t-test (* $p<0.05$, ** $p<0.001$).

### 2.4.9 Protein Steady-State Levels in Isolated Mitochondria

Isolated mitochondria as prepared in section 2.4.1 were flash thawed and mitochondria pelleted by centrifugation at 16,000g for 5 minutes at 4°C. Mitochondria were resuspended in breaking buffer pH7.4 and concentration of mitochondrial proteins measured as per section 2.4.1. Mitochondria were diluted in 2x Laemlli buffer to give the desired concentration and proteins separated via SDS-PAGE gel. Western blotting was used to detect steady state levels of protein of interests.

## 2.5 In vivo Assays

### 2..5.1 Yeast Spot Assay

Yeast colonies were selected and grown overnight at 30°C in YPD medium. $OD_{600}$ was measured and yeast diluted to 0.1OD units in sterile dd$H_2O$. Serial dilutions were performed four times to create dilutions at 0.1, 0.01, 0.001, 0.0001, 0.00001 OD units. 5µl of each dilution was spotted onto either YPD or YPLac agar plates and grown for 48 hours at 30°C. Agar plates

were supplemented with $H_2O_2$ after autoclaving media and pouring the plates fresh before the spot assay.

# Chapter 3: Characterising the Import and Localisation of yeast Methionine Sulfoxide Reductase 2 in Mitochondria

## 3.1 Introduction

As previously discussed in section 1.4.3 yeast cells contain three different Mxr enzymes termed fRMsr, Mxr1 and Mxr2 that reduce different stereoisomers of oxidised methionine sulfoxide groups in proteins. It has been shown that Mxr1 is a cytosolic protein and Mxr2 is targeted to mitochondria (Kaya *et al.*, 2010a).A localisation study determined that Mxr2 was sub-localised to the mitochondrial matrix within the mitochondria (Allu *et al.*, 2015). Indeed interaction studies have determined that Mxr2 is involved in regulating the co-chaperone Mge1, found in the matrix, further emphasising the presence of Mxr2 in this compartment (Allu *et al.*, 2015).

As Mxr2 is believed only to be localised to the matrix, and there are no other discovered Mxr enzymes within the mitochondria then this suggests no other reductase enzymes are present in other compartments of the mitochondria such as the IMS. A previous mass spectrometry analysis of the essential protein Erv1, localised to the IMS, revealed that this protein could become methionine sulfoxidated (Met-O) (Lionaki *et al.*, 2010). This creates a conundrum where this protein is believed to become modified by Met-O but there are no proposed reductase enzymes in the compartment to remove this modification. As Met-O is a harmful protein modification that induces protein unfolding, the failure to reduce these adducts can render the protein dysfunctional (Tarrago *et al.*, 2012). Due to the essential nature of Erv1's role in the MIA pathway this is likely to cause profound consequences for the organelle **(Fig**

**1.2)**. This poses the question of how do mitochondria cope with Met-O stress in other compartments of the organelle out-with the matrix if there are no other reductase enzymes present?

It may be possible that there are undiscovered Mxr enzymes that are also targeted to the mitochondria, particularly those involved with the reduction of the Met-(S)-O form. As Mxr2 only acts on Met-(R)-O there is no mechanism for reduction of the other stereoisomer in the mitochondria **(Fig 1.4)**. An alternative hypothesis that can be tested is that Mxr2 is indeed a dually localised protein within the mitochondria found in both the IMS and Matrix where it can reduce Met-O proteins throughout the organelle. Previously proteins such as peroxiredoxin 1 (Prx1) and Apurinic/apyrimindic endonuclease 1 (APE1) have been demonstrated to be dually localised within this organelle, and translocated into specific compartments under conditions of changes in oxidative stress (Gomes *et al.*, 2017; Barchiesi *et al.*, 2020).

The components of the import machinery required for the import of Mxr2 have not been well characterised. Sequence analysis suggests that the protein possesses a mitochondrial targeting sequence to follow the classical matrix imported pathway, but this has not been tested biochemically. There are also several conserved cysteines in the sequence which could introduce the possibility of disulphide formation and links to the MIA pathway. If Mxr2 is indeed a dually localised protein inside the mitochondria, then this introduces a further level of import regulation to ensure the protein is in the correct compartment when required.

This chapter aims to further confirm the localisation of Mxr2 inside mitochondria and begin elucidating the components of the import pathways that are required for successful import.

## 3.2 Aims

There were two key aims of this chapter. The first was to test the import of Mxr1 and Mxr2 into mitochondria, and if they are successfully imported characterise the localisation of the proteins within the organelle.

Secondly, through sequence analysis of Mxr2 and the use of mitochondrial strains devoid of key components of the mitochondrial import machinery determine the proteins involved in the successful import of this protein.

## 3.3 Results

### 3.3.1 The Import and Localisation of Mxr2 into Mitochondria

Mxr1 and Mxr2 yeast sequences were cloned into pSP64 constructs to allow the radiolabelled translation of these proteins using the rabbit reticulocyte lysate Transcription and Translation (TNT) system. Sequence comparison between Mxr1 and Mxr2 is shown in **Fig 3.1**. A pairwise protein alignment revealed the low level of conservation between the two Mxr enzymes in *S. Cerevisiae*. The mitochondrial targeting sequence (MTS) is present in the Mxr2 sequence but absent from Mxr1 which suggested that only Mxr2 should be imported into the mitochondria **(Fig 3.1)**. Radiolabelled Mxr1 and Mxr2 were first tested to see if they could be imported into mitochondria isolated from WT D273-10B yeast strains. Mxr1 was not imported into the mitochondria as when trypsin was added to the import there was complete loss of radioactive signal suggesting the protein was not protected from the protease. **(Fig 3.2A)**. Mxr2 on the other hand was imported; when trypsin was added there was protection of the protein from the protease **(Fig 3.2B)**. The import of each enzyme was tested in the presence or absence of an inner mitochondrial membrane potential ($\Delta\psi$). **(Fig 3.2A)**. Loss of $\Delta\psi$ did significantly reduce the amount of imported Mxr2 **(Fig 3.2B)**. This suggests that the import of Mxr2 is dependent on the presence of a $\Delta\psi$ in the inner membrane. Triton-X (Tx) was added as a control to completely solubilise the mitochondria and render all proteins subject to trypsin degradation. The loss of Por1 in the presence of Tx acts as a control to confirm the Tx was active and all proteins in the lane have been subjected to proteolytic degredation.

```
>Mxr1
------------------------------------------------------------
------------------------------------------------------------MS
-SSKTKYDAKDKTACGCWGTHMYRKYNDRVDCKVGYANGSKKDSSSVSYKRVCGGDTDAV
VSYNKVTRTDRHDTTSNSGDKGTYRSGAHSDADKAKKWKWGNKATVKNYDAYHYDKNGYA
CTHYRM

>MXR2
MNKWSRYVTVRRTGRRNVTYWNKSKKMSDSNDVKWNDATMVRDKATRNTGAYHTNSGVYH
CANCDRYSSKAKDARCGWAYVSGATYHRDNSMARVCCARCGGHGHVGGWKNKDTRHCVNS
ASNK-K-D------------------------------------------------------
------------------------------------------------------------
------
```

**Figure 3.1 Sequence Comparison of Methionine Sulfoxide Reductase 1 (Mxr1) and Mxr2 in *S. Cerevisiae***. A pairwise protein sequence alignment of the Mxr1 and Mxr2 sequences from *S. Cerevisiae* localised proteins. The mitochondrial targeting sequence (MTS) is highlighted in green and is present only in the Mxr2 sequence.

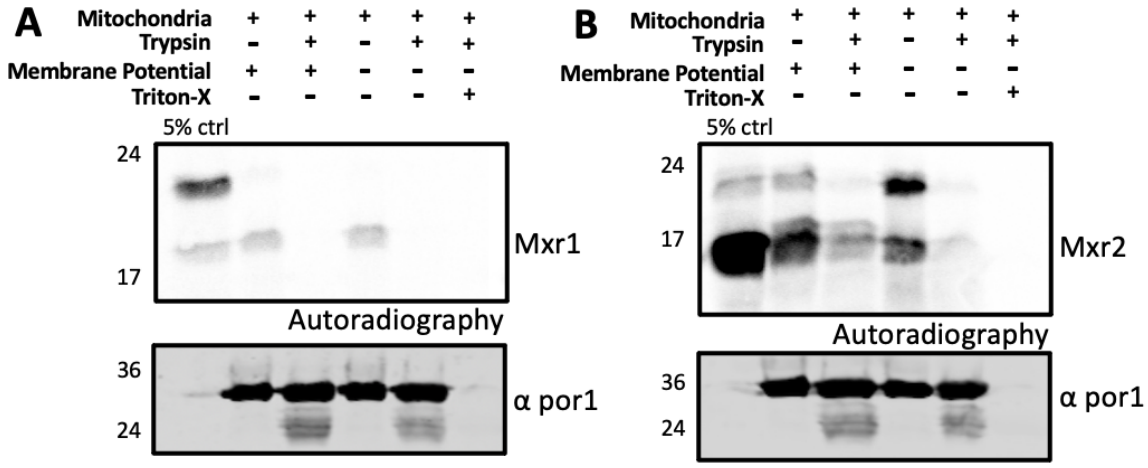


**Figure 3.2 Import of radiolabelled Methionine Sulfoxide Reductase 1/2 (Mxr1/ Mxr2) precursors into mitochondria.** Mxr1 (A) and Mxr2 (B) were translated as radiolabelled precursors and imported into isolated wild-type (WT) yeast mitochondria. Precursors were imported for 30 minutes at 30$^{o}$C and treated with Trypsin (0.1mg/ml) and SBTI (1mg/ml) post import to degrade any unimported precursor proteins. Triton-X100 (Tx) (10%) was used alongside Trypsin as a negative control. 5% of the precursor protein presented to each of the import reactions was loaded as a positive control. Radioactive material was detected using a phosphoimager. Western blotting for Porin 1 (Por1) was used as a loading control. Samples were loaded on an SDS gel.

The 5% control lanes for both Mxr1/2 show the translation of two protein products at approximately 20kDa and 17kDa respectively. For Mxr1 as neither translated protein did not import, we were not interested in characterising these bands. However, as Mxr2 was successfully imported, it was important to understand what each of these translation products corresponded with. It was hypothesised that there may be a secondary start codon in the sequence which could lead to the translation of a smaller truncated product. This is also possibly true for Mxr1 but the focus of the project was on the mitochondrial targeted Mxr enzymes.

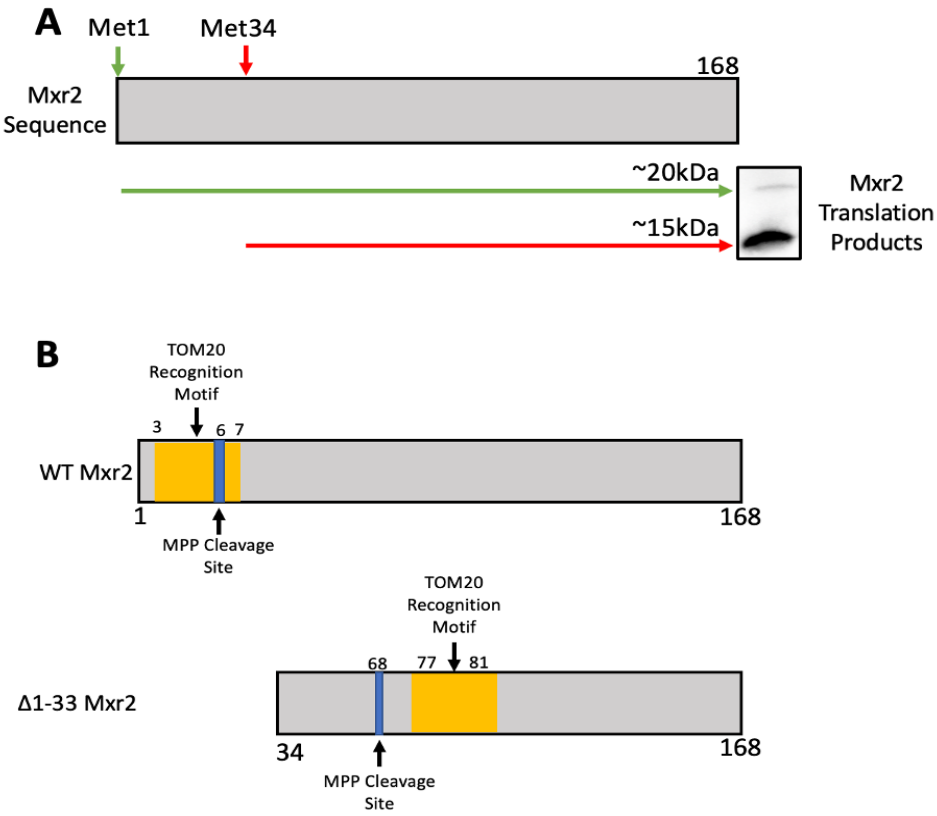


**Figure 3.3 Mxr2 translation products and sequence analysis.** (A) Mxr2 has two alternative start methionine codons. Depending on if translation starts at Methionine (Met) 1 or 34 results in the translation of a 20kDa or 15kDa protein product respectively. The translation of these products is aligned with the detection of these two products through autoradiography. (B) Sequence analysis of the WT Mxr2 and the alternative start codon Mxr2 (Δ1-33 Mxr2) using Mitofates software predicts the presence of Translocase of the Outer Membrane 20 (TOM20) receptor recognition motifs and matrix processing peptidase (MPP) cleavage sites in the sequence, at varying residues between the translation products.

Data from ribosome profiling and mRNA sequence reading of Mxr2 revealed that there was aggregation of sequence reads around Met34 which could suggest the use of this methionine as an alternative start codon to produce a shorter translated product of Mxr2 (Nicklow and

Sevier, 2020). Wild type (WT) Mxr2 has an approximate molecular weight (MW) of 20kDa in accordance with the upper translation product seen on SDS PAGE gels **(Fig 3.2A)**. Calculating the approximate MW of this alternatively translated Met34 Mxr2 suggests a protein of 15kDa. This was in line with the size determined on the SDS gels. From this it is believed that the two translated protein bands of Mxr2 correspond to WT (upper) and Met34 start (lower) Mxr2 proteins. The schematic in **Fig 3.3A** illustrates the alternative Met start codon hypothesis for translation of Mxr2 sequences. To test this hypothesis, primers were designed (**Table 2.2**) to mutagenize the Met34 residue to a glycine, with the hypothesis that this would prevent translation of the MW Mxr2 product. In addition, primers were used to create a Δ1-33 Mxr2 construct, to promote the plasmid to translate Mxr2 from Met34 only. PCR was used to successfully amplify these constructs, but work is still ongoing to clone the sequences into the pSP64 vector for radiolabelled protein translation. Interestingly the protein translation system preferred to translate the Met34 Mxr2 as the band intensity was much greater than the WT Mxr2 in the control lane **(Fig 3.2A)**. Following the successful import of Mxr2 into the mitochondria, the import reaction was assessed at several different timepoints to determine the kinetics of import. From here Tris-Tricine SDS gels were used to enhance the resolution

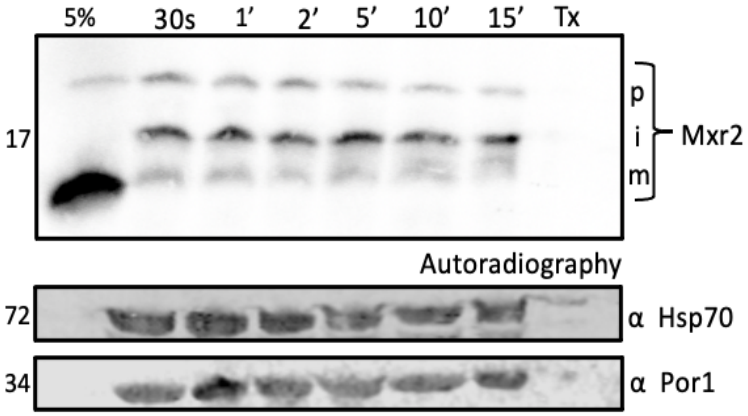


**Figure 3.4 Import kinetics of Methionine Sulfoxide Reductase 2 (Mxr2) into mitochondria.** Import of radiolabelled Mxr2 precursor into yeast mitochondria at different specified timepoints. All samples were treated with Trypsin (0.1mg/ml) and SBTI (1mg/ml). Triton-X100 (Tx) (10%) was used alongside trypsin as a negative control. 5% represents 5% of the TNT reaction mix presented to the mitochondria loaded as a positive control. Radioactivity was detected using a phosphoimager. Three forms of Mxr2 were detected referred to as precursor (p), intermediate (i) and mature (m). Western blots of mitochondrial Hsp70 (Hsp70) and Porin 1 (Por1) used as loading controls. Samples were loaded on a 14% Tris-Tricine SDS gel.

The import kinetics of Mxr2 into yeast mitochondria suggests that Mxr2 is a very efficiently imported protein with high levels of protein import detected after just 30 seconds **(Fig 3.4)**. The level of import did not appear to be enhanced significantly at longer times up to 15 minutes. The higher resolution gel used for this import detected three different forms of Mxr2 opposed to the band pattern seen on the SDS gels **(Fig 3.2)**. The upper band is referred to as the precursor (p) Mxr2. It runs at 20kDa and appears to be the unmodified higher MW protein seen in the 5% control lane, confirming that it is the WT Mxr2 and not the Met34 Mxr2 that is first imported. This precursor protein is imported into yeast mitochondria where it undergoes several processing events inside this organelle to generate smaller MW forms of Mxr2. Next there is the intermediate (i) Mxr2 that runs below this and appears to be a processed form of Mxr2 that becomes cleaved or modified inside the mitochondria resulting in a loss of molecular weight. And lastly there is the mature (m) form of Mxr2 that runs slightly above the Met34 translated Mxr2 in the control lane suggesting that this is not the import of Met34 Mxr2 but instead a further processed form of Mxr2, possibly into its mature conformation. Interestingly the intensity of the intermediate Mxr2 is greatest suggesting it is the preferred form of Mxr2 inside the organelle. It is also of note that despite the WT Mxr2 being translated at a much lesser efficiency than the Met34 Mxr2, it appears this is the form that becomes imported. The results in Fig 3.4 suggest that WT Mxr2 is highly efficiently imported into the mitochondria as a precursor protein, where it undergoes two uncharacterised processing events to generate an intermediate and mature form of Mxr2 inside this organelle at distinct molecular weight.

Following on from the import kinetics into yeast mitochondria, the capacity of yeast Mxr2 to be imported in mammalian mitochondria was determined. Mitochondria were harvested from HEK293 cells as per section 2.4.5. Radiolabelled Mxr2 was presented to these isolated mitochondria and the import is shown in **Fig 3.5**. In the presence of trypsin Mxr2 was protected from protease degradation suggesting it was successfully imported into the mammalian mitochondria. Two forms of Mxr2 were detected: precursor (p) and mature (m) Mxr2. This differs from the import into the yeast system as no intermediate form of Mxr2 was detected suggesting that Mxr2 is processed differently in the mammalian system. In the absence of membrane potential, the ability of Mxr2 to import was substantially reduced, in line with the findings in yeast mitochondria. While Mxr2 was been shown to be imported into

both the yeast and mammalian mitochondrial systems these results do not inform in which compartments of the organelle the protein becomes localised to. To determine this Mitoplasting and Sodium Carbonate extractions were performed.

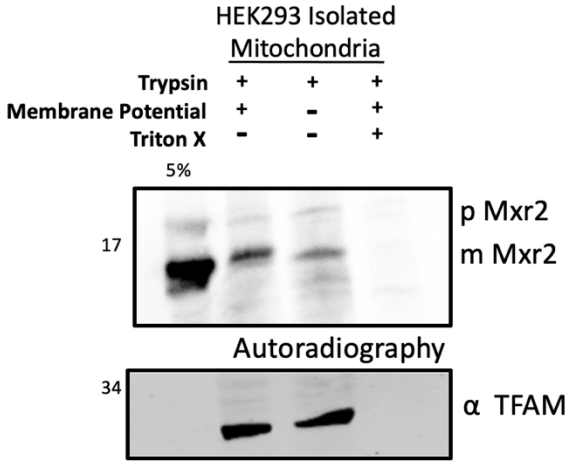


**Figure 3.5 Import of Methionine Sulfoxide Reductase 2 (Mxr2) into mammalian mitochondria.** Import of radiolabelled Mxr2 precursor into HEK293 isolated mitochondria for 30 minutes. All samples were treated with Trypsin (0.1mg/ml) and SBTI (1mg/ml). Triton-X100 (Tx) (10%) was used alongside trypsin as a negative control. 5% represents 5% of the TNT reaction mix presented to the mitochondria loaded as a positive control. Radioactivity was detected using a phosphoimager. Precursor (p) and mature (m) forms of Mxr2 detected. Western blot of human TFAM used as a loading control. Samples were loaded on a 14% Tris-Tricine SDS gel.

Yeast mitoplasts were generated using osmotic shock to rupture the outer membrane and cause leakage of soluble IMS proteins. Mitoplasts were pelleted through centrifugation to separate the IMS proteins into the supernatant (sup) fraction and membrane/ matrix proteins into the pellet (pel). In **Fig 3.6A** Mxr2 was predominantly found in the pellet fraction of the mitoplasts without proteinase K (PK) treatment suggesting that Mxr2 is predominantly found in either the inner membrane or the matrix. The 5% control lane suggests that less than 5% of imported Mxr2 was found in the supernatant, opposed to >5% in the pellet, suggesting that this protein can also be localised to the IMS. The band of Mxr2 found here in the supernatant fraction corresponds to the MW of the mature Mxr2 while all the precursor, intermediate and mature forms of Mxr2 were found in the pellet fraction. When the mitoplasts were treated with PK there was loss of Mxr2 in the supernatant which was expected as soluble IMS proteins are accessible to protease degradation in the mitoplasts. However, the Mxr2 in the pellet fraction of the mitoplasts was also degraded which would suggest over rupturing of the mitoplast inner membrane exposing the matrix proteins to the protease. Alternatively, if

Mxr2 was found embedded in the IMM then the enzyme would be susceptible to protease treatment.

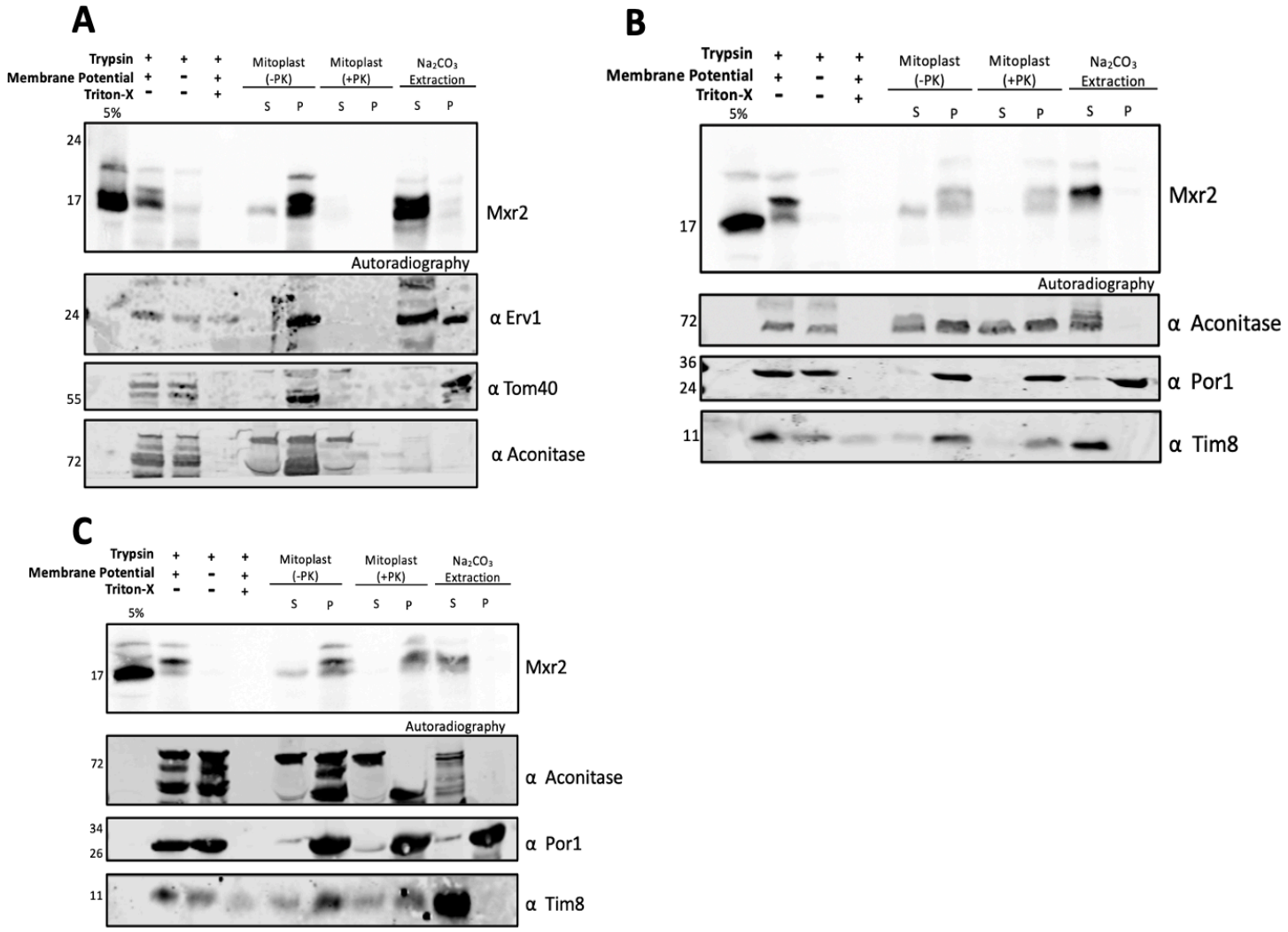


**Figure 3.6 Import and localisation of Mxr2 into WT Mitochondria.** Radiolabelled Mxr2 was imported into WT mitochondria for 15 minutes followed by addition of trypsin (0.1mg ml) treatment to remove any unimported material or Triton-X100 treatment (Tx) (10%) as a control to solubilise mitochondria. Osmotic shock was used to rupture the outer membrane and produce mitoplasts that consist of inner membrane and matrix proteins (P) and soluble IMS proteins (S). Proteinase K (PK) treatment (0.1mg/ ml) was used as a control for the mitoplasting. Sodium carbonate ($Na_2CO_3$) extraction was used to separate the soluble matrix/ IMS proteins (S) from the lipid associated & embedded proteins of the inner and outer mitochondrial membranes (P). Western blots to probe for matrix localised proteins (Acon), IMS proteins (Tim8/ Erv1) and membrane protein (Por1/ Tom40) were used. Samples were loaded on a 14% Tris-Tricine SDS gel. A, B and C were triplicate repeats of the localisation.

The mitoplasting was repeated a further two times and the same dual localisation of Mxr2 between predominantly the matrix/ inner membrane and a small fraction in the IMS was

observed **(Fig 3.6B/C)**. However, this time in the mitoplasts (+PK) pellet lanes Mxr2 was protected from protease degradation as the mitoplasts were not over ruptured and the inner membrane was still intact. This was confirmed by the western blot of Aconitase which demonstrated the protection of this matrix targeted protein in the presence of PK **(Fig 3.6 B/C)**. From the repeats of the Mitoplasting it can be concluded that all three forms of Mxr2 were mainly found in either the matrix or the inner membrane. Sodium carbonate extraction was carried out to further localise the protein between these two compartments. In addition, a small proportion of the mature Mxr2 was found dually localised into the soluble IMS fraction, providing the first evidence for a methionine sulfoxide reductase enzyme in the IMS.

Sodium carbonate ($Na_2CO_3$) extraction was used to further localise Mxr2 between the matrix and the inner membrane. Carbonate extraction (CE) separates soluble proteins from those either embedded or associated with a membrane through carbonate ions out competing the proteins for the lipids. Following the $Na_2CO_3$ extraction, the mitochondria were centrifuged to separate the soluble proteins (supernatant) from the membrane proteins (pel). Tom40 and Por1 controls were used for the CE to confirm these membrane proteins were only found in the pellet **(Fig 3.6A-C)**. In each of the three CE repeats Mxr2 was found in the supernatant fraction, implying it as a soluble protein not associated with a membrane **(Fig 3.6A-C)**. Taken alongside the Mitoplasting data, the Mxr2 that is found in the pellet of the mitoplasts seems to be localised entirely to the mitochondrial matrix. From the localisation studies it can be concluded that precursor and intermediate forms of Mxr2 are entirely localised to the mitochondrial matrix. Interestingly the mature form of Mxr2 is the only form becomes dually localised to both the IMS and the matrix. It is not clear what processing events result in this form of Mxr2 also becoming localised into the IMS. It was hypothesised that under conditions of stress, i.e generation of reactive oxygen species (ROS) there could be a loss of inner mitochondrial membrane potential that may prevent the translocation of Mxr2 across the membrane thereby trapping a portion of the protein inside the IMS. To test this Mxr2 was imported into mitochondria harvested from yeast cells acutely stressed with 1mM $H_2O_2$.

When Mxr2 was imported into WT mitochondria this time there was an appearance of a $4^{th}$ Mxr2 band termed intermediate 2 (i2) **(Fig 3.7)**. This was the only time this import pattern for Mxr2 was seen and it is unknown why this extra processed Mxr2 product appeared. Mxr2

was also successfully imported into the stressed mitochondria **(Fig 3.7)** however the intensity of the i2 band was less than that of the WT import. In addition, the intensity of the mature band was increased suggesting more Mxr2 was processed to its mature form in the $H_2O_2$ stressed mitochondria relative to the WT when subjected to import for the same length of

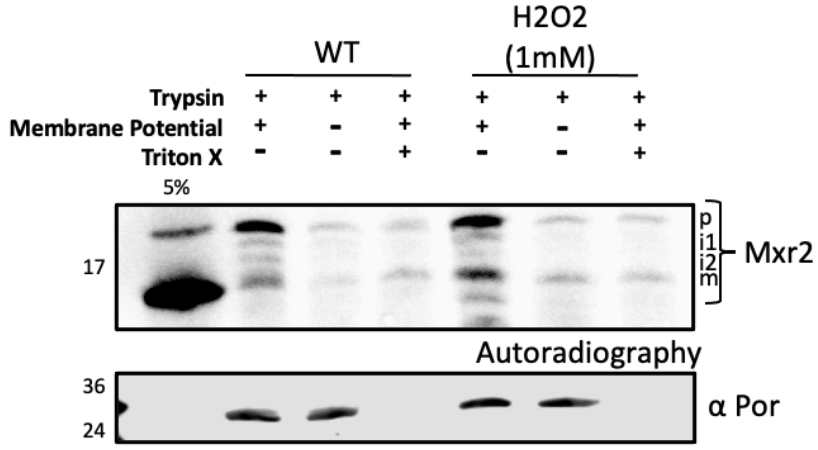


**Figure 3.7 Import of Mxr2 into WT and $H_2O_2$ stressed mitochondria.** Import of radiolabelled Mxr2 for 15 minutes into WT and $H_2O_2$ stressed mitochondria. Yeast cells were stressed with 1mM $H_2O_2$ overnight prior to isolation of mitochondria. Post import samples were treated with Trypsin (0.1mg/ml) and SBTI (1mg/ml) to remove any unimported material. Triton-X100 (Tx) (10%) was used as a control to solubilise mitochondria. 5% refers to 5% of radiolabelled protein presented for import as a positive control. Several forms of Mxr2 were detected via autoradiography referred to as precursor (p), intermediate 1 (i1), intermediate 2 (i2) and mature (m) Mxr2. Western blot of Porin 1 (Por1) was used as a loading control. Samples were run on 14% Tris-Tricine SDS gel.

time.

### 3.3.2 Mxr2 Import into Yeast Mitochondria Requires the Tom20 Import Receptor

With the import and localisation of Mxr2 in mitochondria now established the next aim was to determine which components of the protein import machinery were required. The online software Mitofates was used to analyse the sequence of WT Mxr2 and Δ1-33 Mxr2 for the presence of any mitochondrial targeting sequence regions or peptidase cleavage sites (Fukasawa *et al.*, 2015). It was discovered that WT Mxr2 had a TOM20 recognition motif at residues 3-7 and matrix processing peptidase (MPP) cleavage site at residue 8 **(Fig 3.3B)**. As discussed in section 1.2.1 Tom20 is a receptor component of the TOM complex at the outer membrane exposed to the cytosol. It is involved in the recognition of preproteins containing a mitochondrial targeting sequence destined for import into this organelle through the matrix targeting pathway. The prediction of this Tom20 recognition motif is in line with the

localisation data in **Fig 3.6** that Mxr2 is predominantly localised to the mitochondrial matrix. To test if Tom20 was required a knockout yeast strain of Tom20 was cultured and the mitochondria harvested.

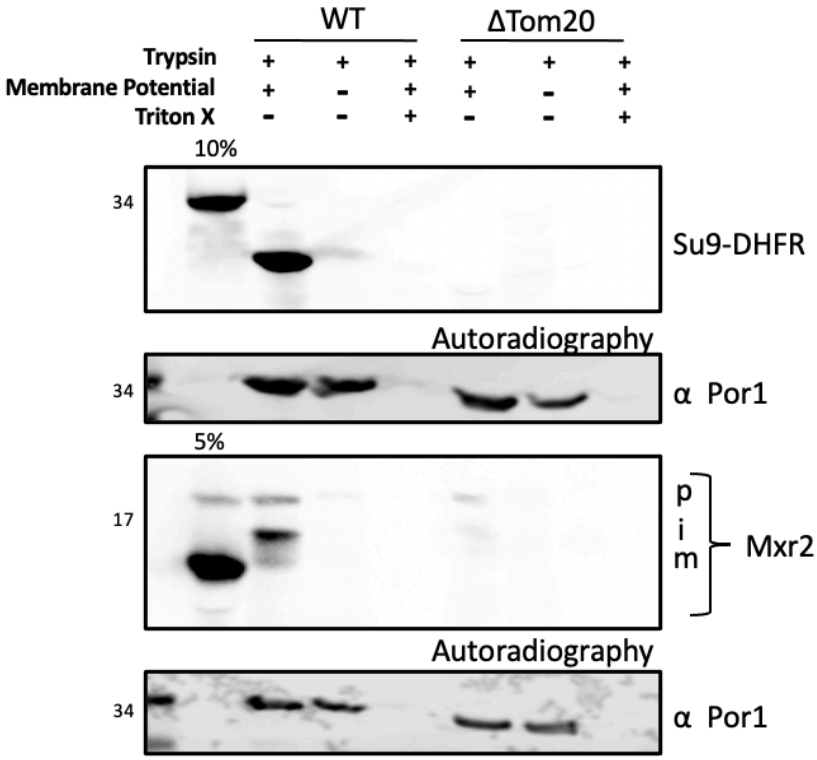


**Figure 3.8 Import of Su9-DHFR and Mxr2 into WT and ΔTom20 mitochondria.** Radiolabelled Su9-DHFR and Mxr2 were imported into WT and ΔTom20 mitochondria for 15 minutes. Samples were treated with Trypsin (0.1mg/ml) and SBTI (1mg/ml) post import to remove any unimported material. Triton-X100 (Tx) (10%) was used as a control to solubilise the mitochondria. 10% and 5% refers to the % of radiolabelled Su9-DHFR and Mxr2 respectively presented for import loaded as a control. Three forms of Mxr2 were detected: precursor (p), intermediate (i) and mature (m). Western blotting of Porin 1 used as a loading control. Samples were loaded on a 14% Tris-Tricine SDS gel.

To determine if knockout of Tom20 (ΔTom20) in the mitochondria was successful of the import of a Su9-DHFR construct was tested. Su9-DHFR is a well-characterised import protein that is localised to the matrix and requires the presence of Tom20 receptor (Yamamoto *et al.*, 2011). In WT mitochondria the Su9-DHFR construct is imported in the presence of a membrane potential and the protein runs at a lower molecular weight relative to the 10% control as it undergoes a cleavage processing event to generate the mature protein inside the organelle **(Fig 3.8)**. When Su9-DHFR is presented to the ΔTom20 for import all protein is subject to trypsin degradation as the protein is no longer imported into the organelle in the absence of the receptor. While there was a slight error in the Por1 loading control, with less

ΔTom20 mitochondria loaded relative to the WT, the difference was not strong enough to account for the total loss of Su9-DHFR import. From this control it was concluded that the mitochondria were deficient in the Tom20 receptor.

When Mxr2 was presented for import to the ΔTom20 cell line there was a substantial loss of import of the protein relative to the WT mitochondria. A small portion of precursor (p) Mxr2 can be seen in the ΔTom20 but the levels of intermediate (i) and mature (m) protein are significantly reduced (Fig 3.8). This finding aligns with the sequence prediction data **(Fig 3.3B)** that Mxr2 contains a Tom20 recognition motif and confirms that the import of Mxr2 is dependent on the presence of Tom20 in the outer membrane and further suggests that Mxr2 follows the classic matrix targeting pathway.

### 3.3.3 Presence of Mia40 is Required for Efficient Mitochondrial Import of Mxr2

Further sequence analysis found that Mxr2 contains several conserved cysteine residues including a redox active disulphide bond between Cys97 and Cys157 (Allu *et al.*, 2015). These cysteines form the active site and resolving cysteine of Mxr2 respectively. Due to the presence of these conserved residues, it was hypothesised that they may be involved in the import of the IMS-localised fraction of Mxr2 through the mitochondrial import and assembly (MIA) pathway with the cysteines being involved in disulphide bond formation that trap the protein in the IMS through interaction with Mia40. To test for this yeast cell lines knocked down in Mia40 were generated under the gal promoter and the mitochondria were isolated. The import of Mxr2 was tested into these mitochondria.

To ensure that the GalMia40 mitochondria were devoid of Mia40 two controls were employed. First the small Tim chaperone Tim9, a known substrate of the MIA pathway was imported into these mitochondria. When imported into the GalMia mitochondria Tim9 displayed a severe import defect relative to the Wild-Type mitochondria **(Fig 3.9A).** Probing for Mia40 via western blot also confirmed the loss of this protein in the mitochondria. This result demonstrated that Mia40 was absent from the mitochondria, and this resulted in a defect in import of a known substrates of the MIA pathway.

Interestingly Mxr2 displayed an import defect with less precursor being imported into the GalMia mitochondria relative to the WT mitos **(Fig 3.9B)**. Por1 loading control suggests that

there was unequal loading of mitochondria, with more GalMia mitos loaded in this experiment but despite these levels of imported Mxr2 were still less than those in the WT. Western blot of Mia40 again confirmed the knockdown of this protein.

Lastly the import of the matrix-targeted Su9-DHFR construct was imported into the GalMia as a control to ensure that loss of Mia40 did not affect any non-MIA substrate import pathways. Import of Su9-DHFR appeared to be relatively consistent between the WT and GalMIa40 mitochondria **(Fig 3.9C)**. There might be a slight decrease in import in the GalMia mitochondria but certainly not to the extent of loss of Mxr2 import capacity. The results in **Fig 3.9** suggest that in the absence of Mia40, Mxr2 is much less efficiently imported. This is an intriguing result as there are not many characterised substrates that interact with Mia40 which are ultimately targeted to the mitochondrial matrix. It is not clear from this result however if this is a direct effect of losing a possible interaction with Mia40 for import or a downstream effect from loss of Mia40 impacting the import of proteins dependent on the MIA pathway and further experimental evidence is needed to characterise this.

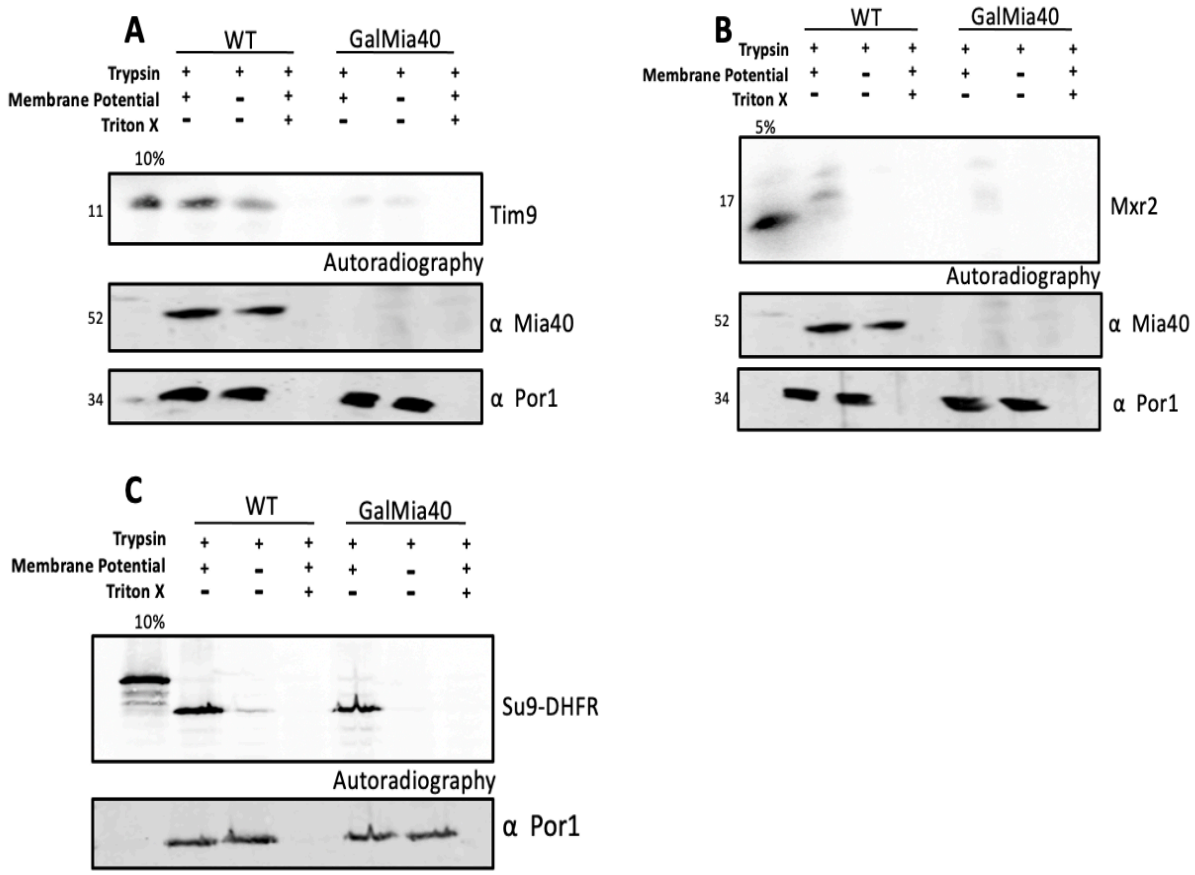


**Figure 3.9 Import of Tim9, Mxr2 and Su9-DHFR into WT and GalMia40 mitochondria.** Radiolabelled Tim9 (A), Mxr2 (B) and Su9-DHFR (C) were imported into WT and GalMia40 mitochondria for 15 minutes. Samples were treated with Trypsin (0.1mg/ml) and SBTI (1mg/ml) post import to remove and unimported material. Triton-X100 (Tx) (10%) was used as a control to solubilise the mitochondria. 10% and 5% refer to the % of radiolabelled Tim9/ Su9-DHFR and Mxr2 respectively presented to each import reaction. Western blotting of Mia40 was used to confirm knockdown of Mia40 in the GalMia40 mitochondria and Por1 blots used to confirm equal lading. Samples were loaded on a 14% Tris-Tricine SDS gel.

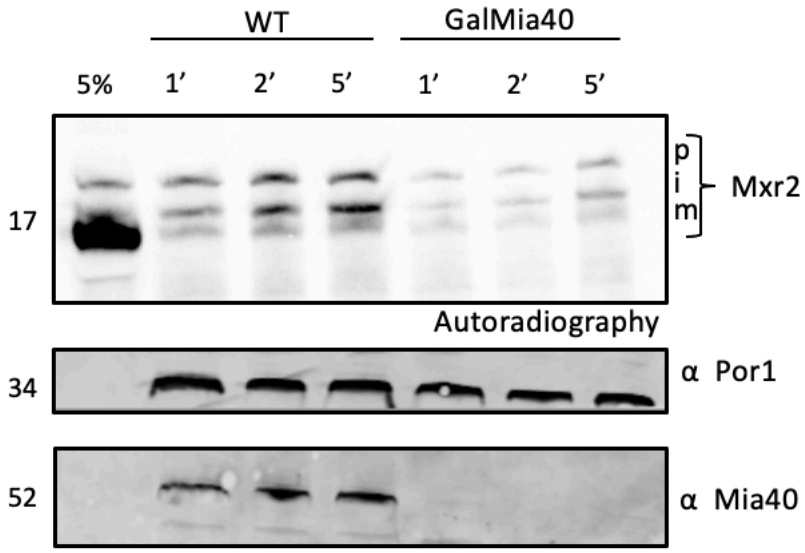


**Figure 3.10 Import kinetics of Mxr2 into WT and GalMia40 mitochondria.** Import of radiolabelled Mxr2 precursor into WT and GalMia40 yeast mitochondria at different specified timepoints. All samples were treated with Trypsin (0.1mg/ml) and SBTI (1mg/ml). 5% represents radiolabelled protein presented to the mitochondria loaded as a positive control. Radioactivity was detected using a phosphoimager. Western blot of and Porin 1 (Por1) was as loading control while Mia40 western blot used to confirm its knockdown in the GalMia40 yeast strain. Samples were loaded on a 14% Tris-Tricine SDS gel.

Mxr2 was imported into WT and GalMia mitochondria at three different timepoints of 1, 2 and 5 minutes to determine the kinetics of import **(Fig 3.10)**. At each timepoint the level of imported protein was substantially reduced in the GalMia mitochondria relative to the WT control, further confirming a defect in the import of Mxr2 when Mia40 is absent (confirmed by western blotting). Inside the GalMia mitochondria, precursor, intermediate and mature Mxr2 were all detected suggesting that processing of Mxr2 can still occur in the absence of Mia40. As it was hypothesised that Mia40 was involved in the trapping of Mia40 in the IMS, the import kinetics was followed on with a localisation study. It was predicted that in the GalMia mitochondria Mxr2 would no longer be present in the IMS soluble fraction.

The import and localisation of Mxr2 into GalMia40 mitochondria revealed a very weak import of the protein relative to the 5% control sample loaded, providing further evidence of the reduced import of this protein in the absence of Mia40 **(Fig 3.11)**. Mitoplasting revealed the presence of a band of Mxr2 in the supernatant (-PK) sample that was removed once the protease was added suggesting that a fraction of the Mxr2 had once again localised to the

IMS even in the absence of Mia40. The rest of the protein was found not associated with a membrane from the results of the carbonate extraction, and therefore was found in the matrix when pelleted from the mitoplasts. From this it can be concluded that the loss of Mia40 in mitochondria results in a substantial defect in the ability of Mxr2 to import into the mitochondria over several timepoints. However, it does not change the localisation of the protein within the organelle as the fraction of Mxr2 that is found in the IMS can still be detected in the GalMia mitochondria, albeit to a lesser extent.

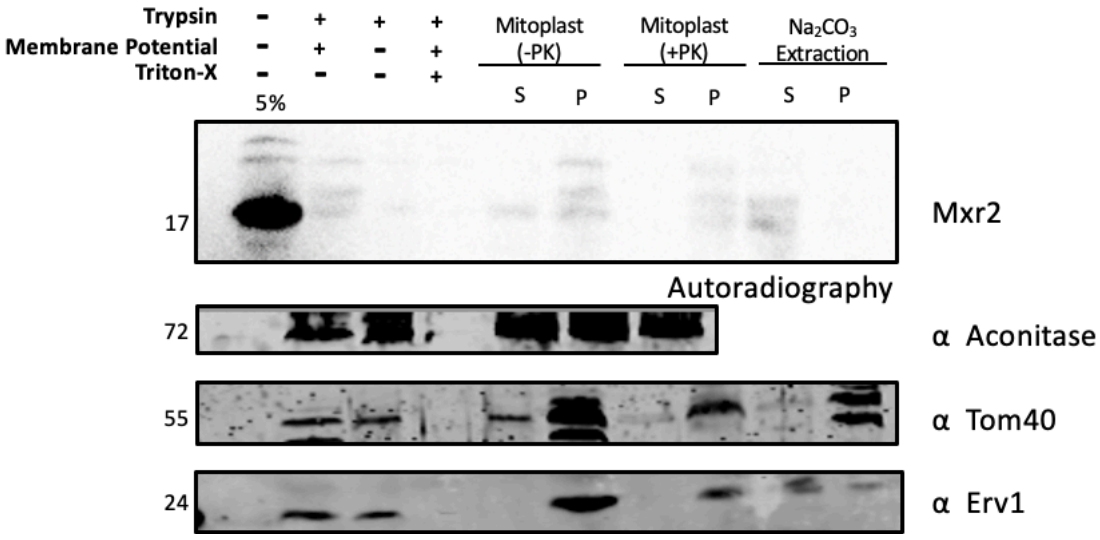


**Figure 3.11 Import and localisation of Mxr2 into GalMia40 Mitochondria.** Radiolabelled Mxr2 was imported into GalMia40 mitochondria for 15 minutes followed by trypsin (0.1mg ml) treatment to remove anu unimported material or Triton-X100 treatment (Tx) (10%) as a control to solubilise mitochondria. Osmotic shock was used to rupture the outer membrane and produce mitoplasts that consist of inner membrane and matrix proteins (P) and soluble IMS proteins (S). Proteinase K (PK) treatment (0.1mg/ ml) was used as a control for the mitoplasting. Sodium carbonate ($Na_2CO_3$) extraction was used to separate the soluble matrix/ IMS proteins (S) from the lipid associated & embedded proteins of the inner and outer mitochondrial membranes (P). Western blots to probe for matrix localised proteins (Acon), IMS proteins (Erv1) and membrane proteins (Tom40) were used. Samples were loaded on a 14% Tris-Tricine SDS gel.

## 3.4 Discussion

Previous studies on Mxr2 had characterised this reductase enzyme as a mitochondrial targeted protein believed to be localised to the mitochondrial matrix (Allu *et al.*, 2015). However, little was known about the components of the import machinery required for import, how the protein crossed the OM and IM and how Mxr2 is processed in the mitochondria into its mature form. In this chapter these unknowns were addressed and novel findings on the import mechanism of Mxr2 into the mitochondria were discovered.

### 3.4.1 Mxr2 is imported into the mitochondria as a precursor and undergoes several processing events to generate the mature protein

The import assay in **Fig 3.2** confirmed previous findings that Mxr1 was a cytoplasmic protein and was unable to be imported into isolated yeast mitochondria (Kaya *et al.*, 2010a), while Mxr2 was able to successfully import. An import kinetic study demonstrated that Mxr2 showed quick kinetics for import and could be imported in as fast as 30 seconds **(Fig 3.4)**. This assay also provided the first evidence showing the processing of Mxr2 into two smaller MW products upon import lending credence to the idea that Mxr2 is imported into the mitochondria as a precursor protein and once inside the mitochondria becomes cleaved into its mature form. The exact mechanism and possible proteases involved in this processing are yet unknown. The sequence analysis in **Fig 3.3** based on mitofates software revealed a predicted matrix processing peptidase (MPP) cleavage site near the N-terminus of the protein suggesting that Mxr2 possesses an N-terminal presequence region (Fukasawa *et al.*, 2015). These presequence regions are involved with targeting proteins to the mitochondrial matrix, which subsequent assays have demonstrated Mxr2 to become targeted to **(Fig 3.6)**. Once in the matrix Mxr2 may interact with MPP to cleave this N-terminal presequence resulting in the mature Mxr2 protein. To test this a knockdown strain of mitochondria could be generated devoid of MPP. As MPP is an essential protein a knockout strain would not be viable. Mxr2 could then be imported into these mitochondria to determine if the precursor protein no longer becomes proteolytically processed. However, this would only account for one processed form of Mxr2 found upon import and does not explain why precursor Mxr2 undergoes two processing events.

It is hypothesised that Mxr2 is cleaved into an intermediate form before undergoing a final processing event to generate the mature protein, however this has not been demonstrated experimentally and it is equally possible that these are two distinct processing events to produce two unique sub populations of Mxr2, both of which are in themselves in their mature form. There are numerous proteases in the mitochondria that could give rise to the mature protein such as inner membrane peptidase (IMP) complex, or the octapeptidyl aminopeptidase 1 (Oct1). As before knockdown strains devoid of these proteases could be created and the import tested to determine if Mxr2 no longer becomes processed to indicate if these peptidases are involved in proteolytic cleavage of Mxr2 inside the mitochondria.

A recent study on the yeast peroxiredoxin Prx1 has highlighted how proteolytic cleavage by two different proteases controls the localisation of this protein to different sub-compartments of the mitochondria. Prx1 is a mitochondrial localised, cysteine contain peroxiredoxin involved in catalysing the reduction of endogenously generated $H_2O_2$ (Cox, Winterbourn and Hampton, 2010). Prx1 precursor protein is released into the lipid bilayer and is subsequently cleaved by the IMP protease releasing the soluble protein into the IMS (Gomes *et al.*, 2017). Interestingly Prx1 was also found to be localised to the mitochondrial matrix and during its import becomes sequentially cleaved by MPP and Oct1 to generate the mature Prx1. This demonstrates how differential cleavage of Prx1 can control the localisation of the protein into distinct mitochondrial compartments, possibly to contribute to redox processes in different regions of the organelle. Characterising the interaction of Mxr2 with these different proteases could account for the various processed forms of Mxr2 seen in the import assay.

When Mxr2 was imported into the mammalian mitochondrial system **(Fig 3.5)** the intermediate fraction of Mxr2 did not appear suggesting that the protein was unable to be processed inside the mammalian isolated mitochondria. This could suggest that either the protease is only present in yeast cells or the homology of the enzyme between yeast and mammals is not well conserved and thus the protease was not able to recognise the yeast Mxr2 sequence. Or it could be that the human Mxr2 homologue undergoes a different maturation pathway compared to the yeast enzyme.

### 3.4.2 Mxr2 is a dually localised IMS and matrix mitochondrial protein in yeast mitochondria

As discussed before, previous mitoplasting studies suggested that Mxr2 was localised to the mitochondrial matrix (Allu *et al.*, 2015). The finding that this is the sole methionine reductase enzyme found in yeast mitochondria only localised to the matrix has the consequence that Met-O groups can only be reduced in this compartment. But it is known that Met-O can also occur in the IMS, and proteins such as Erv1 have been demonstrated through mass spec to become modified (Lionaki *et al.*, 2010). Therefore, this created a conundrum of how Met-O groups would be reduced in this compartment Through triplicate repeats of the mitoplasting and CE experiments with appropriate controls of levels of membrane, IMS and matrix proteins it is now established that while the majority of Mxr2 is localised to the mitochondrial matrix, a small subset is also found in the soluble IMS **(Fig 3.6)**. This provides the first evidence of a methionine sulfoxide reductase enzyme inside this compartment of yeast mitochondria. Though it does introduce new questions and queries about the regulation of localisation of Mxr2 between these two compartments.

Another mitochondrial protein recently discovered to have a dual localisation within this organelle is Apurinic/Apyrimidinic Endonuclease 1 (APE1), a protein that plays a key role in the base excision repair (BER) pathway. The BER pathway is responsible for repairing non-helix distorting base lesions in mtDNA that becomes damaged through oxidative stress condition (Prakash and Doublié, 2015). This study uncovered that while APE1 is normally found in the IMS, under conditions of increased oxidative stress this protein became translocated to the mitochondrial matrix through the TIM23/ PAM complex where it can interact with the mtDNA (Barchiesi *et al.*, 2020). One hypothesis is that Mxr2 may be regulated in a similar mechanism, where increases in oxidative stress conditions (which could in turn lead to increased Met-O) could trigger the translocation of this protein into a different compartment.

The import of Mxr2 into WT and stressed mitochondria was tested to confirm this hypothesis of stress conditions being involved in modifying the localisation of Mxr2 in the mitochondria. The import intriguingly revealed the presence of a second intermediate Mxr2 band **(Fig 3.7)** when imported into WT mitochondria but appeared to disappear when the mitochondria

were isolated from $H_2O_2$ induced oxidatively stressed cells. As this was the only import where this Mxr2 band was seen it is unknown if it is an artifact or a genuine result. The SDS PAGE gel may have been run at a lower voltage for longer allowing greater separation and resolution of the bands. However, the isolation of mitochondria from oxidatively stressed cells did not negatively affect the import of precursor Mxr2, or its processing into intermediate or mature Mxr2. It would be interesting to follow this up with a localisation study within the stressed mitochondria to confirm protein is still found in both compartments. It is also possible that the addition of $H_2O_2$ did not represent accurately stressed conditions in vivo.

### 3.4.3 Import of Mxr2 is dependent on the Tom20 receptor and the presence of Mia40

At the onset of this project there was little information in the literature detailing the components of the mitochondrial protein import machinery required for translocation of Mxr2 into the mitochondria. Sequence analysis of Mxr2 **(Fig 3.3)** gave the first indication that Mxr2 appeared to possess a Tom20 recognition motif and through studies with ΔTom20 mitochondria this receptor was confirmed to be essential for the import of Mxr2 **(Fig 3.)**. Another method to test the involvement of the Tom20 receptor in the import of Mxr2 would be to mutagenize the putative Tom20 binding motif and test the import of Mxr2 in the presence of Tom20. If this binding motif is recognised by Tom20 then mutagenesis of this region should prevent the binding to the receptor and diminish the import capacity. As such, interaction with this receptor would in turn suggest that Mxr2 enters the mitochondria through the Tom40 translocation pore that forms part of the TOM complex with Tom20. This could be followed up by harvesting Tom40 temperature sensitive (ts) mitochondria, as Tom40 is itself essential and testing for the reduction of Mxr2 import in the absence of the translocation pore.

Once in the IMS however it has been not characterised how the protein is further translocated into the matrix through the inner membrane. Most matrix targeted proteins that are imported through recognition of Tom20 receptor pass through the TIM23 translocase embedded in the IM.

There are two conformations of the TIM23 translocase machinery termed $TIM23_{PAM}$ and $TIM23_{SORT}$ that promote release into the matrix and IMS respectively as detailed in section 1.2.2. The passage of Mxr2 through this translocase could account for the dual localisation demonstrated, where depending on the conformation of TIM23 promotes either matrix or IMS import. Mitofates sequence analysis suggests the presence of a max positively charged amphiphilic region in Mxr2 that may potentially arrest in the lipid bilayer(Fukasawa *et al.*, 2015). This mechanism of translocation through the different conformations of the TIM23 complex may account for how Mxr2 is localised into the IMS though further studies including the use of knockout components of the TIM23 complex are required to test this hypothesis.

### 3.4.4 The Role of Mia40 in the Import of Mxr2

The results in **Fig 3.9-3.11** demonstrate that import of Mxr2 is substantially reduced in the absence of Mia40. Import was demonstrated to be diminished using import studies, kinetics of import and localisation studies. However, it is unclear the mechanism that results in decreased import of Mxr2 whether Mxr2 directly interacts with Mia40 or if there are downstream effects of loss of Mia40. One method to test for a direct interaction could be to use a small molecule inhibitor of Mia40, such as the ITS peptide. The peptide binds directly to Mia40 inhibiting it. Supplementing WT mitochondria with this inhibitor prior to import of Mxr2 could provide a direct mechanism to test if Mia40 is directly involved. Alternatively, the GalMia mitochondria could be supplemented with Mia40 to determine if this rescues the import capacity of Mxr2. To test for an interaction a Co-immunoprecipitation assay could be carried out to determine if radiolabelled Mxr2 is detected when precipitating Mia40 using anti-Mia40 antibodies. In addition, mutants construct of Mxr2 could be created mutating individual cysteines in the sequence to alanine residues and testing the import of Mxr2 in the presence/ absence of Mia40. It is likely that if there is an interaction this would be cysteine dependent. The localisation study in **Fig 3.11** suggests that even in the absence of Mia40, Mxr2 can still be found in the IMS. From this it is believed that the protein does not rely on disulphide folding for import and while Mia40 plays a role in the import but not via the default oxidatively import pathway. These findings provide an intriguing result that implies the presence of Mia40 is required for the import of a protein that is not localised to the IMS.

### 3.4.5 Conclusions and Future Work

In conclusion the results in this chapter demonstrate that despite previous studies Mxr2 is a mitochondrial protein targeted to both the IMS and the matrix. Import of Mxr2 is dependent on the presence of a membrane potential and the protein appears to be imported as a precursor protein. Once inside the organelle the protein appears to undergo two processing events to generate an intermediate and a mature form of Mxr2. Sequence analysis predicted import was dependent on interaction with the Tom20 import receptor on the outer membrane and this was confirmed biochemically with the use of ΔTom20 isolated mitochondria. The most striking finding however was that in the absence of Mia40, the import capacity of Mxr2 was substantially impaired. Reduced import was found for the Mxr2 protein localised to not only the IMS, but also impacted the protein normally targeted to the mitochondrial matrix. While this chapter does not provide a full overview of the exact mechanism by which Mxr2 becomes imported, it does provide some novel research on the components of the import machinery involved.

Future work should focus on further elucidating the components of the import machinery involved in the import of Mxr2, particularly the TIM23 complex and its different conformations. Characterising the processing events of Mxr2 once inside mitochondria through the use cell lines that have become knocked out of specific proteases may also reveal how this protein becomes dually localised. Lastly more studies are required to determine if the loss of Mxr2 import in the absence of Mia40 is through loss of a direct interaction or indirect effects. If Mia40 is in fact directly involved in the import of Mxr2, in both the IMS and the matrix this would provide some of the first evidence implicating Mia40 as being an important import component required for the translocation of matrix targeted proteins.

# Chapter 4: The Effects of Loss of Methionine Sulfoxide Reductase 2 (Mxr2) on Yeast Cells and Isolated Mitochondria

## 4.1 Introduction

Aside from the general reductase activity of Mxr2 inside the mitochondria, very little is understood about specific substrates of this enzyme, or the effects loss of this reductase enzyme has on the mitochondria. Yeast two-hybrid system analysis revealed that Mxr2 interacts with the OM protein Uth1, that plays a role in mitochondrial biogenesis and induction of autophagy (Bandara *et al.*, 1998; Camougrand *et al.*, 2003; Kiššová *et al.*, 2004). Despite this no biochemical or biophysical interaction between the two proteins have been characterised.

Previous studies with mitochondria isolated from cells devoid of either Mxr1, Mxr2 or a double mutant revealed that the cells displayed a growth defect when cultured in the presence of the respiratory substrates lactate and ethanol (Kaya et al., 2010). A subsequent flow cytometry analysis of these mutant cell lines revealed that in the absence of the Mxr enzymes levels of respiration competent mitochondria were substantially reduced especially for the double mutant and ΔMxr1 strains. Levels of cytochrome C were also found to be reduced in these mitochondria, but only at the protein level and not at level of RNA expression as determined through cDNA microarray analysis.

Oxidative stress is linked to the process of programmed cell death (apoptosis) through the release of cytochrome C (Cyt C) from the mitochondria into the cytosol. Cyt C itself has a highly conserved methionine residue involved in both coordinating the haem iron and redox regulation of the protein (Ivanetich, Bradshaw and Kaminsky, 1976; Feinberg, Bedore and Ferguson-Miller, 1986). This Met residue is a target for oxidation by ROS and the oxidised form was demonstrated to be compromised in electron transfer capability. Cyt C is involved

in shuttling electrons from CIII to CIV in yeast mitochondria (Zara, Conte and Trumpower, 2009). The current data in the literature suggests that Cyt C is susceptible to oxidation, particularly in the absence of Mxr enzymes in the mitochondria (Feinberg et al., 1986; Kaya et al., 2010). This has the potential to result in mitochondrial dysfunction and impairment of the electron transport chain due to a deficit of electron shuttling by Cyt C in its oxidised state which cannot be reduced in the absence of Mxr enzymes.

More recently Mxr2 has been implicated in the regulation of protein import due to evidence demonstrating that Mge1 is a physiological substrate of this reductase enzyme. Preproteins destined for the mitochondrial matrix pass through the TIM23 complex as discussed in section 1.2.2. As the preprotein emerges from the translocation pore it binds Tim44 and mtHsp70 in an ATP dependent manner (D'Silva *et al.*, 2004). mtHsp70 forms part of the translocation motor that also consists of the Pam16 and Pam18 subunits alongside the nucleotide exchange factor Mge1 (Stojanovski, Pfanner and Wiedemann, 2007; Schiller *et al.*, 2008). ATP hydrolysis on Hsp70 results in formation of an ADP-Hsp70 complex which displays high affinity for incoming precursor proteins. The Mge1 subunit is a nucleotide exchange factor and when in its active dimeric form replaces ADP for ATP on Hsp70. This in turn leads to the release of the precursor protein from this complex (Mayer and Bukau, 2005).

Mge1 is responsive to oxidative stress. Under these conditions the protein is in a monomeric form and is therefore unable to interact with the ADP-Hsp70 complex with the consequence of stalling protein import into the matrix. The oxidative sensor function of this protein has been pinpointed to a specific Met155 residue (Marada *et al.*, 2013). Studies involving mutagenizing this Met to Leucine (Leu) halted the proteins' ability to respond to oxidative stress. In vivo and in vitro studies have recently demonstrated that Mxr2 can interact with the oxidised form of Mge1 and reduce this sulfoxide modification thereby promoting dimerisation of Mge1 and therefore subsequent protein import (Allu *et al.*, 2015). This demonstrates how reversible regulation of an oxidised Met residue in Mge1 through the action of Mxr2 allows the mitochondria to respond to oxidative stress to control protein import into the mitochondrial matrix **(Fig 4.1)**.

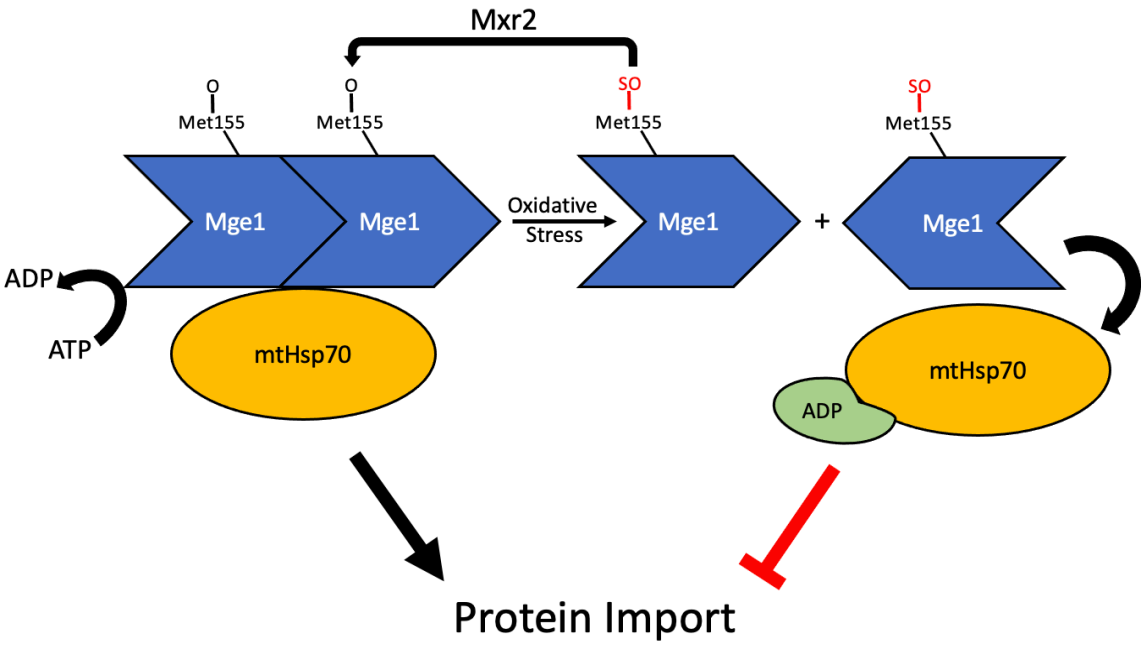


**Figure 4.1: Redox regulation of Mge1 controls protein import.** Dimeric Mge1 acts as a nucleotide exchange factor to replace ADP with ATP on mitochondrial Hsp70 (mtHsp70) The methionine 155 (Met155) residue of the Mge1 protein is susceptible to oxidation in response to oxidative stress conditions. The resulting methionine sulfoxidation (Met-SO) of Mge1 results in the monomerization of the protein thus preventing interaction with the ADP-mtHsp70 complex and stalling protein import. The reductase enzyme methionine sulfoxide reductase 2 (Mxr2) can reduce Met-SO in Mge1 groups back to Met-O. This in turn allows dimerisation of Mge1 promoting protein import.

The focus of this chapter was to build upon the limited studies in the literature to further investigate the function of Mxr2 in the mitochondria, primarily using a ΔMxr2 yeast strain.

## 4.2 Aims

The overarching aim of this chapter was to investigate how loss of Mxr2 in the mitochondria imparted phenotypic changes at the level of the whole cell and isolated mitochondria. Research primarily focused on expanding upon previous data including how mitochondria devoid of Mxr2 could tolerate oxidative stress and measuring the oxygen consumption rates and respiratory capacity of these mitochondria. As Met-O is a harmful modification an aim was devised to determine how loss of Mxr2 may affect the steady state levels of essential mitochondrial proteins. From these findings a new aim was established to further characterise how loss of Mxr2 resulted in a defect in the steady state levels of the small Tim proteins in isolated mitochondria.

## 4.3 Results

### 4.3.1 Tolerance to Oxidative Stress and Protein Steady State Levels in the Absence of Mxr2

Yeast strains devoid of ΔMxr1 and ΔMxr2, that encode the cytosolic and matrix localised methionine reductase enzymes respectively, alongside the parental WT BY4751 strain were cultured overnight in YPD media. $OD_{600}$ was measured and the cultured yeast diluted in $ddH_2O$ to an OD of 0.1 and further diluted to produce 1:10 serial dilutions between 0.1 – 0.0001 OD. These dilutions were spotted on YPD and YP lac plates and grown for 48 hours. The cells grown on YP lac rely on lactate as an energy source that can only be utilised through cellular respiration and electron transfer through the ETC complexes. Thus, cell growth on this media is dependent on functional mitochondria. ATP can be produced through glycolysis on YPD media so there is less reliance on functional mitochondria for cellular growth.

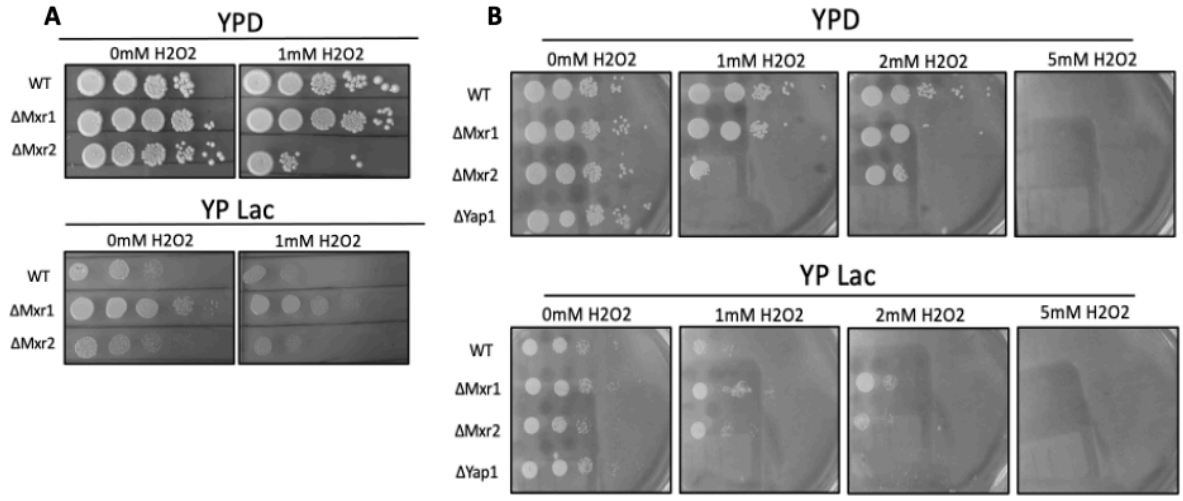


**Figure 4.2: Yeast cell lines devoid of Mxr2 display growth defects.** (A) Spot assay of WT, ΔMxr1 and ΔMxr2 yeast cells cultured on glucose (YPD) or lactate containing medium in the presence or absence of 1mM $H_2O_2$ to induce oxidative stress conditions. (B) Spot assay was repeated incorporating a ΔYap1 strain and using a titration of $H_2O_2$ of 0, 1, 2 and 5mM $H_2O_2$.

The results of the spot assay in **Fig 4.2A** demonstrated that WT and ΔMxr1 cells display similar growth patterns on YPD media in the presence or absence of $H_2O_2$. The ΔMxr2 cells however display a severe growth defect in the presence of 1mM $H_2O_2$ on YPD suggesting that these cells are less capable of tolerating oxidative stress conditions. The WT cells did not grow as

well on YPlac media and this was further stunted in the presence of $H_2O_2$. ΔMxr1 cells displayed a similar growth pattern on both YPD and YPlac media irrespective of oxidative stress conditions. The ΔMxr2 strain grew worse on YPlac media but was able to tolerate oxidative stress conditions better when the cells were forced to rely on mitochondria for respiration and energy production. It is unclear why these ΔMxr2 mitochondria tolerate the oxidative better on YPlac media when functional mitochondria are essential for cell growth and survival using this lactate as a substrate for energy production compared to YPD media. The spot assay was repeated, this time incorporating a ΔYap1 control and a titration of [$H_2O_2$].

Yap1 is a transcription factor involved in regulating an antioxidant response in response to increased levels of hydrogen peroxide (Delaunay, Isnard and Toledano, 2000). The ΔYap1 strain was incorporated as a control to ensure $H_2O_2$ was added and active in the media. In the absence of Yap1 the cells cannot produce an antioxidant response to tolerate the stress conditions. A titration of $H_2O_2$ concentrations was used to provide more information on how levels of this oxidative stressor affected yeast cell growth in the absence of the Mxr enzymes. While the ΔYap1 strain grew similar to the WT on YPD, in the presence of 1, 2 and 5mM $H_2O_2$ growth was totally abolished **(Fig 4.2B)**. This confirmed that the $H_2O_2$ was active and present in the agar media. WT cells were able to tolerate 1mM and 2mM $H_2O_2$ but at 5mM concentration growth was abolished. At 5mM the hydrogen peroxide kills the cells while at lower concentrations acts as a stressor but does not kill the cells The growth of ΔMxr1 and ΔMxr2 yeast cells was comparable to the WT strain in the absence of $H_2O_2$. However, in the presence of 1mM $H_2O_2$ the ΔMxr2 yeast cells displayed a severe growth defect similar to that seen in **Fig 4.2A**. At 2mM $H_2O_2$ the ΔMxr1 and ΔMxr2 yeast cells both displayed a growth defect though surprisingly the ΔMxr2 grew slightly better than in 1mM $H_2O_2$ but worse than in the absence of $H_2O_2$. This severe growth defect of ΔMxr2 was replicable in both **Fig 4.2A/B**.

On YPLac media all strains showed similar levels of growth in the absence of $H_2O_2$. In the presence of 1mM $H_2O_2$ WT and ΔMxr2 cells displayed a similar growth defect whereas ΔMxr1 appeared to tolerate the stress conditions better. This suggests that loss of Mxr2 in the mitochondria did not induce a cumulative defect on growth of yeast cells on oxidatively stressed conditions. As ΔMxr1 grew better than WT it suggests that loss of this protein may in fact provide a protective effect to the mitochondria. It was hypothesised that when levels

of ROS increase, there is an increase in methionine sulfoxidation of proteins within the mitochondria. As this is a harmful modification it is predicted this would lead to enhanced protein degradation and therefore reduced cellular viability, demonstrated through impaired cellular growth. To test this hypothesis the isolated mitochondria were resuspended in 2X Laemmli buffer and the proteins separated via SDS PAGE. Specific proteins were probed for via western blotting to determine the steady state levels in WT and knockout mitochondrial strains.

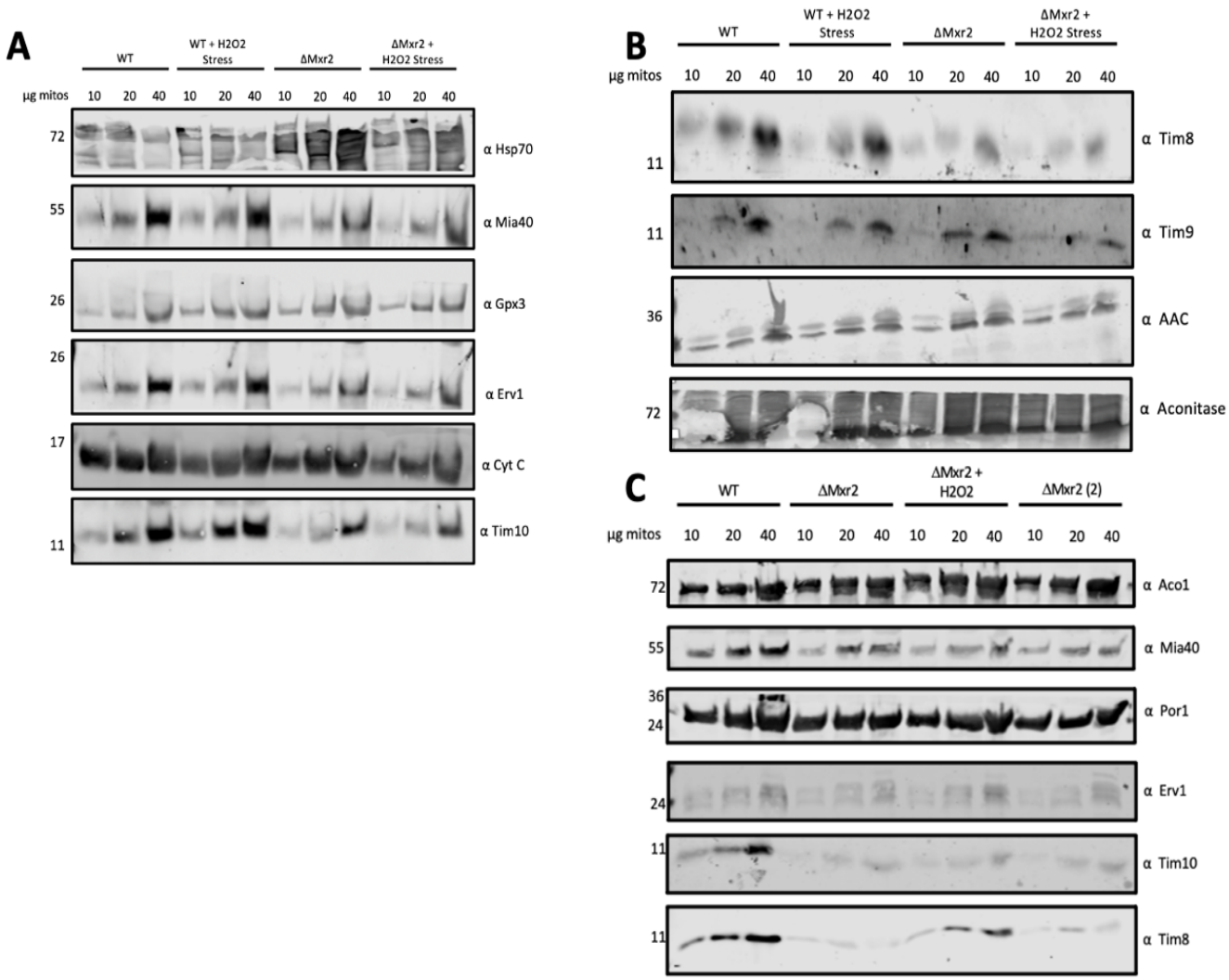


**Figure 4.3: Analysis of protein steady state levels in the ΔMxr2 isolated mitochondria.** WT and ΔMxr2 mitochondria were isolated from yeast cells and proteins separated through SDS PAGE. Western blotting was used to probe for differences in protein levels. (A) WT and ΔMxr2 were isolated from unstressed and stressed (1mM $H_2O_2$) yeast cells. Western blotting probed for mitochondrial Hsp70 (Hsp70), Mia40, Gpx3, Erv1 and Cyt C. (B) Steady state assay was repeated using the same mitochondrial strains as (A) instead probing for Tim8, Erv1 and AAC. (C) A second preparation of ΔMxr2 mitochondria were isolated termed ΔMxr2 (2) to have an independent repeat of the protein steady state levels

Initially steady state levels of several mitochondrial proteins were compared between WT and ΔMxr2 mitochondria with corresponding $H_2O_2$ stressed mitochondria. Steady state levels of Hsp70 were probed as a loading control and results suggest that higher levels of the ΔMxr2 mitochondria had been loaded **(Fig 4.3A)**. Alternatively it is possible that in response to deletion of Mxr2, there was an upregulation of expression of Hsp70. However, despite this the levels of Mia40, Erv1 and Tim10 were reduced in the ΔMxr2, most notably seen in the 40µg mitochondrial lane. Despite a possible uneven loading of mitochondria, with more ΔMxr2 mitochondria present the levels of these proteins were still reduced relative to the WT mitochondria. The presence or absence of oxidative stress appeared to have no effect on the steady state levels of these proteins, induced by the addition of $H_2O_2$. Interestingly each of these are essential mitochondrial proteins found in the IMS. The decreased levels of these proteins in the IMS compartment further lends credence to the argument that Mxr2 is also localised to the IMS. If Mxr2 is a solely matrix localised protein it would be difficult to explain why loss of this reductase enzyme in the matrix would affect steady state levels of essential IMS proteins. Levels of Gpx3 were unaffected as were the levels of Cyt C between WT and ΔMxr2 mitochondria. However, when ΔMxr2 mitochondria were stressed prior to isolation a reduction in steady state levels of Cyt C was observed.

With the knowledge that both Mia40 and Erv1 levels were reduced in the ΔMxr2 mitochondria alongside the levels of Tim10 (a substrate for Mia40) then it was decided to determine if more of the small Tim chaperones were affected in the absence of Mxr2. These findings were not quantified so it is possible there is not a statistically significant decrease in the relative abundance of Mia40 and Erv1 protein levels between the two strains of mitochondria. The steady states in **Fig 4.3B** show that levels of Tim8 were also decreased irrespective of oxidative stress conditions. No significant difference was seen for the levels of Tim9 when comparing WT and ΔMxr2 mitochondria, however, there does appear to be a slight decrease in levels when the ΔMxr2 mitochondria were subjected to oxidative stress (40µg lane). The levels of the carrier metabolite ADP/ ATP carrier (AAC) were also tested as this protein requires the functional Tim9-Tim10 chaperone complex for its import. No decrease in protein levels of AAC were detected despite the reduction in Tim10 levels. Aconitase was probed for as a loading control for the assay. The steady state levels repeat

suggests that levels of Tim8 and possibly Tim9 are reduced in the absence of Mxr2, alongside Tim10 from the previous experiment **(Fig 4.3A)**. Despite the loss of these small Tim chaperones, it does not appear to cause a decrease in steady state levels of AAC protein.

To further characterise the decreased steady state levels a second ΔMxr2 mitochondrial preparation was performed, growing the cells fresh from glycerol stocks to provide an independent repeat and determine protein levels in two separate stocks of isolated ΔMxr2 mitochondria. These were termed ΔMxr2 and ΔMxr2 (2). Levels of Porin 1 and aconitase were probed as two separate loading controls and showed equal loading of all strains of mitochondria. The steady state results confirmed that levels of Mia40, Tim8, and Tim10 showed decreased protein levels in both preparations of ΔMxr2 mitochondria, relative to WT mitochondria **(Fig 4.3C)**. The decrease in protein levels characterised in at least two independent repeats in two different preparations of the mitochondria highlighting the validity of this finding. It is interesting to note that in the ΔMxr2 +$H_2O_2$ mitochondria, levels of Tim8 appear to be slightly increased relative to the unstressed mitochondria. From the steady state experiments while it is clear there is a reduction in the levels of these essential IMS proteins in the absence of Mxr2 it is not understood why. It is hypothesised that in the absence of Mxr2 uncontrolled methionine sulfoxidation occurs and these harmful protein modifications cannot be reduced. This in turn leads to the degradation of these proteins accounting for the decreased steady state levels. However, there is still no direct evidence to suggest that these proteins do become Met-O in vivo or that they interact with Mxr2 to reduce these groups. This is clearly something worthwhile investigating in the future

### 4.3.2 Respiratory Capacity and Substrate Utilisation through the Electron Transport Chain

With the essential components of the MIA pathway such as Mia40 and Erv1 and substrates of this pathway such as the small Tims seemingly affected in the ΔMxr2 mitochondria, it was decided to test if the respiratory capacity of these mitochondria was affected. Many assembly factors required for the biogenesis and maturation of the respiratory chain complexes are MIA pathway substrates so it was hypothesised that some of these components may be affected by the decrease of components of this pathway which could in turn lead to a functional defect in mitochondrial respiratory capacity. Indeed, previous studies in the

literature have linked loss of Mxr enzymes with deficits in respiratory capacity (Kaya et al., 2010). To measure this the Clark Electrode was used which measures the levels of oxygen in solution. The electrode consists of a platinum cathode and silver anode that is covered by an oxygen-permeable membrane. The diffused oxygen that passes through the membrane is reduced by a fixed voltage, generating a current that is proportional to the oxygen in solution. This system allows the measurement of oxygen consumption over time to produce an oxygen consumption rate of actively respiring isolated mitochondria. The Clark electrode was set up as per section 2.4.8. The assessment of mitochondrial respiratory capacity was repeated in triplicate for each mitochondrial strain to generate average oxygen consumption rate (OCR) and statistical analysis determined using an unpaired t-test. Statistical significance was determined by $p < 0.05$.

Baseline respiratory rates were initially measured by addition of 300µg of mitochondria to the sealed chamber and measuring respiration in the absence of any exogenous substrates. The ΔMxr2 mitochondria showed increased levels of basal respiration **(Fig 4.4)** relative to the WT and this was deemed to be statistically significant ($p<0.05$), suggesting that basal respiration rates were higher in ΔMxr2 mitochondria. Next, malate glutamate (MG) was added to promote state 2 respiration. Any oxygen consumption in the absence of adenylates utilising MG reflects respiration specific to complex I activity. Malate and glutamate are substrates for dehydrogenase reactions in the TCA cycle to generate NADH. This NADH is subsequently oxidised by complex I, the NADH dehydrogenase in mammalian cells. Therefore, oxygen consumption in the presence of MG must be linked to activity at this complex. Yeast however do not possess complex I but instead have monomeric NADH dehydrogenases (Nde and Ndi) (Luttik *et al.*, 1998). In the ΔMxr2 mitochondria, OCR in the presence of malate glutamate was significantly increased ($p<0.001$) relative to the WT suggesting that when Mxr2 is absent from the mitochondria production of NADH is increased and greater activity at the NADH dehydrogenase enzymes to consume oxygen. Next pyruvate was introduced into the system as a substrate for respiration. Pyruvate is normally produced through glycolysis in vivo and is converted into acetyl-CoA which enters the TCA Cycle to promote aerobic respiration and oxygen consumption. OCR in the ΔMxr2 mitochondria was increased upon the addition of pyruvate though this increase was not statistically significant. State 3 respiration was measured by the addition of saturating levels of ADP to maximally stimulate respiration in the

presence of glutamate and malate substrates. Interestingly, for unknown reasons, the WT mitochondria did not respond as expected to the addition of ADP and OCR was similar to pyruvate treatment. ΔMxr2 mitochondria showed a significant increase in OCR when ADP was added ($p<0.05$) much more in line with the expected results demonstrating maximal respiration. Oligomycin was added to inhibit the $F_0$ subunit of the ATP synthase inducing state 4 respiration. Blocking $F_0$ blocks the return flow of protons through the proton channel eliminating ATP production. Oxygen consumption can still occur and is attributed to proton leak across the IM. Thus, the addition of oligomycin indicates the extent of proton leakage. The differences in OCR between WT and ΔMxr2 were not statistically significant during this treatment stage ($p>0.05$). CCCP was used as an uncoupler due to its ability to dissipate the proton gradient across the IM and induce maximal oxidative capacity of the mitochondria. Indeed, upon addition of CCCP WT OCR drastically increased representative of maximal capacity, and ΔMxr2 OCR was higher than that of the previous oligomycin stage. Lastly sodium azide was added as an inhibitor of mitochondrial respiration that blocks CIV activity. OCR fell harshly once azide was added to the system as expected suggesting inhibition of the ETC,

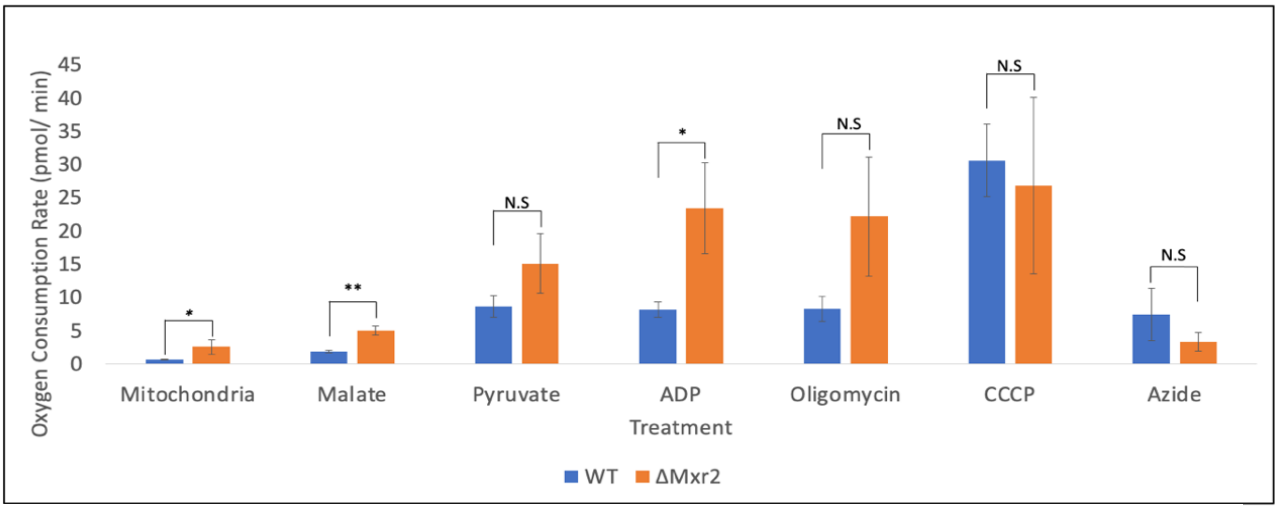


**Figure 4.4: Comparison of Oxygen Consumption Rates (OCR) between WT and ΔMxr2 isolated mitochondria in response to treatments.** 300µg mitochondria were added to obtain the basal respiration rate. Following this substrates malate glutamate (1M each), sodium pyruvate (1M) and ADP (0.1M) were added to obtain OCR of each substrate's utilisation by the mitochondria. Next 1mM Oligomycin was added to obtain proton leak-linked OCR followed by the uncoupler CCCP (0.25mM) to obtain maximal OCR. Lastly 5mM sodium azide was added to inhibit the electron transport chain (ETC) and obtain excess OCR. Each bar represents the mean of three independent repeat experiments. Error bars represent standard deviation of triplicate results. Unpaired t-test performed to determine statistical significance denoted by $p < 0.05$ (*) or $p < 0.001$ (**).

though some oxygen consumption remained. It is possible that this represents non-mitochondrial respiration in the system, or a lack of azide added to efficiently inhibit the complexes. No statistical differences in azide treatment were noticed between the WT and ΔMxr2 mitochondria.

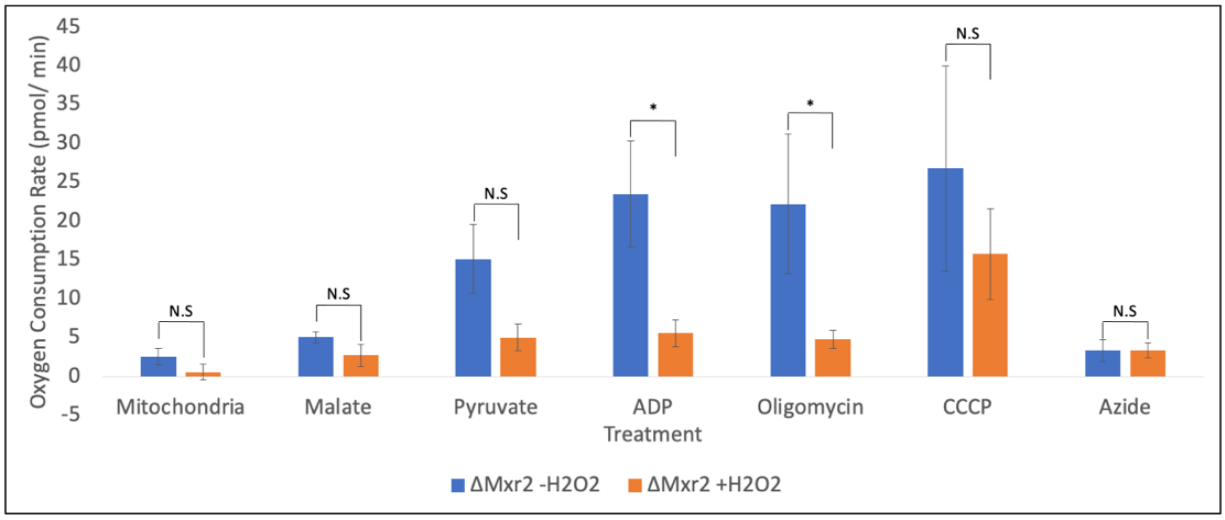


**Figure 4.5: Comparison of Oxygen Consumption Rates (OCR) between ΔMxr2 -$H_2O_2$ and ΔMxr2 + $H_2O_2$ isolated mitochondria in response to treatments.** 300µg mitochondria were added to obtain the basal respiration rate. Following this substrates malate glutamate, (1M each) sodium pyruvate (1M) and ADP (0.1M) were added to obtain OCR of each substrate's utilisation by the mitochondria. Next Oligomycin (1mM) was added to obtain proton leak-linked OCR followed by the uncoupler CCCP (0.25mM) to obtain maximal OCR. Lastly sodium azide (5mM) was added to inhibit the electron transport chain (ETC) and obtain excess OCR. Each bar represents the mean of three independent repeat experiments. Unpaired t-test performed to determine statistical significance denoted by $p < 0.05$ (*) or $p < 0.001$ (**).

The Clark Electrode experiment was repeated with ΔMxr2 mitochondria isolated from $H_2O_2$ induced oxidatively stressed cells to determine if the presence of stress affected mitochondrial respiratory capacity. Statistically significant changes in OCR ($p<0.05$) between the +/- $H_2O_2$ stressed ΔMxr2 mitochondria were demonstrated after ADP and oligomycin treatment **(Fig 4.5)**. In each case the + stressed mitochondria displayed OCR rates much more similarly to the previous WT mitochondria. No direct comparison between WT and ΔMxr2 + $H_2O_2$ mitochondria was made due to the addition of two changed variables (loss of Mxr2 and induction of oxidative stress). The addition of $H_2O_2$ WT mitochondria has the effect of inducing oxidative stress/ damage and subsequent modification of key proteins within the organelle. From the results in **Fig 4.4-4.5** it was concluded that in the absence of Mxr2, basal respiration rates and oxygen consumption at complex I of the ETC was increased relative to

the WT mitochondria. In addition, when ΔMxr2 mitochondria were isolated from oxidatively stressed conditions the mitochondria did not respond to addition of ADP to promote respiration to the same extent of the unstressed cells implying a defect in respiratory capacity. As an extension of the results of the Clark Electrode, mitochondrial function was assayed using the BioLog machinery. This involved a high throughput analysis of the rate of substrate metabolism in different strains of mitochondria. The assay functions by measuring the rate of electron flow into/ through the ETC from numerous metabolic substrates such as succinate, malate etc. Each substrate follows a different pathway which involves the requirement for different dehydrogenase and transporter proteins. As substrates are utilized the electrons flow from complex I/II to the end of the ETC where they are accepted by a terminal electron acceptor tetrazolium redox dye (MC). Upon reduction of this dye, it undergoes a colour change which is measured by the BioLog machinery over time to determine substrate utilisation by the mitochondria. Each plate contained 96 wells each with a different substrate to be measured. Triplicate repeats for WT and ΔMxr2 were performed, and average rates calculated.

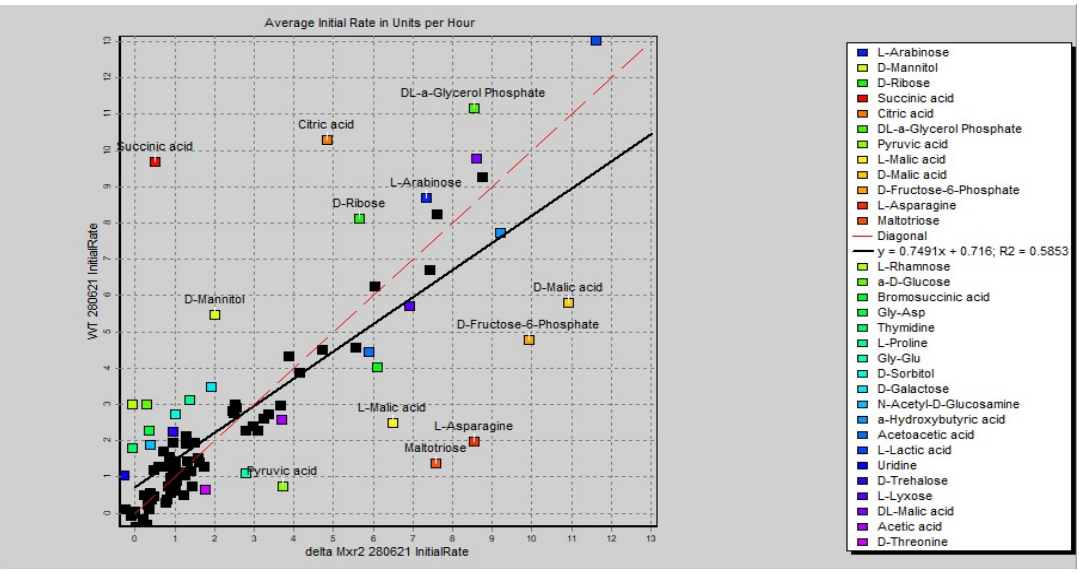


**Figure 4.6: Biolog mitochondrial function assay comparison between WT and ΔMxr2 yeast cells.** Biolog mitoplates were used to determine rates of substrate metabolism in WT and ΔMxr2 yeast cells by measuring rate of electron flow into the electron transport chain. Assay involved the use of a tetrazolium redox dye that acts as terminal electron acceptor and changes colour upon reduction. Omnilog machinery measured the change in dye colour over time to determine utilisation of substrates in a high throughput assay. Rate of substrate utilisation of WT yeast was compared to that of ΔMxr2 yeast. Three independent repeats were performed on separate dates and average rate for each yeast strain calculated.

The results of the Biolog mitochondrial function assay revealed differences in the utilisation of several substrates to produce energy through the ETC between the WT and the ΔMxr2 mitochondria **(Fig 4.6)**. In the absence of Mxr2 rate of substrate metabolism of succinic acid, citric acid and many other substrates were reduced relative to the WT mitochondria. On the other hand, substrate metabolism of both L- and D- Malic acid, and pyruvic acid were all upregulated when Mxr2 was absent from the mitochondria. Interestingly this upregulation in substrate metabolism corroborated the findings from the Clark Electrode that demonstrated an increase in OCR when these substrates were utilised in the ΔMxr2 mitochondria. Though it should be noted that this occurred in the absence of adenylates in the Clark Electrode experiment preventing a direct comparison. The Biolog assay monitored the changes in over 90 different substrates to provide a detailed overview of many of the mitochondrial metabolite pathways involved in energy production within this organelle. An in-depth analysis of each of these pathways however was beyond the scope of this thesis.

### 4.3.3 Impaired Complex Assembly and Function of the Tim9-Tim10 Chaperones

Due to the decrease in the levels of both Tim 8 and Tim 10 shown in the steady state experiment in ΔMxr2 mitochondria **(Fig 4.3)** a new aim was devised to investigate why the levels of the small Tim chaperones were decreased in the absence of this reductase. It was hypothesised that in the absence of Mxr2 increased levels of Met-O occurred on the Tim proteins. This would result in the unfolding and subsequent degradation of these proteins thus explaining the lower steady state levels. However, from these results it was unclear whether the loss of protein was due to a fault at the level of protein import, level of complex assembly or the increased levels of Met-O of the fully formed small Tims in mature complex form. It was decided that the intital focus would be to characterise the reduction in Tim10 as this showed the most striking decrease in steady state levels.

Initially the import of Tim10 into ΔMxr2 was tested relative to Wild type to ensure that levels of Tim10 were not reduced due a decrease in the levels of protein import. Import of Tim9 was simultaneously tested as once inside the mitochondria it associates and forms a complex with Tim10. The import of Tim9 **(Fig 4.7A)** shows that levels of Tim9 were not decreased in the

ΔMxr2 mitochondria suggesting that loss of this reductase does not cause a defect in import capacity. The Por1 loading control shows that slightly less ΔMxr2 mitochondria were added but despite these levels of Tim9 were not decreased relative to WT. The import of Tim10 **(Fig 4.7B)** was relatively unaffected in the ΔMxr2 mitochondria and levels of Por1 suggested more equal loading of mitochondria. This suggests that the decreased levels of Tim10 in the ΔMxr2 mitochondria were not a result of a defect of protein import. Western blot of Mia40 confirmed that the levels were reduced compared to WT corroborating the previous steady state results **(Fig 4.3)**.

As Mia40 is required for the successful import of the small Tim proteins and its levels were

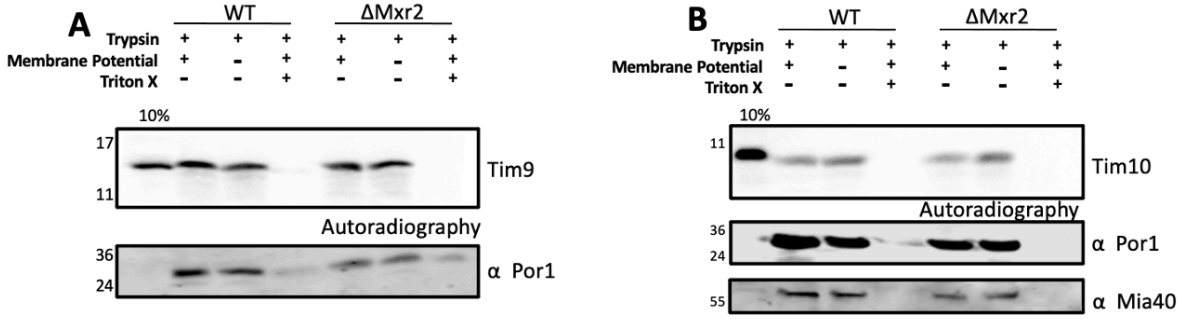


**Figure 4.7: Import of the small Tim proteins into WT and ΔMxr2 mitochondria.** Radiolabelled Tim9 (A) and Tim10 (B) were imported into isolated WT and ΔMxr2 mitochondria for 15 minutes. Samples were treated with trypsin (0.1mg/ml) and SBTI (1mg/ml) post import to remove any unimported material. Triton-X100 (Tx) (10%) was used as a control to solubilise the mitochondria. 10% refers to 10% of the radiolabelled protein presented for import. Radiolabelled Tim10 was visualised via autoradiography. Western blotting of Por1 was used as a loading control.

reduced, the import of Mia40 itself was tested. Unfortunately, due to time constraints ΔMxr2 mitochondria isolated from $H_2O_2$ stressed cells had to be used and were compared to their stressed WT counterparts. An 8% Tris-Tricine gel was used, and the gel ran at a low voltage for the duration to enhance the resolution of the intermediates of the Mia40 import pathway.

Mia40 was imported at 6 different timepoints between 1 and 40 minutes to capture the stages of successful import of Mia40. Within the first three timepoints Mia40 was found in a reduced state and not until the 10-minute timepoint was there a very slight decrease in MW suggesting that Mia40 was now oxidised in the WT + $H_2O_2$ mitochondria. From the 10' timepoint at the top of the autoradiography a new band appeared believed to correspond to the Mia40-Mia40 intermediate and below that a series of bands that correspond to a Mia40

intermediate with Erv1. Following the appearance of these intermediate bands of Mia40 import pathway then the shift to oxidised Mia40 is present. In the ΔMxr2 + $H_2O_2$ the overall

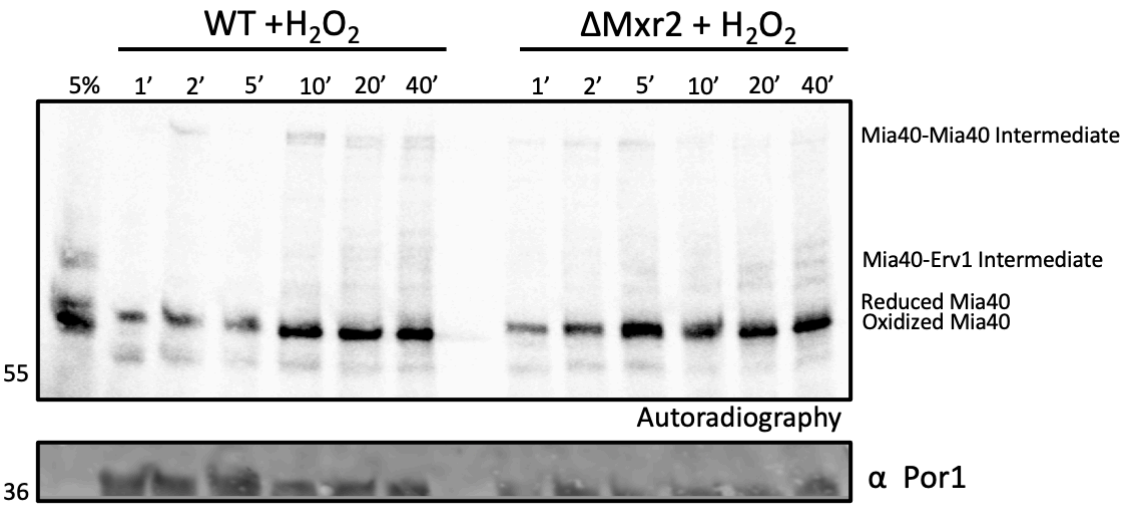


**Figure 4.8: Import of Mia40 into WT + $H_2O_2$ and ΔMxr2 + $H_2O_2$ mitochondria.** Radiolabelled Mia40 was imported into isolated WT + $H_2O_2$ and ΔMxr2 + $H_2O_2$ mitochondria for indicated time. Samples were treated with trypsin (0.1mg/ml) and SBTI (1mg/ml) post import to remove any unimported material. Triton-X100 (Tx) (10%) was used as a control to solubilise the mitochondria. 5% refers to 5% of the radiolabelled protein presented for import. Radiolabelled Mia40 was visualised via autoradiography. Western blotting of Por1 was used as a loading control. Samples run on an 8% Tris-Tricine gel.

levels of imported Mia40 appear to be the same. The distinction between reduced and oxidised Mia40 is much less clear however. The presence of the Mia40-Mia40 and Mia40-Erv1 intermediates appear more strongly at the 5' minute timepoint suggesting that the import kinetics of Mia40 in these mitochondria may be quicker and these interactions occur faster. Overall, the import of Mia40 into ΔMxr2 appears to be unaffected by the loss of Mxr2 and is not believed to account for the decreased steady state levels of Mia40 or Tim10 demonstrated.

As import of Tim9, Tim10 and Mia40 did not seem to be affected in the ΔMxr2 mitochondria it was concluded that the decrease in Tim10 levels were not because of a defect at the level of protein import and instead research focused on determining if there were any alterations in the redox state of the protein or its ability to become incorporated into the mature hexameric Tim9-Tim10 complex. The thiol reactive compound AMS was used to determine the redox state of Tim10 in vivo. AMS binds to free thiols on a protein resulting in a 0.5kDa shift per free thiol modified. Tim10 contains four cysteine residues (Allen *et al.*, 2003)

meaning that there was potential for four molecules of AMS to bind to Tim10 giving a maximum Mwt increase of 2kDa on an SDS PAGE gel. Tim10 protein was incubated either untreated, with AMS, or with a combination of AMS and DTT to fully reduce the protein.

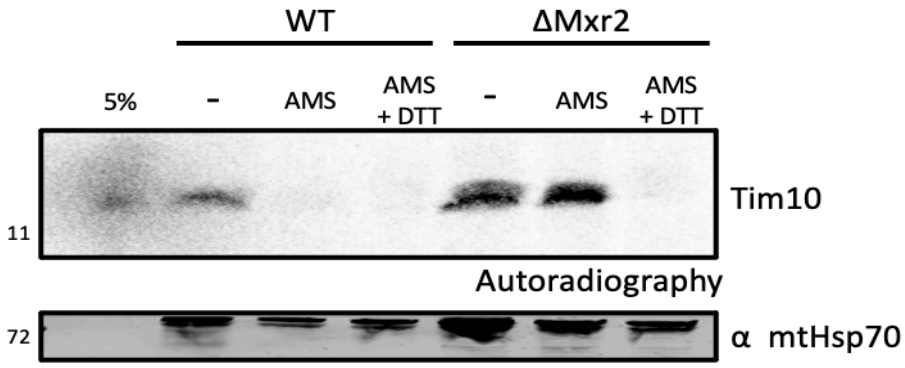


**Figure 4.9: Determining the in organello redox state of Tim10 in WT and ΔMxr2 mitochondria.** Radiolabelled Tim10 protein was imported into WT and ΔMxr2 mitochondria. Proteins were precipitated using 10% TCA and either untreated (- lanes), treated with AMS, or treated with a combination of AMS/ DTT. Tim10 was detected using autoradiography and mtHsp70 detected via western blotting as a loading control.

The results of the thiol oxidation experiment in **Fig 4.9** were inconclusive. Despite several attempts to AMS label the protein there was a complete loss of radioactive signal in many of the lanes. From the limited results available it appears that the Tim10 in the AMS lane of the ΔMxr2 mitochondria runs at the same Mwt as the untreated WT mitochondrial lane suggesting that in the knockout mitochondria AMS was unable to bind to any free thiols or they were all fully reduced. However, without the corresponding AMS labelled Tim10 in the WT mitochondria it is impossible to draw any real conclusions.

Following on from this, the assembly of Tim10 into its mature Tim9-Tim10 complex was monitored via Blue-Native PAGE analysis. Samples were run under native conditions to maintain the small Tim assembly complexes in their native conformation and capture the intermediates of assembly to determine if there were any defects in any stage of the complex assembly when Mxr2 was absent.

Radiolabelled Tim10 was imported into WT and ΔMxr2 mitochondria for either 10, 20 or 30 minutes to capture all stages of complex assembly. The import was presented in two panels; the Coomassie stained blue native gel showing the respiratory chain complexes, and the autoradiograph of the radiolabelled Tim10 with the annotated stages of complex assembly. These include the high molecular weight trimeric complex between Tim9-Tim10-Tim22, the Tim10-Mia40 intermediate, and the hexameric Tim9-Tim10 complex that runs at the bottom

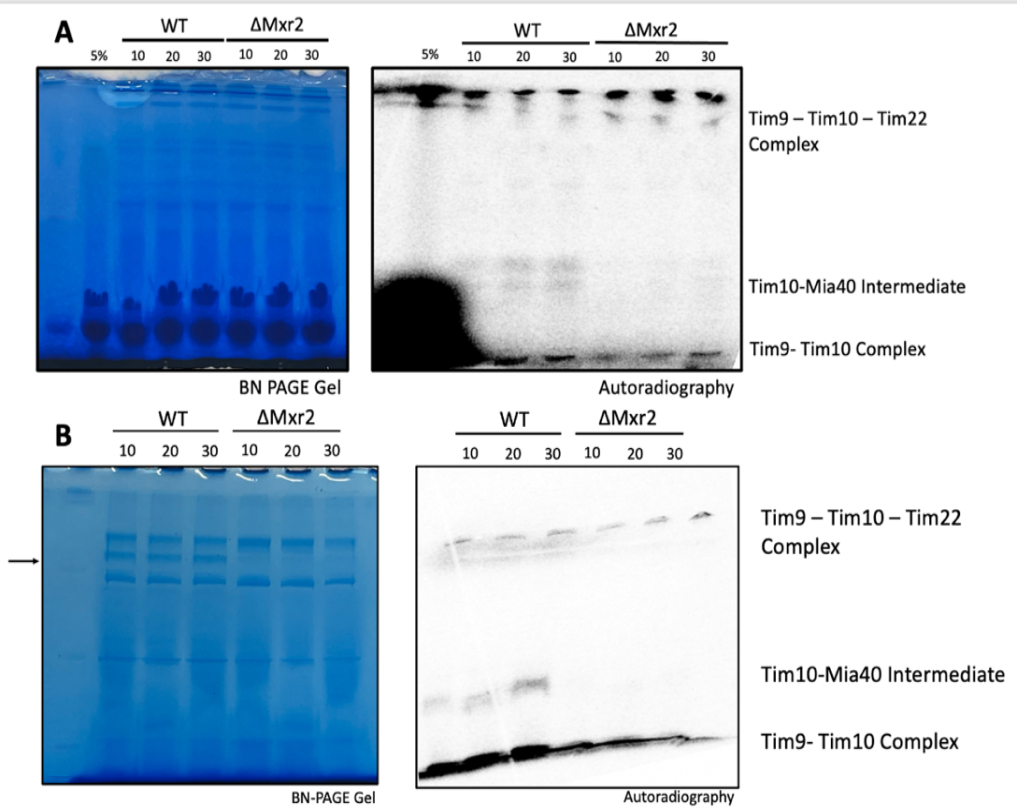


**Figure 4.10: Blue-Native PAGE analysis of Tim10 complex assembly formation.** Radiolabelled Tim10 was imported into WT and ΔMxr2 mitochondria for different specified timepoints and samples loaded on a BN PAGE gel. Autoradiography used to detect the radiolabelled Tim10 and speculated stages of Tim10 complex assembly. (A) and (B) are two independent repeats of the import experiment. Blank arrow in (B) refers to missing unknown complex in the Coomassie stained BN PAGE gel.

of the gel. The BN analysis revealed that there is a loss of radioactivity corresponding to the Tim10-Mia40 in the ΔMxr2 mitochondria **(Fig 4.10A)**. This suggests when Mxr2 is absent, Tim10 is less able to form an intermediate with Mia40 – a key stage in its assembly into the mature complex and indeed the levels of Tim9-Tim10 complex do appear to be decreased in these ΔMxr2 mitochondria. The large blot of radioactivity to the left of this image corresponds to the 5% TNT control added to the gel however this proved to be too intense for visualising the BN PAGE and the contrast had to be adjusted to see the intermediate bands in complex

assembly. This experiment was repeated and again the results suggested that there was a lack of Tim10-Mia40 intermediate formed in the knockout mitochondria again confirming that complex assembly of Tim10 was affected **(Fig 4.10B)**. It is hypothesised therefore that while Tim10 is imported into the mitochondria as normal in the ΔMxr2 it is unable to efficiently form its mature complex in the IMS. As a result, unincorporated Tim10 is likely subject to degradation accounting for the loss of Tim10 steady state levels in **Fig 4.3**. However, the mechanism or reasoning for why the loss of this reductase enzyme would prevent the proper assembly of this complex. The Coomassie stained BN gel in **Fig 4.10B** was subject to destaining buffer for 30 minutes to allow greater visualisation of the respiratory complexes and Mwt markers. Intriguingly one of the believed respiratory complex bands was absent in the ΔMxr2 mitochondria, denoted by the black arrow. Without the molecular weight markers and further analysis of this band it is difficult to know what complex it represents. Aligning the complexes in **Fig 4.10B** with a previous blue native supercomplex analysis in *S. cerevisiae* (Schägger and Pfeiffer, 2000) indicates that the upper band above the arrow may be the dimeric form of CV which would make the unknown complex a supercomplex between CIII and CIV (either $III_2$-$IV_2$ or $III_2$-$IV_2$). More research is required to provide a more accurate analysis of the nature of this complex

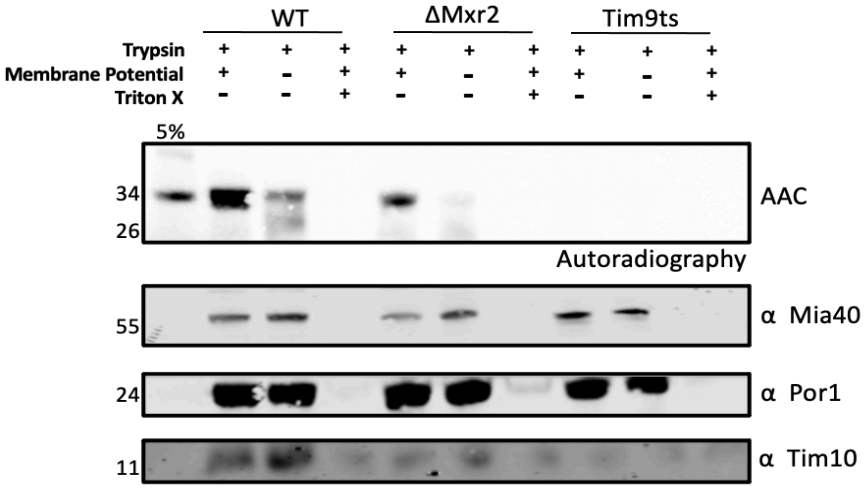


**Figure 4.11: Import of AAC into WT, ΔMxr2 and Tim9ts mitochondria.** Radiolabelled AAC was imported into WT, ΔMxr2 and Tim9ts mitochondria for 15 minutes. Post import samples were treated with trypsin (0.1mg/ ml) and SBTI (1mg/ ml) to remove any unimported material. Trypsin-X100 (Tx) (10%) was used as a negative control to solubilise mitochondria. 5% refers to 5% of radiolabelled protein presented to the import reaction loaded. Western blot of Por1 used to show equal loading.

With the decreased levels of Tim10 in the ΔMxr2 now presumed to be a result of impaired complex assembly, it was decided to test if this resulted in a functional deficit in the mitochondria. The small Tim9-Tim10 chaperone complex is involved in the import of large inner membrane carrier proteins such as the ADP/ ATP carrier (AAC) (Webb *et al.*, 2006). It was hypothesised that when levels of Tim10 were decreased this would result in a decrease in the levels of imports of these carrier proteins.

Radiolabelled AAC was imported into WT, ΔMxr2 and Tim9ts mitochondria to test this hypothesis. In the WT mitochondria AAC was efficiently imported and this appeared to be dependent on the presence of membrane potential as in when this was dissipated levels of AAC import were decreased **(Fig 4.11)**. A Tim9ts mutant strain was used, and the mitochondria were incubated at 37$^{o}$C for 30 minutes, the non-permissive temperature, as Tim9 protein becomes unstable at elevated temperatures in this strain. As Tim9 is an essential protein it cannot be knocked out. This mutant strain was used as a positive control as Tim9 is required for the import of AAC. As expected, import of AAC was completely abolished in the Tim9ts mitochondria. Western blotting revealed that levels of Tim10 were also decreased, which was to be expected as it requires Tim9 for complex assembly. In the ΔMxr2 mitochondria AAC import capacity was negatively affected but not completely abolished in the presence of membrane potential relative to import in the WT mitochondria. Western blotting confirmed that levels of Tim10 were in fact significantly reduced in these ΔMxr2 mitochondria but also the levels of Mia40 were decreased as well. Despite levels of Tim10 being significantly decreased in the ΔMxr2 and Tim9ts mitochondria, there was not a complete loss of AAC import in both strains. It is unclear why some AAC was still able to be imported. It is possible that AAC is a very stable protein and even if little protein is imported it persists. However, the results in **Fig 4.11** show a clear defect in protein import of AAC in the absence of Mxr2 and subsequently Tim10. The loss of Mxr2 not only results in a decrease in the levels of the essential protein Tim10 but this also manifests as a functional defect in the import of one of its substrate proteins.

## 4.4 Discussion

This chapter focused on elucidating the phenotypic effects of mitochondria in the absence of Mxr2 to give insights and further our understanding on the role of this enzyme in the mitochondria. There were three main areas of focus including the effect of oxidative stress on the mitochondria, respiratory capacity, and the import and assembly of the small Tim chaperone into the IMS. The findings in this chapter build upon the limited research on the function of Mxr2 inside the mitochondria and provide indications of new potential substrates of these reductase enzymes.

### 4.4.1 Mitochondrial Oxidative Stress Tolerance and Effects on Relative Protein Abundance

In the absence of Mxr2, yeast cells were demonstrated to display a severe growth defect when cultured on glucose containing medium in the presence of 1mM $H_2O_2$ to induce oxidative stress conditions **(Fig 4.2A/B)**. This finding is in line with a previous $H_2O_2$ sensitivity assay indicating a severe growth defect of ΔMxr2 in the presence of 1mM $H_2O_2$ (Allu *et al.*, 2015). This suggests that in the absence of the reductase enzyme the yeast cells are unable able to tolerate oxidative stress conditions. Oxidative stress is linked to an increase in Met-O, and it is hypothesised in the absence of Mxr2, uncontrolled Met-O occurs which cannot be reduced (Cabreiro *et al.*, 2006). As this is a harmful protein modification it may cause unfolding and degradation of essential mitochondrial proteins that in turn results in cell death as demonstrated by the growth defects on cultured media. Interestingly this defect was observed when cells were cultured in the presence of glucose for energy. Glucose can be utilised to generate ATP through glycolysis bypassing the need for functional mitochondria to ensure cell survival. It is therefore intriguing that potential oxidative damage in the mitochondria still resulted in cell death and growth inhibition when cells can utilise this energy source without the requirement of functional mitochondria.

Growth of ΔMxr2 yeast cells utilising a titration of [$H_2O_2$] revealed that the growth defect was more severe at 1mM opposed to 2mM **(Fig 4.2B)**. This contrasts with the hypothesis that increased oxidative stress conditions are more harmful to the mitochondria and instead suggests that loss of Mxr2 is in fact protective to the mitochondria at higher concentrations of $H_2O_2$. This experiment needs to be replicated to determine if this is reproducible finding,

possibly incorporating a greater titration of [$H_2O_2$] to determine if there is a protective dose response relationship between concentration and cell growth in absence of Mxr2.

The findings in **Fig 4.2B** also revealed that growth of yeast cells in the absence of either Mxr1 or Mxr2 were consistent with WT on both glucose and lactic acid containing media. A previous study demonstrated that yeast cells with a double Mxr1, Mxr2 knockout mutation displayed reduced growth on lactic acid media (Kaya et al., 2010). This suggests that loss of no single Mxr enzyme is sufficient to induce a growth defect in the presence of respiratory substrates, but instead a combination of loss of both reductase enzymes in yeast is required. It would be interesting to test the growth of the double Mxr mutant in the presence of $H_2O_2$ to test if this induces a cumulative growth defect especially at lower concentrations (<1mM) of $H_2O_2$. In addition, a rescue experiment needs to be performed involving transformation of the ΔMxr2 mitochondria with a plasmid encoding the Mxr2 protein to determine if this would rescue the growth defect. This would confirm if the growth defect was specific to loss of Mxr2. To further elucidate this phenotype, Mxr2 constructs with either a Su9- or cytochrome b2- mitochondrial targeting sequence could be used to rescue the knockout strains. These constructs could target Mxr2 to either the matrix or the IMS respectively to test where in the mitochondria Mxr2 is required to prevent the growth defect and presumably reduce Met-O proteins that result in cell death.

While hypothesised that the increase in oxidative stress conditions results in an increase in Met-O of substrates in mitochondria that cannot be reduced there is little evidence to support this, let alone if Mxr2 is a substrate for many of these mitochondrial proteins. Very few substrates for Mxr2 have been biochemically characterised. Mge1, a component of the protein import machinery was the first and only well characterised substrate as of the beginning of this project (Allu *et al.*, 2015). Steady state levels of mitochondrial proteins were determined between WT and ΔMxr2 isolated mitochondria to characterise the relative abundance of proteins.

The steady state levels results revealed that relative levels of Mia40, Erv1 and Tim10 were reduced in the ΔMxr2 mitochondria **(Fig 4.3A)**. Each of these three proteins is encoded by an essential gene and the translated protein localised to the IMS. The loss of these IMS proteins

when Mxr2 is absent from the mitochondria further emphasises the findings in Chapter 3 that suggested Mxr2 was also localised to the IMS. This is contradicting with the previous localisation studies. If Mxr2 was strictly matrix bound, then it would be unclear why loss of Mxr2 in this compartment would affect steady state levels of proteins in the IMS. The reduction in protein levels does not necessarily imply an interaction with Mxr2, nor an overabundance of Met-O of the affected proteins though this is the current working hypothesis. The reduction in levels of Mia40 and Tim10 was replicated, this time in two separately prepared ΔMxr2 mitochondrial isolations allowing the characterisation of loss of these two essential proteins as a real defect in the absence of Mxr2 **(Fig 4.3C)**. As Tim10 is a substrate of the MIA pathway for which Mia40 and Erv1 are the two main components it was unknown if loss of Tim10 was a result of the increased Met-O hypothesis or loss of import capacity in the MIA pathway. The levels of other small Tim chaperones that are also substrates of this pathway were tested. Levels of Tim8 were confirmed to be reduced in the ΔMxr2 **(Fig 4.3B/C)**. Tim9 levels were decreased but only when the ΔMxr2 mitochondria were subjected to $H_2O_2$ induced oxidative stress **(Fig 4.3B)**. The results displayed here do suggest an overall defect in the levels of the small Tim chaperones in the mitochondria though levels of both Tim12 and Tim13 would need to be tested. Lastly despite a decrease in levels of Tim8 in the ΔMxr2 mitochondria when these mitochondria were oxidatively challenged steady state levels of Tim8 appeared to increase **(Fig 4.3C)**. It is unclear as to why this protein would be upregulated in response to oxidative stress. Tim8 is a non-essential protein unlike Tim9/10 and functions as a chaperone to assist in import and insertion of multiple-spanning transmembrane proteins embedded in the IMS such as Tim23 and citrin a member of the solute carrier family (Davis *et al.*, 2007; Beverly *et al.*, 2008). Mutations in the human *TIM88A* gene have been linked to Mohr-Tranebjærg syndrome (MTS), a neurodegenerative disorder characterised by hearing loss, dystonia and blindness (Tranebjærg *et al.*, 1995; Koehler *et al.*, 1999). Knock out of hTim8a protein was shown to result in defects in CIV assembly linking loss of the Tim8 protein to respiratory defects (Kang *et al.*, 2019). Upregulation of Cyt C was also demonstrated in this study in response to knock-out of Tim8.

Previous experimental evidence determined that Cyt C levels were significantly reduced in single/ double mutant Mxr1, Mxr2 yeast strains (Kaya et al., 2010). The steady state results in **Fig 4.3A** revealed that levels of Cyt C were relatively unchanged between WT and ΔMxr2

mitochondria inconsistent with the previous studies. However, levels of this protein were decreased in the ΔMxr2 + $H_2O_2$ suggesting loss of Cyt C in the mitochondria under conditions of oxidative stress **(Fig 4.3)**. Cyt C has been demonstrated to be tightly linked to oxidative stress due to its role as an electron carrier and an ability to induce apoptosis in response to oxidative stress (Guerra-Castellano *et al.*, 2018). Cyt C and can become modified through phosphorylation events and lipid modifications when cells are oxidatively challenged (Guerra-Castellano *et al.*, 2018; Jenkins *et al.*, 2018).

The substantial defect in the levels of the small Tim chaperones Tim8 and Tim10 piqued research interests to further investigate in detail how loss of Mxr2 in the mitochondria resulted in a defect in steady state levels of these proteins in this chapter.

### 4.4.2 Respiratory Capacity and Metabolic Substrate Profiling

Previous studies had implicated Cyt C as being susceptible to redox regulation at a Met residue and the function of this protein modified in the absence of Mxr enzymes (Feinberg et al., 1986; Kaya et al., 2010). Due to the role of Cyt C in the electron transfer required for energy production, oxygen consumption rates and respiratory capacity of the mitochondria were monitored using a Clark Electrode to determine any differences when Mxr2 was absent from the organelle.

The results from the Clark Electrode determined that loss of Mxr2 resulted in the alteration of the respiratory capacity of isolated ΔMxr2 mitochondria relative to the WT mitochondria. Basal respiratory rates were increased in the absence of Mxr2, and these mitochondria also displayed increased utilisation of malate, glutamate, pyruvate, and ADP as respiratory substrates for energy production. In addition, the introduction of oxidative stress induced by $H_2O_2$ further modulated the respiratory capacity of the mitochondria with significant changes in oxygen consumption in response to ADP and oligomycin treatments relative to the unstressed isolated mitochondria. It is unclear whether the increased utilisation of these substrates was a result of increased activity of substrate metabolite transporters or increased activity of enzymes involved in the metabolism of these substrates into intermediates for the TCA cycle.

The results of the Biolog experiment demonstrated an increased utilisation and metabolism of substrates such as malate and pyruvate, corroborating the findings from the Clark Electrode on. Together these independent experimental techniques demonstrate how mitochondria devoid of Mxr2 display an altered mitochondrial substrate metabolism capacity. The Biolog experiments provided an in-depth analysis of over 90 substrates involved in energy production within this organelle. While an in-depth analysis was beyond the scope of this project it would be interesting to follow up this in the future and fully understand the metabolic changes and differences in substrate utilisation in the absence of Mxr2.

### 4.4.3 Defects in the Assembly of Tim10 in absence of Mxr2

The final portion of this chapter was focused on further investigating the decreased levels of the small Tim chaperone Tim10 demonstrated to occur in the absence of Mxr2 **(Fig 4.3A/C)**. The results demonstrated that this loss of Tim10 was not because of impaired import of Tim10 itself **(Fig 4.7)** or that of Mia40 **(Fig 4.8)** which is an essential protein required for the oxidative folding and import of Tim10. However, a defect in the assembly of Tim10 into its mature complex once inside the mitochondria was detected via a BN-PAGE analysis **(Fig 4.10)**.

A previous study by Milenkovic et al characterised the stages of assembly and intermediate complex formation of Tim9 which follows a similar import pathway to become associated with Tim10 in a mature hexameric complex (Milenkovic *et al.*, 2007). The BN analysis revealed the presence of three protein MW complexes with radiolabelled Tim9 incorporated into the Tim9-Tim10 complex, the Tim9-Mia40 intermediate and finally the Tim9-TIM22 complex from lowest to highest Mwt. The separation of the Tim assesmbly complex proteins was also demonstrated with kinetic resolution (Sideris and Tokatlidis, 2007, 2010). This trio of complexes was also seen when radiolabelled Tim10 was imported **(Fig 4.10)**.

Interestingly in the absence of Mxr2 the Tim10-Mia40 intermediate was lost when analysed on a BN gel relative to WT mitochondria counterpart. As previously indicated levels of Mia40 have been shown to be reduced in the ΔMxr2 mitochondria possibly accounting for loss of interaction between these two proteins. The previous BN analysis of Tim9 also investigated how the loss of cysteine residues resulted in loss of interaction with Mia40, indicating these

Cys are crucial for interaction with Mia40. Due to the similarities between Tim9/Tim10 it is therefore likely that this principle applies to Tim10 as well and it is possible in the ΔMxr2 mitochondria the redox state of the cysteine residues has been altered and therefore interaction with Mia40 is no longer feasible. The AMS labelling experiment aimed to test this hypothesis that the Cys of Tim10 are in a different oxidation stage in the absence of Mxr2 though the results were inconclusive **(Fig 4.9)**. Future work is required to optimise the conditions for the AMS labelling, or alternatively use another thiol-reactive compound Maleimide (Mal) PEG to characterise the redox state of Tim10.

From these results a direct interaction between Mxr2 and Tim10 cannot be characterised. The alterations in assembly and steady state levels may be due to downstream effects of loss of this reductase rather from a lack of direct interaction. It would be beneficial to attempt to characterise an interaction through either Co-immunoprecipitation or more direct biophysical methods such as fluorescence resonance energy transfer (FRET). In addition, there is no evidence of Tim10 itself becoming Met-O in the literature, which is the main hypothesis of why levels of this protein are reduced in the absence of Mxr2.

To test if Tim10 becomes Met-O, and if levels of this modification are enhanced in the absence of Mxr2 mass spectrometry (MS) could be used. By radiolabelling Tim10 and importing it into WT and ΔMxr2 prior to MS analysis of the imported protein, the extent of Met-O between the two mitochondrial strains could be determined. It is hypothesised that Tim10 isolated post import from the ΔMxr2 mitochondria would display greater levels of Met-O modifications due to the lack of a reductase enzyme to remove these adducts.

The BN analysis of Tim10 import revealed the loss of a respiratory complex in the absence of Mxr2 through Coomassie staining. Under BN conditions, the respiratory chain complexes I-V and accompanying supercomplex structures in mitochondria are preserved and can be separated using PAGE (Timón-Gómez *et al.*, 2020). The loss of a respiratory complex or supercomplex in the absence of Mxr2 would provide a striking result though more experimental evidence is needed to characterise this complex. To determine the complex composition a two-dimension (2D) BN/SDS PAGE analysis could be performed. The first dimension BN-PAGE shown in **Fig 4.10** separates the intact OXPHOS complexes, while a

second electrophoresis using the denaturing agent SDS would resolve the individual subunits of each complex. From here western blotting could be used to probe for specific assembly factors and respiratory complex proteins to help characterise the respiratory complex band absent in the ΔMxr2 mitochondria. As many assembly factors of the respiratory chain complexes particularly CIV are Cys containing proteins that rely on the MIA pathway for their import, then in the absence of Mxr2 which in turn leads to a defect in levels of Mia40 **(Fig 4.3A/C)** this could account for a defect in protein import of assembly factors required for maturation of this defected complex.

Lastly in the absence of Mxr2, a defect in the import of the carrier protein AAC was determined **(Fig 4.11)**. As AAC is a substrate for the Tim9-Tim10 chaperone proteins essential for import then as levels of Tim10 have been characterised to be defected in the knockout mitochondria it was hypothesised this would account for the decrease in AAC import. To test this, a two-stage import could be trialled; first Tim10 imported into the ΔMxr2 mitochondria followed by a second import of AAC. If AAC import appears to be rescued when the mitochondria are supplemented with Tim10 then it is likely that it is loss of this chaperone inducing the defect rather than a downstream indirect effect. In addition, testing the import capacity of other substrates for Tim10 would be beneficial to see if there is a general import defect or if this is specific to AAC.

### 4.4.4 Conclusions and Future Work

In conclusions this chapter further elucidated the functional role of Mxr2 inside the mitochondria using a ΔMxr2 yeast cell line. In the absence of Mxr2, yeast cells were demonstrated to display a growth defect in the presence of $H_2O_2$ stress conditions. Analysis of protein steady state levels revealed a decrease in the levels of essential IMS localised protein such as Mia40, Erv1 and the small Tim chaperones in the knockout cell line. However, differences in protein levels due to modifications in gene expression were not tested or accounted for and these changes may account for the reduction in steady state levels demonstrated. in the Alterations in mitochondrial respiratory capacity and oxygen consumption in response to specific treatments were generated and the results corroborated with the metabolic substrate utilisation Biolog analysis. Lastly the decreased levels of Tim10

demonstrated were determined to be a result of impaired assembly into its native conformation and a defect in respiratory supercomplex assembly was observed.

Future work should focus on further characterising the observed phenotypes observed in the absence of Mxr2 and the appropriate rescue experiments performed to ensure these defects are a consequence of loss of Mxr2 itself and not a downstream effect. Further work is required to characterise the defect in respiratory complex assembly in terms of the specific complex that is affected and how Mxr2 may interact with specific respiratory complexes or assembly factors. Despite the evidence provided on the potential role of Mxr2 in the mitochondria very little is still characterised on specific interactions and mechanisms of Mxr2 with mitochondrial proteins. It would be particularly interesting to test for protein-protein interactions using biochemical and biophysical techniques between Mxr2 and primarily the proteins demonstrated to show reduced steady state levels in the absence of Mxr2.

# Chapter 5: The Import and Redox Regulation of Cytochrome C Oxidase Assembly Factor 8 (COA8) into Mitochondria

## 5.1 Introduction

The human *APOPT1* gene encodes the cytochrome C oxidase assembly factor 8 (COA8) protein that is translated on cytosolic ribosomes and subsequently translocated to the mitochondria. COA8 is translated as a 206 amino acid precursor protein with an N-terminal mitochondrial targeting sequence (MTS) **(Fig 5.1)** to aid translocation to the organelle. A combination of multiple sequence alignments and Mitofates analysis predicted the presence of this MTS (Fukasawa *et al.*, 2015). COA8 displays a positively charged amphiphilic region within its first 30 residues. The presence of these positively charged residues and the ability to form an amphiphilic α-helix are two key characteristics of the MTS (von Heijne, 1986; Roise *et al.*, 1988). In addition, the presence of a Tom20 recognition motif suggests that this is the main import receptor required for recognition and import inside the mitochondria. Lastly, the presence of a MPP cleavage site suggests COA8 follows the classical matrix import pathway to target the protein to the matrix where MPP is involved in the cleavage of the N-terminal

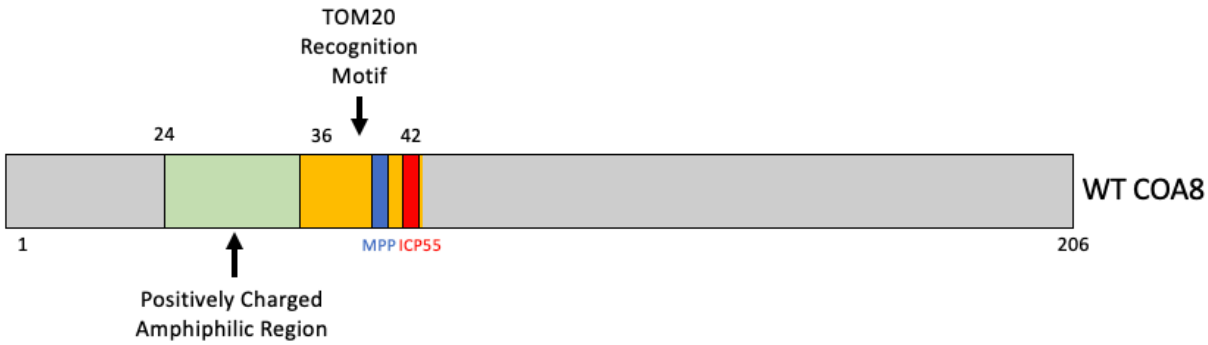


**Figure 5.1 Sequence analysis of the Wild-Type COA8 Protein encoded by the APOPT1 gene.** The *APOPT1* gene in humans encodes the 206 amino acid containing protein COA8 as a precursor. Mitofates analysis and sequence alignment predict the presence of an N-terminal mitochondrial targeting sequence in COA8 within the first 42 residues of the protein. Protein possesses a max positively charged amphiphilic region. A Tom20 receptor recognition motif can be found between residues 36 and 42. A matrix processing peptidase (MPP) and intermediate cleaving peptidase 55 (ICP55) cleavage sites are predicted at residues 41 and 42 respectively.

Previously unpublished data demonstrated that protein levels of an HA-tagged COA8 construct was downregulated under hypoxic (5% $O_2$) conditions (Erika Fernandez-Vizarra *et al.,* unpublished data) but the mechanism to regulate the stability or abundance of COA8 in these conditions is unclear. COA8 contains four conserved cysteine residues, two present within the MTS and two outside this region that are hypothesised to become redox regulated. Initial studies involving the use of GFP-tagged COA8 mutants in each of the Cys residues revealed that the Cys37Ala and Cys59Ala mutants displayed altered levels of import under conditions of $H_2O_2$ induced oxidative stress **(Fig 5.2)** (Erika Fernandez-Vizarra *et al.,* unpublished data). The Cys37Ala mutants displayed a reduced import while the Cys59Ala mutants demonstrated increased imports in response to $H_2O_2$ relative to the WT COA8 import. It is hypothesised that redox regulation of the cysteine residues by factors such as $H_2O_2$ may alter import capacity of COA8 protein. If true, this would demonstrate the first-time cysteine residues have been involved in regulating the import of a matrix-targeted protein.

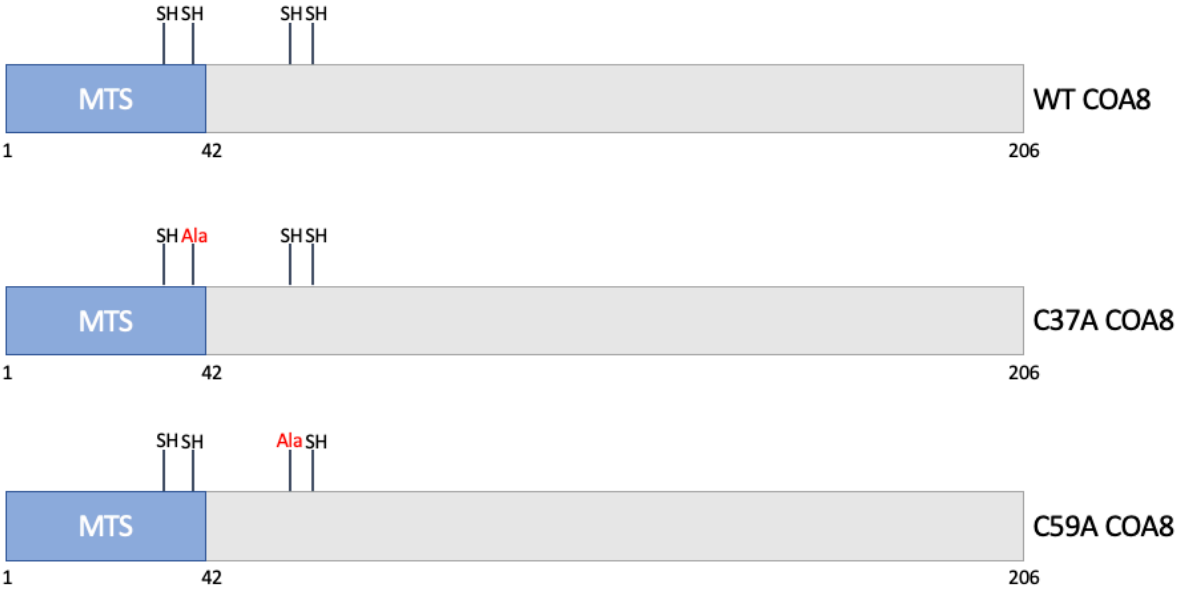


**Figure 5.2: Presence of conserved Cysteine Residues in COA8.** COA8 contains four conserved cysteine (-SH) residues in its sequence. Two of these residues are located within the mitochondrial targeting sequence and two out-with this region. The cysteines are located at residues 29, 37, 59 and 65. Mutant COA8 constructs were created mutating the either the cysteine 37 or 59 for an alanine (Ala) residue. These constructs were termed C37A COA8 and C59A COA8 respectively.

## 5.2 Aims

There were two main aims of this chapter. The first was to investigate the conditions under which COA8 could be translocated into either yeast or mammalian mitochondria and elucidate the components of the import machinery required for import. The second aim was to clone the C37A and C59A COA8 mutants into a pSP64/65 plasmid vector to allow radiolabelled expression of this protein for subsequent import assays. Generation of these constructs would enable the import of the mutants to be tested in response to oxidative stress conditions in vitro.

## 5.3 Results

### 5.3.1 The Import of COA8 into Yeast and Mammalian Mitochondria

Before the import capacity of the Cys mutant COA8 constructs could be tested, first the import of WT COA8 had to characterised. COA8 is only present in metazoans but due to the practical simplicity of the yeast mitochondria import system we first tested import in yeast mitochondria. There is the potential of artificial results associated with using this system. *S.cerevisiae* mitochondria can be stored at -80 without losing their Δψ, unlike those isolated from mammalian systems making them a much more robust system to study protein import. Initially a WT COA8 HA tagged protein construct was used while the untagged protein was cloned. COA8-HA was radiolabelled using the TNT coupled system and the resulting protein presented to WT yeast mitochondria for import.

The import results in **Fig 5.3** revealed that WT COA8-HA could not be imported into the yeast mitochondria system. The TNT system produces a ~20kDa protein corresponding to the WT COA8-HA protein as shown in the 5% control lane. Import reactions were performed in the presence or absence of the protease trypsin. When trypsin was added to the import lanes there was a significant loss in radioactive signal corresponding to the loss of COA8 protein. As COA8 was not imported into the mitochondria it was not protected from degradation. In the presence of membrane potential and trypsin there is a very faint band of COA8 present however it is not believed that this is the imported protein and in fact just over spill when loading the SDS gel as this band in the + trypsin lane was not seen in any subsequent import experiments. As COA8 is translated as a precursor protein, once inside the mitochondria it is

expected to be cleaved near the end of the MTS to produce the mature protein. As the molecular weight of the protein in this lane was the same as the minus trypsin lane then it was concluded to not be imported material. A smaller truncated form of COA8 was detected via autoradiography in both the control lanes and the import lanes. The MW is lower than the expected MW of COA8 and more experimental evidence was required to identify this translation product.

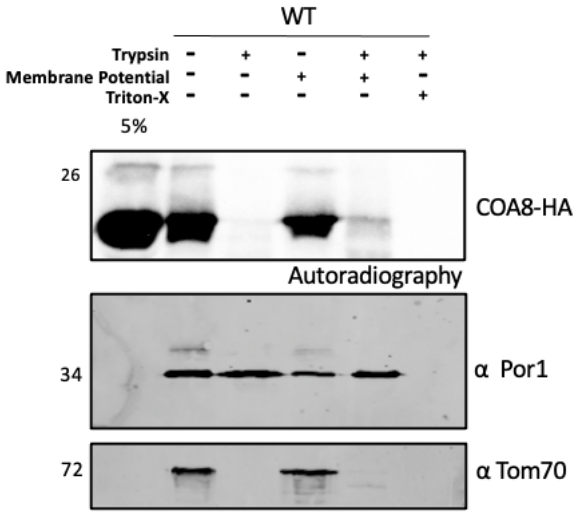


**Figure 5.3 - Import of radiolabelled Cytochrome C assembly factor 8 (COA8) into yeast mitochondria.** COA8-HA was translated as radiolabelled precursor and imported into isolated wild-type (WT) yeast mitochondria. Protein was imported for 30 minutes at 30°C and treated with Trypsin (0.1mg/ml) and SBTI (1mg/ml) post-import to degrade any unimported precursor proteins. Triton-X100 (Tx) (10%) was used alongside Trypsin as a negative control. 5% of the precursor protein presented to each of the import reactions was loaded as a positive control. Radioactive material was detected using a phosphoimager. Western blotting for Porin 1 (Por1) was used as a loading control and Tom70 to test for trypsinisation.

Western blotting of porin 1 (Por1) was used as loading control to determine equal loading. Tom70 was probed as a control for the trypsinisation as Tom70 is an OM protein with a large cytosolic domain. With the addition of trypsin this results in the degradation of this receptor which can be demonstrated in the western blot **(Fig 5.3)**. Following on from this result it was decided to continue with the yeast system and attempt to import COA8 under varying conditions. It was hypothesised that this protein may enter the mitochondria in a denatured form or even as a fully reduced protein due to the presence of cysteines that may form disulphide bonds. Following the radiolabelling process, the COA8 protein was suspended in a urea buffer (see section 2.3.4) to promote denaturation of the protein prior to import.

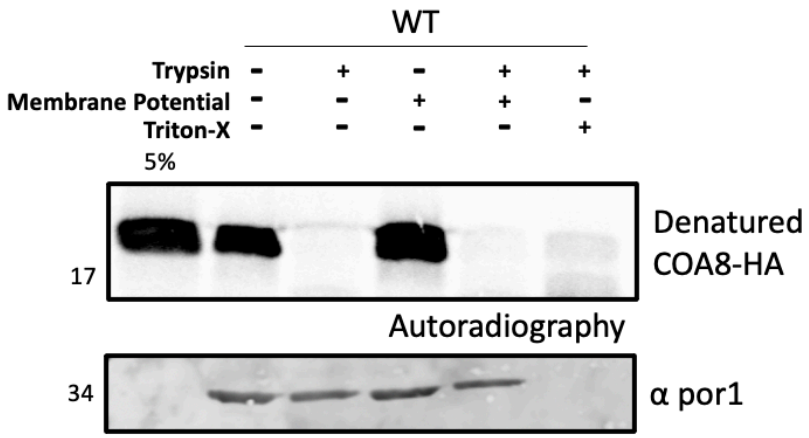


**Figure 5.4 - Import of radiolabelled Cytochrome C assembly factor 8 (COA8) into yeast mitochondria under denaturing conditions.** COA8-HA was translated as radiolabelled precursor and denatured and reduced in urea buffer prior to import. Protein was subsequently imported into isolated wild-type (WT) yeast mitochondria. for 30 minutes at 30$^{o}$C and treated with Trypsin (0.1mg/ml) and SBTI (1mg/ml) post import to degrade any unimported precursor proteins. Triton-X100 (Tx) (10%) was used alongside Trypsin as a negative control. 5% of the precursor protein presented to each of the import reactions was loaded as a positive control. Radioactive material was detected using a phosphoimager. Western blotting for Porin 1 (Por1) was used as a loading control.

Despite attempts to denature the protein to promote its import the COA8 was still unsuccessfully imported into the yeast mitochondria **(Fig 5.4)**. Again, in the presence of trypsin COA8 was susceptible to protease degradation and therefore not protected inside the mitochondria. As stated above COA8 is not found in yeast or fungi so it was concluded that the protein was just unable to be imported into this system. All subsequent import reactions involved the isolation of mitochondria from HEK293 cultured mammalian cells, where COA8 is natively found. The import of the tagged construct was repeated in the mammalian mitochondria.

Surprisingly, despite importing COA8 into a system where the protein is natively localised, it was found that the protein was still unable to be imported even into WT mammalian mitochondria under native conditions **(Fig 5.5)**. Once the untagged COA8 construct was successfully cloned, the import was again tested into HEK293 isolated mitochondria in case the presence of the tag was interfering with the import capacity of the protein.

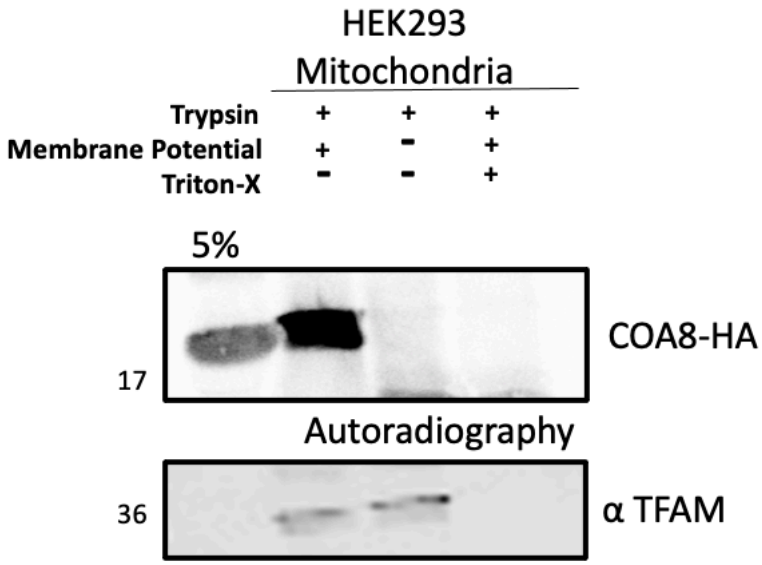


**Figure 5.5 - Import of radiolabelled Cytochrome C assembly factor 8 (COA8) into mammalian mitochondria.** COA8-HA was translated as radiolabelled precursor and imported into isolated wild-type (WT) HEK293 isolated mitochondria. Protein was imported for 30 minutes at 30°C and treated with Trypsin (0.05mg/ml) and SBTI (0.5mg/ml) post import to degrade any unimported precursor proteins. Triton-X100 (Tx) (10%) was used alongside Trypsin as a negative control. 5% of the precursor protein presented to each of the import reactions was loaded as a positive control. Radioactive material was detected using a phosphoimager. Western blotting for TFAM was used as a loading control.

The import of WT COA8 into the HEK293 mitochondria in the presence or absence of 1mM $H_2O_2$ was tested. $H_2O_2$ was added to induce oxidative stress conditions for the mitochondria which may promote the import of COA8 and speed up the import kinetics. Unfortunately, the import was unsuccessful, and despite a smear of radioactivity detected no clear band of COA8 was protected from proteolytic degradation **(Fig 5.6)**. The induction of oxidative stress had no effect on the import capacity of COA8 either. Western blotting of the mammalian protein TFAM confirmed equal loading of mitochondria into the import lanes.

### 5.3.2 Cloning of the COA8 Cysteine Mutant Constructs

Concurrent to the COA8 import experiments cloning work was undertaken to clone WT and cysteine mutant COA8 sequences into the pSP64 plasmid vector to allow radiolabelled translation of the encoded proteins for subsequent import experiments. PCR was initially used to amplify the COA8 sequences using the primer sequences detailed in **Table 2.2.**

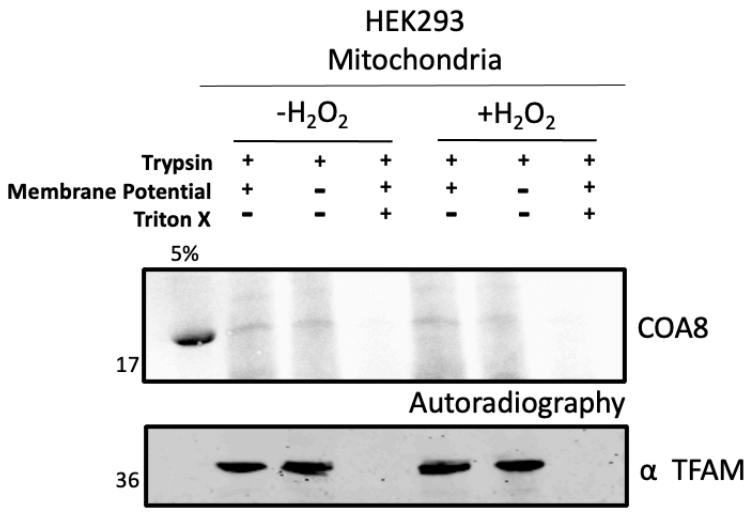


**Figure 5.6 - Import of radiolabelled Cytochrome C assembly factor 8 (COA8) into mammalian mitochondria under oxidative stress conditions.** COA8 was translated as radiolabelled precursor and imported into isolated wild-type (WT) HEK293 isolated mitochondria in the presence or absence of 1mM $H_2O_2$. Protein was imported for 30 minutes at 30$^{o}$C and treated with Trypsin (0.05mg/ml) and SBTI (0.5mg/ml) post import to degrade any unimported precursor proteins. Triton-X100 (Tx) (10%) was used alongside Trypsin as a negative control. 5% of the precursor protein presented to each of the import reactions was loaded as a positive control. Radioactive material was detected using a phosphoimager. Western blotting for TFAM was used as a loading control.

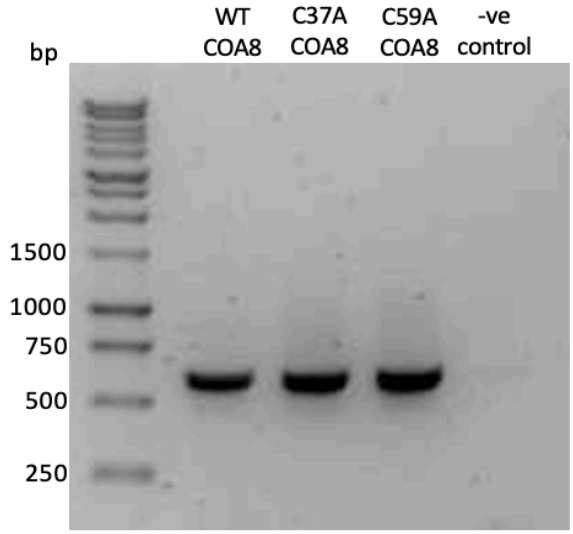


**Figure 5.7: PCR amplification of COA8 sequences.** Cytochrome C Oxidase Assembly Factor 8 (COA8) constructs were amplified via PCR using Taq polymerase. The PCR products were separated by electrophoresis on a 1.25% TAE agarose gel stained with SYBR safe. Lanes contain wild-type (WT), Cys39Ala (C37A) COA8, Cys59Ala (C59A) COA8, and water as a negative (-ve) control.

The resulting agarose gel demonstrated the successful amplification of the WT, C37A, and C59A COA8 sequences amplified through PCR generating a DNA fragment at approximately

600bp (Fig 5.6). Point mutations were incorporated from the use of specific primers to change Cysteine (C) to Alanine (A) at the desired residue. From here the Taq-amplified PCR products were sequenced to confirm introduction of the point mutation. PCR products were subsequently ligation into the pCR2.1 TOPO TA vector using T4 DNA ligase and transformed into DH5α cells using blue-white colony screening as a selection marker. White colonies were chosen as having been successfully transformed with the pCR2.1 COA8 containing vector and the resulting DNA miniprepped from overnight cultures.

Digestion reactions were carried out overnight to ensure COA8 sequence was present in the plasmid vector using the EcoR1 restriction enzyme.

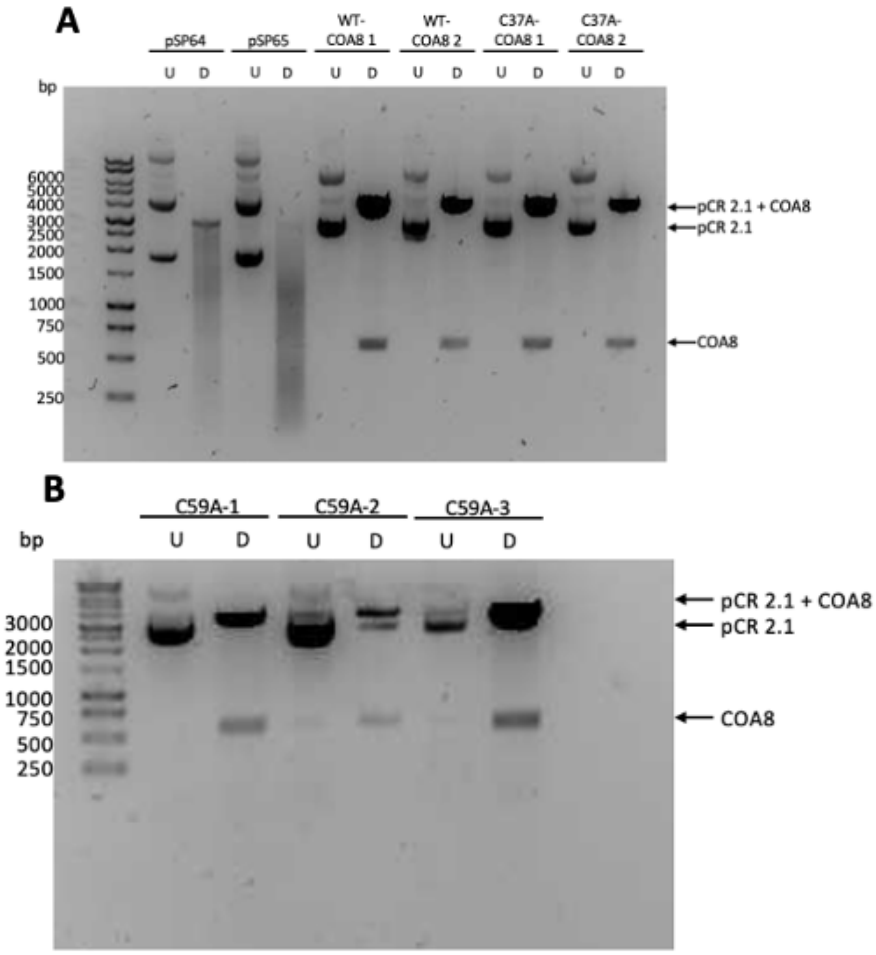


**Figure 5.8: Digestion of pCR2.1-COA8 sequences and pSP64/65 plasmids.** The pCR2.1 COA8 ligations and pSP64/65 plasmid vectors were digested using the EcoR1 restriction enzyme for 2 hours at 37°C. Wild-type (WT), Cys37Ala (C37A), and Cys59Ala (C59A) COA8 sequences were run. Undigested (U) samples run alongside the digested (D) samples as a control on a 1% agarose gel.

For the digestion of the COA8 constructs, the undigested lane revealed the presence of two high DNA base pair (bp) products that correspond to the size of the pCR2.1 with COA8 insert in either a coiled or supercoiled structure **(Fig 5.7)**. Following digestion (D) of the samples a new DNA product appeared at approximately 600bp that is the COA8 insert. This runs at the same bp as the PCR amplified COA8 constructs (Fig 5.6). The release of COA8 from the pCR2.1 digest was seen for the WT, C37A, and C59A constructs. pSP64/65 vectors were also digested with EcoR1 enzyme to linearise the vector for subsequent ligation of the COA8 constructs into this plasmid for TNT coupled translation of the protein. However, the digest of these vectors revealed a smear of DNA product that was not sufficient for subsequent ligation. The digest of the pSP64/65 vectors needs to be repeated before the ligation can be performed. Due to time constraints and issues with the in vitro import of COA8 into mitochondria the cloning project was put on hiatus.

## 5.4 Discussion

The main aim of this chapter was to elucidate how the redox regulation of cysteine residues in the sequence of COA8 affected the import of this matrix targeted protein into the mitochondria. However due to the difficulties in optimising the in vitro import of this protein into isolated mitochondria efforts to attempt to investigate this aim were largely unsuccessful.

### 5.4.1 Challenges Associated with the Import of COA8

The lack of COA8 import into WT yeast isolated mitochondria was not surprising due to the fact this protein is found in metazoans only but was worth testing due to the conserved homology of the components of the protein import machinery between yeast and mammals **(Fig 5.3)**. Attempts to import the protein in an unfolded state to aid passage through the TOM complex were also unsuccessful **(Fig 5.4)**. As a future experiment the COA8 protein could be incubated with DTT to fully reduce the cysteine residues in the sequence in the hopes this would leave COA8 in a conformation that is import capable. Ideally future in vitro imports should rely on using the mammalian mitochondrial system where this protein is natively found. Experiments involving reducing and denaturing the protein prior to import could be repeated using the mammalian system. Alternatively, it is possible that COA8 relies on other

cytoplasmic proteins for its import, and during the process to isolate mitochondria these import factors are lost. To compensate for this the cytoplasmic fraction of the cells produced during the mitochondrial preparation could be saved and supplemented into the import reaction mix. Potential cytoplasmic proteins in this fraction may aid or guide the import of COA8 into the mitochondria.

Until the optimum conditions to import even the WT COA8 into mitochondria can be determined the use of the in vitro import system to investigate how the cysteine COA8 mutants respond to oxidative stress cannot be tested. Work on cloning these mutant constructs is nearly complete, the digested COA8 proteins from the pCR2.1 vector are ready to be ligated into digested pSP64 vector and sequence for use in the TNT coupled system to radiolabel the protein for subsequent import experiments **(Fig 5.7)**. Experimental work was stopped at this stage due to the COVID-19 situation which resulted in a loss of time in the lab for over three months. Upon return to the lab much of the experimental research was focused on the Mxr2 chapters.

### 5.4.2 Future Research to Characterise the Redox Regulation and Links to COX Deficiency

Additional future work could characterise the oxidation stage of COA8 and that of the cysteine mutants using thiol trap assays. This involves the use of chemicals such as AMS that bind to free thiol groups in proteins. Using these assays, the oxidative state of COA8 could be compared between normal, hypoxic and $H_2O_2$ stressed conditions to determine if this alters the redox state of the protein. The mutant cysteine constructs could be tested to pinpoint which of the cysteine residues can become modified. While much of the research in this chapter focused on the C37 and C59 residues, the protein also possesses two others conserved Cys residues **(Fig 5.2)** that may also become modified, though this might not affect the import capacity. If the cysteines do undergo redox regulation in the mitochondria this introduces the possibility that these residues may in turn be reduced by reducing systems in the mitochondria such as the thioredoxin and peroxiredoxin systems introducing a new layer of regulation of COA8 inside the mitochondria (Holmgren and Lu, 2010; Perkins *et al.*, 2015).

Lastly patient derived fibroblasts cell lines are available isolated from individuals with characterised mutations in the *APOPT1* gene that manifests as mitochondrial leukoencephalopathy (Hedberg-Oldfors *et al.*, 2020). Due to the links with COX deficiency future work could aim to establish a clearer biochemical link between mutations in *APOPT1* and the clinical phenotype. Further research could aim to characterise the assembly state of the modules in these fibroblasts cell lines to determine a defect in COX assembly or alternatively monitor the enzymatic activity of this complex, under normal and stressed conditions.

# Bibliography


Aachmann, F. L. *et al.* (2011) 'Structural and biochemical analysis of mammalian methionine sulfoxide reductase B2', *Proteins: Structure, Function and Bioinformatics*, 79(11), pp. 3123–3131. doi: 10.1002/prot.23141.

Ahting, U. *et al.* (2001) 'Tom40, the pore-forming component of the protein-conducting TOM channel in the outer membrane of mitochondria', *Journal of Cell Biology*, 153(6), pp. 1151–1160. doi: 10.1083/jcb.153.6.1151.

Allen, S. *et al.* (2003) 'Juxtaposition of the two distal CX3C motifs via intrachain disulfide bonding is essential for the folding of Tim10', *Journal of Biological Chemistry*, 278(40), pp. 38505–38513. doi: 10.1074/jbc.M306027200.

Allen, S. *et al.* (2005) 'Erv1 mediates the Mia40-dependent protein import pathway and provides a functional link to the respiratory chain by shuttling electrons to cytochrome c', *Journal of Molecular Biology*, 353(5), pp. 937–944. doi: 10.1016/j.jmb.2005.08.049.

Allu, P. K. *et al.* (2015) 'Methionine sulfoxide reductase 2 reversibly regulates Mge1, a cochaperone of mitochondrial Hsp70, during oxidative stress', *Molecular Biology of the Cell*, 26(3), pp. 406–419. doi: 10.1091/mbc.E14-09-1371.

Araiso, Y. *et al.* (2019) 'Structure of the mitochondrial import gate reveals distinct preprotein paths', *Nature*, 575(7782), pp. 395–401. doi: 10.1038/s41586-019-1680-7.

Backes, S. *et al.* (2018) 'Tom70 enhances mitochondrial preprotein import efficiency by binding to internal targeting sequences', *Journal of Cell Biology*, 217(4), pp. 1369–1382. doi: 10.1083/jcb.201708044.

Baertling, F. *et al.* (2015) 'Mutations in COA6 cause cytochrome c oxidase deficiency and neonatal hypertrophic cardiomyopathy', *Human Mutation*, 36(1), pp. 34–38. doi: 10.1002/humu.22715.

Banci, L. *et al.* (2009) 'MIA40 is an oxidoreductase that catalyzes oxidative protein folding in mitochondria', *Nature Structural and Molecular Biology*, 16(2), pp. 198–206. doi: 10.1038/nsmb.1553.

Banci, L. *et al.* (2011) 'Molecular recognition and substrate mimicry drive the electron-transfer process between MIA40 and ALR', *Proceedings of the National Academy of Sciences of the United States of America*, 108(12), pp. 4811–4816. doi: 10.1073/pnas.1014542108.

Banci, L. *et al.* (2012) 'An electron-transfer path through an extended disulfide relay system: The case of the redox protein ALR', *Journal of the American Chemical Society*, 134(3), pp. 1442–1445. doi: 10.1021/ja209881f.

Banci, L. *et al.* (2013) 'An intrinsically disordered domain has a dual function coupled to compartment-dependent redox control', *Journal of Molecular Biology*, 425(3), pp. 594–608. doi: 10.1016/j.jmb.2012.11.032.

Bandara, P. D. S. *et al.* (1998) 'Involvement of the Saccharomyces cerevisiae UTH1 gene in the oxidative-stress response', *Current Genetics*, 34(4), pp. 259–268. doi: 10.1007/s002940050395.

Barchiesi, A. *et al.* (2020) 'Mitochondrial Oxidative Stress Induces Rapid Intermembrane Space/Matrix Translocation of Apurinic/Apyrimidinic Endonuclease 1 Protein through TIM23 Complex', *Journal of Molecular Biology*, 432(24). doi: 10.1016/j.jmb.2020.11.012.

Bausewein, T. *et al.* (2017) 'Cryo-EM Structure of the TOM Core Complex from Neurospora crassa', *Cell*, 170(4), pp. 693-700.e7. doi: 10.1016/j.cell.2017.07.012.

Becker, L. *et al.* (2005) 'Preprotein translocase of the outer mitochondrial membrane: Reconstituted Tom40 forms a characteristic TOM pore', *Journal of Molecular Biology*, 353(5),

pp. 1011–1020. doi: 10.1016/j.jmb.2005.09.019.
Becker, T. *et al.* (2010) 'Assembly of the mitochondrial protein import channel: Role of Tom5 in two-stage interaction of Tom40 with the SAM complex', *Molecular Biology of the Cell*, 21(18), pp. 3106–3113. doi: 10.1091/mbc.E10-06-0518.
Becker, T. *et al.* (2011) 'The mitochondrial import protein Mim1 promotes biogenesis of multispanning outer membrane proteins', *Journal of Cell Biology*, 194(3), pp. 387–395. doi: 10.1083/jcb.201102044.
Beverly, K. N. *et al.* (2008) 'The Tim8-Tim13 Complex Has Multiple Substrate Binding Sites and Binds Cooperatively to Tim23', *Journal of Molecular Biology*, 382(5), pp. 1144–1156. doi: 10.1016/j.jmb.2008.07.069.
Boschi-Muller, S. *et al.* (2005) 'The enzymology and biochemistry of methionine sulfoxide reductases', *Biochimica et Biophysica Acta - Proteins and Proteomics*, pp. 231–238. doi: 10.1016/j.bbapap.2004.09.016.
Boschi-Muller, S., Gand, A. and Branlant, G. (2008) 'The methionine sulfoxide reductases: Catalysis and substrate specificities', *Archives of Biochemistry and Biophysics*, pp. 266–273. doi: 10.1016/j.abb.2008.02.007.
Bourens, M. *et al.* (2013) 'Redox and reactive oxygen species regulation of mitochondrial cytochrome C oxidase biogenesis', *Antioxidants and Redox Signaling*, pp. 1940–1952. doi: 10.1089/ars.2012.4847.
Boveris, A. *et al.* (2006) 'Mitochondrial metabolic states regulate nitric oxide and hydrogen peroxide diffusion to the cytosol', *Biochimica et Biophysica Acta - Bioenergetics*, 1757(5–6), pp. 535–542. doi: 10.1016/j.bbabio.2006.02.010.
Brachmann, C. B. *et al.* (1998) 'Designer Deletion Strains derived from', *Yeast*, 132(2), pp. 115–132.
Brand, M. D. (2010) 'The sites and topology of mitochondrial superoxide production', *Experimental Gerontology*, 45(7–8), pp. 466–472. doi: 10.1016/j.exger.2010.01.003.
Brand, M. D. (2016) 'Mitochondrial generation of superoxide and hydrogen peroxide as the source of mitochondrial redox signaling', *Free Radical Biology and Medicine*, pp. 14–31. doi: 10.1016/j.freeradbiomed.2016.04.001.
Brix, J., Dietmeier, K. and Pfanner, N. (1997) 'Differential recognition of preproteins by the purified cytosolic domains of the mitochondrial import receptors Tom20, Tom22, and Tom70', *Journal of Biological Chemistry*, 272(33), pp. 20730–20735. doi: 10.1074/jbc.272.33.20730.
Cabreiro, F. *et al.* (2006) 'Methionine sulfoxide reductases: Relevance to aging and protection against oxidative stress', in *Annals of the New York Academy of Sciences*, pp. 37–44. doi: 10.1196/annals.1354.006.
Callegari, S. *et al.* (2019) 'A MICOS–TIM22 Association Promotes Carrier Import into Human Mitochondria', *Journal of Molecular Biology*, 431(15), pp. 2835–2851. doi: 10.1016/j.jmb.2019.05.015.
Camougrand, N. *et al.* (2003) 'The product of the UTH1 gene, required for Bax-induced cell death in yeast, is involved in the response to rapamycin', *Molecular Microbiology*, 47(2), pp. 495–506. doi: 10.1046/j.1365-2958.2003.03311.x.
Cao, Z. *et al.* (2018) 'Methionine sulfoxide reductase B3 requires resolving cysteine residues for full activity and can act as a stereospecific methionine oxidase', *Biochemical Journal*, 475(4), pp. 827–838. doi: 10.1042/BCJ20170929.
Chacinska, A. *et al.* (2004) 'Essential role of Mia40 in import and assembly of mitochondrial intermembrane space proteins', *EMBO Journal*, 23(19), pp. 3735–3746. doi:

10.1038/sj.emboj.7600389.
Chacinska, A. *et al.* (2010) 'Distinct Forms of Mitochondrial TOM-TIM Supercomplexes Define Signal-Dependent States of Preprotein Sorting', *Molecular and Cellular Biology*, 30(1), pp. 307–318. doi: 10.1128/mcb.00749-09.
Chan, N. C. and Lithgow, T. (2008) 'The peripheral membrane subunits of the SAM complex function codependently in mitochondrial outer membrane biogenesis', *Molecular Biology of the Cell*, 19(1), pp. 126–136. doi: 10.1091/mbc.E07-08-0796.
Chatzi, A. *et al.* (2013) 'Biogenesis of yeast Mia40 - Uncoupling folding from import and atypical recognition features', in *FEBS Journal*, pp. 4960–4969. doi: 10.1111/febs.12482.
Court, D. A. *et al.* (1996) 'Role of the intermembrane-space domain of the preprotein receptor Tom22 in protein import into mitochondria', *Molecular and Cellular Biology*, 16(8), pp. 4035–4042. doi: 10.1128/mcb.16.8.4035.
Cox, A. G., Winterbourn, C. C. and Hampton, M. B. (2010) 'Mitochondrial peroxiredoxin involvement in antioxidant defence and redox signalling', *Biochemical Journal*, pp. 313–325. doi: 10.1042/BJ20091541.
Curran, S. P. *et al.* (2004) 'The role of Hot13p and redox chemistry in the mitochondrial TIM22 import pathway', *Journal of Biological Chemistry*, 279(42), pp. 43744–43751. doi: 10.1074/jbc.M404878200.
D'Silva, P. *et al.* (2004) 'Regulated interactions of mtHsp70 with Tim44 at the translocon in the mitochondrial inner membrane', *Nature Structural and Molecular Biology*, 11(11), pp. 1084–1091. doi: 10.1038/nsmb846.
Dabir, D. V. *et al.* (2007) 'A role for cytochrome c and cytochrome c peroxidase in electron shuttling from Erv1', *EMBO Journal*, 26(23), pp. 4801–4811. doi: 10.1038/sj.emboj.7601909.
Daithankar, V. N. *et al.* (2012) 'Flavin-linked erv-family sulfhydryl oxidases release superoxide anion during catalytic turnover', *Biochemistry*, 51(1), pp. 265–272. doi: 10.1021/bi201672h.
Daithankar, V. N., Farrell, S. R. and Thorpe, C. (2009) 'Augmenter of liver regeneration: Substrate specificity of a flavin-dependent oxidoreductase from the mitochondrial intermembrane space', *Biochemistry*, 48(22), pp. 4828–4837. doi: 10.1021/bi900347v.
Davis, A. J. *et al.* (2007) 'The Tim9p/10p and Tim8p/13p complexes bind to specific sites on Tim23p during mitochondrial protein import', *Molecular Biology of the Cell*, 18(2), pp. 475–486. doi: 10.1091/mbc.E06-06-0546.
Dayan, D. *et al.* (2019) 'A mutagenesis analysis of Tim50, the major receptor of the TIM23 complex, identifies regions that affect its interaction with Tim23', *Scientific Reports*, 9(1). doi: 10.1038/s41598-018-38353-1.
Delaunay, A., Isnard, A. D. and Toledano, M. B. (2000) 'H2O2 sensing through oxidation of the Yap1 transcription factor', *EMBO Journal*, 19(19), pp. 5157–5166. doi: 10.1093/emboj/19.19.5157.
Dembowski, M. *et al.* (2001) 'Assembly of Tom6 and Tom7 into the TOM Core Complex of Neurospora crassa', *Journal of Biological Chemistry*, 276(21), pp. 17679–17685. doi: 10.1074/jbc.M009653200.
Dimmer, K. S. *et al.* (2012) 'A crucial role for Mim2 in the biogenesis of mitochondrial outer membrane proteins', *Journal of Cell Science*, 125(14), pp. 3464–3473. doi: 10.1242/jcs.103804.
Dogan, S. A. *et al.* (2018) 'Perturbed Redox Signaling Exacerbates a Mitochondrial Myopathy', *Cell Metabolism*, 28(5), pp. 764-775.e5. doi: 10.1016/j.cmet.2018.07.012.
Esaki, M. *et al.* (2003) 'Tom40 protein import channel binds to non-native proteins and prevents their aggregation', *Nature Structural Biology*, 10(12), pp. 988–994. doi:

10.1038/nsb1008.
Esaki, M. *et al.* (2004) 'Mitochondrial protein import. Requirement of presequence elements and TOM components for precursor binding to the TOM complex', *Journal of Biological Chemistry*, 279(44), pp. 45701–45707. doi: 10.1074/jbc.M404591200.
Feinberg, B. A., Bedore, J. E. and Ferguson-Miller, S. (1986) 'Methionine-80-sulfoxide cytochrome c: preparation, purification and electron-transfer capabilities', *BBA - Bioenergetics*, 851(2), pp. 157–165. doi: 10.1016/0005-2728(86)90121-0.
Fernandez-Vizarra, E. and Zeviani, M. (2021) 'Mitochondrial disorders of the OXPHOS system', *FEBS Letters*, pp. 1062–1106. doi: 10.1002/1873-3468.13995.
Di Fonzo, A. *et al.* (2009) 'The Mitochondrial Disulfide Relay System Protein GFER Is Mutated in Autosomal-Recessive Myopathy with Cataract and Combined Respiratory-Chain Deficiency', *American Journal of Human Genetics*, 84(5), pp. 594–604. doi: 10.1016/j.ajhg.2009.04.004.
Fukasawa, Y. *et al.* (2015) 'MitoFates: Improved prediction of mitochondrial targeting sequences and their cleavage sites', *Molecular and Cellular Proteomics*, 14(4), pp. 1113–1126. doi: 10.1074/mcp.M114.043083.
Gabbita, S. P. *et al.* (1999) 'Decrease in peptide methionine sulfoxide reductase in Alzheimer's disease brain', *Journal of Neurochemistry*, 73(4), pp. 1660–1666. doi: 10.1046/j.1471-4159.1999.0731660.x.
Gabriel, K. *et al.* (2007) 'Novel Mitochondrial Intermembrane Space Proteins as Substrates of the MIA Import Pathway', *Journal of Molecular Biology*, 365(3), pp. 612–620. doi: 10.1016/j.jmb.2006.10.038.
Gabriel, K., Egan, B. and Lithgow, T. (2003) 'Tom40, the import channel of the mitochondrial outer membrane, plays an active role in sorting imported proteins', *EMBO Journal*, 22(10), pp. 2380–2386. doi: 10.1093/emboj/cdg229.
Geldon, S., Fernández-Vizarra, E. and Tokatlidis, K. (2021) 'Redox-Mediated Regulation of Mitochondrial Biogenesis, Dynamics, and Respiratory Chain Assembly in Yeast and Human Cells', *Frontiers in Cell and Developmental Biology*, 9(September), pp. 1–24. doi: 10.3389/fcell.2021.720656.
Ghafourifar, P. and Cadenas, E. (2005) 'Mitochondrial nitric oxide synthase', *Trends in Pharmacological Sciences*, pp. 190–195. doi: 10.1016/j.tips.2005.02.005.
Gladyck, S. *et al.* (2021) 'Regulation of COX Assembly and Function by Twin CX9C Proteins-Implications for Human Disease', *Cells*. doi: 10.3390/cells10020197.
Glick, B. S. (1991) 'Chapter 20 Protein Import into Isolated Yeast Mitochondria', *Methods in Cell Biology*, 34(C), pp. 389–399. doi: 10.1016/S0091-679X(08)61693-3.
Gomes, F. *et al.* (2017) 'Proteolytic cleavage by the inner membrane peptidase (IMP) complex or Oct1 peptidase controls the localization of the yeast peroxiredoxin Prx1 to distinct mitochondrial compartments', *Journal of Biological Chemistry*, 292(41), pp. 17011–17024. doi: 10.1074/jbc.M117.788588.
Grevel, A., Pfanner, N. and Becker, T. (2019) 'Coupling of import and assembly pathways in mitochondrial protein biogenesis', *Biological Chemistry*. doi: 10.1515/hsz-2019-0310.
Groß, D. P. *et al.* (2011) 'Mitochondrial Ccs1 contains a structural disulfide bond crucial for the import of this unconventional substrate by the disulfide relay system', *Molecular Biology of the Cell*, 22(20), pp. 3758–3767. doi: 10.1091/mbc.E11-04-0296.
Guerra-Castellano, A. *et al.* (2018) 'Oxidative stress is tightly regulated by cytochrome c phosphorylation and respirasome factors in mitochondria', *Proceedings of the National Academy of Sciences of the United States of America*, 115(31), pp. 7955–7960. doi:

10.1073/pnas.1806833115.
Habich, M. *et al.* (2019) 'Vectorial Import via a Metastable Disulfide-Linked Complex Allows for a Quality Control Step and Import by the Mitochondrial Disulfide Relay', *Cell Reports*, 26(3), pp. 759-774.e5. doi: 10.1016/j.celrep.2018.12.092.
Habich, M., Salscheider, S. L. and Riemer, J. (2019) 'Cysteine residues in mitochondrial intermembrane space proteins: more than just import', *British Journal of Pharmacology*, pp. 514–531. doi: 10.1111/bph.14480.
Han, D. *et al.* (2003) 'Voltage-dependent anion channels control the release of the superoxide anion from mitochondria to cytosol', *Journal of Biological Chemistry*, 278(8), pp. 5557–5563. doi: 10.1074/jbc.M210269200.
Hangen, E. *et al.* (2015) 'Interaction between AIF and CHCHD4 Regulates Respiratory Chain Biogenesis', *Molecular Cell*, 58(6), pp. 1001–1014. doi: 10.1016/j.molcel.2015.04.020.
Hansen, K. G. and Herrmann, J. M. (2019) 'Transport of Proteins into Mitochondria', *Protein Journal*. doi: 10.1007/s10930-019-09819-6.
Hartley, A. M. *et al.* (2019) 'Structure of yeast cytochrome c oxidase in a supercomplex with cytochrome bc 1', *Nature Structural and Molecular Biology*, 26(1), pp. 78–83. doi: 10.1038/s41594-018-0172-z.
Hedberg-Oldfors, C. *et al.* (2020) 'COX deficiency and leukoencephalopathy due to a novel homozygous APOPT1/COA8 mutation', *Neurology: Genetics*, 6(4). doi: 10.1212/NXG.0000000000000464.
von Heijne, G. (1986) 'Mitochondrial targeting sequences may form amphiphilic helices.', *The EMBO journal*, 5(6), pp. 1335–1342. doi: 10.1002/j.1460-2075.1986.tb04364.x.
Hell, K., Neupert, W. and Stuart, R. A. (2001) 'Oxa1p acts as a general membrane insertion machinery for proteins encoded by mitochondrial DNA', *EMBO Journal*, 20(6), pp. 1281–1288. doi: 10.1093/emboj/20.6.1281.
Hofmann, S. *et al.* (2005) 'Functional and mutational characterization of human MIA40 acting during import into the mitochondrial intermembrane space', *Journal of Molecular Biology*, 353(3), pp. 517–528. doi: 10.1016/j.jmb.2005.08.064.
Holmgren, A. and Lu, J. (2010) 'Thioredoxin and thioredoxin reductase: Current research with special reference to human disease', *Biochemical and Biophysical Research Communications*, 396(1), pp. 120–124. doi: 10.1016/j.bbrc.2010.03.083.
Holmström, K. M. and Finkel, T. (2014) 'Cellular mechanisms and physiological consequences of redox-dependent signalling', *Nature Reviews Molecular Cell Biology*, pp. 411–421. doi: 10.1038/nrm3801.
Iñarrea, P. *et al.* (2005) 'Redox activation of mitochondrial intermembrane space Cu,Zn-superoxide dismutase', *Biochemical Journal*, 387(1), pp. 203–209. doi: 10.1042/BJ20041683.
Iñarrea, P. *et al.* (2007) 'Mitochondrial respiratory chain and thioredoxin reductase regulate intermembrane Cu,Zn-superoxide dismutase activity: Implications for mitochondrial energy metabolism and apoptosis', *Biochemical Journal*, 405(1), pp. 173–179. doi: 10.1042/BJ20061809.
Ivanetich, K. M., Bradshaw, J. J. and Kaminsky, L. S. (1976) 'Methionine Sulfoxide Cytochrome c', *Biochemistry*, 15(5), pp. 1144–1153. doi: 10.1021/bi00650a029.
Jenkins, C. M. *et al.* (2018) 'Cytochrome c is an oxidative stress–activated plasmalogenase that cleaves plasmenylcholine and plasmenylethanolamine at the sn-1 vinyl ether linkage', *Journal of Biological Chemistry*, 293(22), pp. 8693–8709. doi: 10.1074/jbc.RA117.001629.
Jensen, R. E. and Johnson, A. E. (2001) 'Opening the door to mitochondrial protein import', *Nature Structural Biology*, pp. 1008–1010. doi: 10.1038/nsb1201-1008.

Ji, L. L. and Yeo, D. (2021) 'Oxidative stress: an evolving definition', *Faculty Reviews*, 10. doi: 10.12703/r/10-13.
Kallergi, E. *et al.* (2012) 'Targeting and maturation of Erv1/ALR in the mitochondrial intermembrane space', *ACS Chemical Biology*, 7(4), pp. 707–714. doi: 10.1021/cb200485b.
Kang, Y. *et al.* (2017) 'Sengers Syndrome-Associated Mitochondrial Acylglycerol Kinase Is a Subunit of the Human TIM22 Protein Import Complex', *Molecular Cell*, 67(3), pp. 457-470.e5. doi: 10.1016/j.molcel.2017.06.014.
Kang, Y. *et al.* (2019) 'Function of hTim8a in complex IV assembly in neuronal cells provides insight into pathomechanism underlying mohr-tranebjærg syndrome', *eLife*, 8. doi: 10.7554/eLife.48828.
Kawano, S. *et al.* (2009) 'Structural basis of yeast Tim40/Mia40 as an oxidative translocator in the mitochondrial intermembrane space', *Proceedings of the National Academy of Sciences of the United States of America*, 106(34), pp. 14403–14407. doi: 10.1073/pnas.0901793106.
Kaya, A. *et al.* (2010a) 'Compartmentalization and regulation of mitochondrial function by methionine sulfoxide reductases in yeast', *Biochemistry*, 49(39), pp. 8618–8625. doi: 10.1021/bi100908v.
Kaya, A. *et al.* (2010b) 'Compartmentalization and regulation of mitochondrial function by methionine sulfoxide reductases in yeast', *Biochemistry*, 49(39), pp. 8618–8625. doi: 10.1021/bi100908v.
Khalimonchuk, O. and Winge, D. R. (2008) 'Function and redox state of mitochondrial localized cysteine-rich proteins important in the assembly of cytochrome c oxidase', *Biochimica et Biophysica Acta - Molecular Cell Research*, pp. 618–628. doi: 10.1016/j.bbamcr.2007.10.016.
Kim, H. Y. and Gladyshev, V. N. (2004) 'Methionine Sulfoxide Reduction in Mammals: Characterization of Methionine-R-Sulfoxide Reductases', *Molecular Biology of the Cell*, 15(3), pp. 1055–1064. doi: 10.1091/mbc.E03-08-0629.
Kim, H. Y. and Kim, J. R. (2008) 'Thioredoxin as a reducing agent for mammalian methionine sulfoxide reductases B lacking resolving cysteine', *Biochemical and Biophysical Research Communications*, 371(3), pp. 490–494. doi: 10.1016/j.bbrc.2008.04.101.
Kimura, Y., Goto, Y. I. and Kimura, H. (2010) 'Hydrogen sulfide increases glutathione production and suppresses oxidative stress in mitochondria', *Antioxidants and Redox Signaling*, 12(1), pp. 1–13. doi: 10.1089/ars.2008.2282.
Kiššová, I. *et al.* (2004) 'Uth1p is involved in the autophagic degradation of mitochondria', *Journal of Biological Chemistry*, 279(37), pp. 39068–39074. doi: 10.1074/jbc.M406960200.
Klein, A. *et al.* (2012) 'Characterization of the insertase for β-barrel proteins of the outer mitochondrial membrane', *Journal of Cell Biology*, 199(4), pp. 599–611. doi: 10.1083/jcb.201207161.
Koch, J. R. and Schmid, F. X. (2014a) 'Mia40 combines thiol oxidase and disulfide isomerase activity to efficiently catalyze oxidative folding in mitochondria', *Journal of Molecular Biology*, 426(24), pp. 4087–4098. doi: 10.1016/j.jmb.2014.10.022.
Koch, J. R. and Schmid, F. X. (2014b) 'Mia40 targets cysteines in a hydrophobic environment to direct oxidative protein folding in the mitochondria', *Nature Communications*, 5. doi: 10.1038/ncomms4041.
Koehler, C. M. *et al.* (1999) 'Human deafness dystonia syndrome is a mitochondrial disease', *Proceedings of the National Academy of Sciences of the United States of America*, 96(5), pp. 2141–2146. doi: 10.1073/pnas.96.5.2141.
Koehler, C. M. (2004) 'The small Tim proteins and the twin Cx3C motif', *Trends in Biochemical*

*Sciences*, pp. 1–4. doi: 10.1016/j.tibs.2003.11.003.
Kritsiligkou, P. *et al.* (2017) 'Unconventional Targeting of a Thiol Peroxidase to the Mitochondrial Intermembrane Space Facilitates Oxidative Protein Folding', *Cell Reports*, 18(11), pp. 2729–2741. doi: 10.1016/j.celrep.2017.02.053.
Krüger, V. *et al.* (2017) 'Identification of new channels by systematic analysis of the mitochondrial outer membrane', *Journal of Cell Biology*, 216(11), pp. 3485–3495. doi: 10.1083/jcb.201706043.
Kutik, S. *et al.* (2008) 'Dissecting Membrane Insertion of Mitochondrial β-Barrel Proteins', *Cell*, 132(6), pp. 1011–1024. doi: 10.1016/j.cell.2008.01.028.
Lambert, A. J. and Brand, M. D. (2009) 'Reactive oxygen species production by mitochondria.', *Methods in molecular biology (Clifton, N.J.)*, pp. 165–181. doi: 10.1007/978-1-59745-521-3_11.
Lange, H. *et al.* (2001) 'An essential function of the mitochondrial sulfhydryl oxidase Erv1p/ALR in the maturation of cytosolic Fe/S proteins', *EMBO Reports*, 2(8), pp. 715–720. doi: 10.1093/embo-reports/kve161.
Le, D. T. *et al.* (2009) 'Functional analysis of free methionine-R-sulfoxide reductase from saccharomyces cerevisiae', *Journal of Biological Chemistry*, 284(7), pp. 4354–4364. doi: 10.1074/jbc.M805891200.
Lee, S. *et al.* (2020) 'The Mgr2 subunit of the TIM23 complex regulates membrane insertion of marginal stop-transfer signals in the mitochondrial inner membrane', *FEBS Letters*, 594(6), pp. 1081–1087. doi: 10.1002/1873-3468.13692.
Letts, J. A. and Sazanov, L. A. (2017) 'Clarifying the supercomplex: The higher-order organization of the mitochondrial electron transport chain', *Nature Structural and Molecular Biology*, pp. 800–808. doi: 10.1038/nsmb.3460.
Lionaki, E. *et al.* (2010) 'The N-terminal shuttle domain of Erv1 determines the affinity for Mia40 and mediates electron transfer to the catalytic Erv1 core in yeast mitochondria', *Antioxidants and Redox Signaling*, 13(9), pp. 1327–1339. doi: 10.1089/ars.2010.3200.
Lobo-Jarne, T. and Ugalde, C. (2018) 'Respiratory chain supercomplexes: Structures, function and biogenesis', *Seminars in Cell and Developmental Biology*, pp. 179–190. doi: 10.1016/j.semcdb.2017.07.021.
Longen, S. *et al.* (2009) 'Systematic Analysis of the Twin Cx9C Protein Family', *Journal of Molecular Biology*, 393(2), pp. 356–368. doi: 10.1016/j.jmb.2009.08.041.
Lu, H. *et al.* (2004) 'Functional TIM10 Chaperone Assembly Is Redox-regulated in Vivo', *Journal of Biological Chemistry*, 279(18), pp. 18952–18958. doi: 10.1074/jbc.M313045200.
De Luca, A. *et al.* (2010) 'Methionine sulfoxide reductase A down-regulation in human breast cancer cells results in a more aggressive phenotype', *Proceedings of the National Academy of Sciences of the United States of America*, 107(43), pp. 18628–18633. doi: 10.1073/pnas.1010171107.
Luttik, M. A. H. *et al.* (1998) 'The Saccharomyces cerevisiae NDE1 and NDE2 genes encode separate mitochondrial NADH dehydrogenases catalyzing the oxidation of cytosolic NADH', *Journal of Biological Chemistry*, 273(38), pp. 24529–24534. doi: 10.1074/jbc.273.38.24529.
Makki, A. *et al.* (2019) 'Triplet-pore structure of a highly divergent TOM complex of hydrogenosomes in Trichomonas vaginalis', *PLoS Biology*, 17(1). doi: 10.1371/journal.pbio.3000098.
Marada, A. *et al.* (2013) 'Mge1, a nucleotide exchange factor of Hsp70, acts as an oxidative sensor to regulate mitochondrial Hsp70 function', *Molecular Biology of the Cell*, 24(6), pp. 692–703. doi: 10.1091/mbc.E12-10-0719.

Mårtensson, C. U. *et al.* (2019) 'Mitochondrial protein translocation-associated degradation', *Nature*, 569(7758), pp. 679–683. doi: 10.1038/s41586-019-1227-y.
Massa, V. *et al.* (2008) 'Severe Infantile Encephalomyopathy Caused by a Mutation in COX6B1, a Nucleus-Encoded Subunit of Cytochrome C Oxidase', *American Journal of Human Genetics*, 82(6), pp. 1281–1289. doi: 10.1016/j.ajhg.2008.05.002.
Matta, S. K., Kumar, A. and D'Silva, P. (2020) 'Mgr2 regulates mitochondrial preprotein import by associating with channel-forming Tim23 subunit', *Molecular Biology of the Cell*, 31(11), pp. 1112–1123. doi: 10.1091/MBC.E19-12-0677.
Mayer, M. P. and Bukau, B. (2005) 'Hsp70 chaperones: Cellular functions and molecular mechanism', *Cellular and Molecular Life Sciences*, pp. 670–684. doi: 10.1007/s00018-004-4464-6.
Melchionda, L. *et al.* (2014) 'Mutations in APOPT1, encoding a mitochondrial protein, cause cavitating leukoencephalopathy with cytochrome c oxidase deficiency', *American Journal of Human Genetics*, 95(3), pp. 315–325. doi: 10.1016/j.ajhg.2014.08.003.
Mesecke, N. *et al.* (2005) 'A disulfide relay system in the intermembrane space of mitochondria that mediates protein import', *Cell*, 121(7), pp. 1059–1069. doi: 10.1016/j.cell.2005.04.011.
Milenkovic, D. *et al.* (2007) 'Biogenesis of the essential Tim9-Tim10 chaperone complex of mitochondria: Site-specific recognition of cysteine residues by the intermembrane space receptor Mia40', *Journal of Biological Chemistry*, 282(31), pp. 22472–22480. doi: 10.1074/jbc.M703294200.
Milenkovic, D. *et al.* (2009) 'Identification of the signal directing Tim9 and Tim10 into the intermembrane space of mitochondria', *Molecular Biology of the Cell*, 20(10), pp. 2530–2539. doi: 10.1091/mbc.E08-11-1108.
Mohanraj, K. *et al.* (2019) 'Inhibition of proteasome rescues a pathogenic variant of respiratory chain assembly factor COA7', *EMBO Molecular Medicine*, 11(5). doi: 10.15252/emmm.201809561.
Muller, F. L., Liu, Y. and Van Remmen, H. (2004) 'Complex III releases superoxide to both sides of the inner mitochondrial membrane', *Journal of Biological Chemistry*, 279(47), pp. 49064–49073. doi: 10.1074/jbc.M407715200.
Murphy, M. P. (2009) 'How mitochondria produce reactive oxygen species', *Biochemical Journal*, pp. 1–13. doi: 10.1042/BJ20081386.
Murschall, L. M. *et al.* (2020) 'The C-terminal region of the oxidoreductase MIA40 stabilizes its cytosolic precursor during mitochondrial import', *BMC Biology*, 18(1). doi: 10.1186/s12915-020-00824-1.
Naoé, M. *et al.* (2004) 'Identification of Tim40 that mediates protein sorting to the mitochondrial intermembrane space', *Journal of Biological Chemistry*, 279(46), pp. 47815–47821. doi: 10.1074/jbc.M410272200.
Neal, S. E. *et al.* (2017) 'Osm1 facilitates the transfer of electrons from Erv1 to fumarate in the redox-regulated import pathway in the mitochondrial intermembrane space', *Molecular Biology of the Cell*, 28(21), pp. 2773–2785. doi: 10.1091/mbc.E16-10-0712.
Nicklow, E. E. and Sevier, C. S. (2020) 'Activity of the yeast cytoplasmic Hsp70 nucleotide-exchange factor Fes1 is regulated by reversible methionine oxidation', *Journal of Biological Chemistry*, 295(2), pp. 552–569. doi: 10.1074/jbc.RA119.010125.
Oien, D. B. *et al.* (2009) 'Clearance and phosphorylation of alpha-synuclein are inhibited in methionine sulfoxide reductase a null yeast cells', *Journal of Molecular Neuroscience*, 39(3), pp. 323–332. doi: 10.1007/s12031-009-9274-8.

Oien, D. B., Carrasco, G. A. and Moskovitz, J. (2011) 'Decreased Phosphorylation and Increased Methionine Oxidation of α-Synuclein in the Methionine Sulfoxide Reductase A Knockout Mouse', *Journal of Amino Acids*, 2011, pp. 1–6. doi: 10.4061/2011/721094.
Otera, H. *et al.* (2007) 'A novel insertion pathway of mitochondrial outer membrane proteins with multiple transmembrane segments', *Journal of Cell Biology*, 179(7), pp. 1355–1363. doi: 10.1083/jcb.200702143.
Pagliarini, D. J. *et al.* (2008) 'A Mitochondrial Protein Compendium Elucidates Complex I Disease Biology', *Cell*, 134(1), pp. 112–123. doi: 10.1016/j.cell.2008.06.016.
Pais, J. E., Schilke, B. and Craig, E. A. (2011) 'Reevaluation of the role of the Pam18:Pam16 interaction in translocation of proteins by the mitochondrial Hsp70-based import motor', *Molecular Biology of the Cell*, 22(24), pp. 4740–4749. doi: 10.1091/mbc.E11-08-0715.
Palmeira, C. M. *et al.* (2019) 'Mitohormesis and metabolic health: The interplay between ROS, cAMP and sirtuins', *Free Radical Biology and Medicine*, pp. 483–491. doi: 10.1016/j.freeradbiomed.2019.07.017.
Paschen, S. A. *et al.* (2003) 'Evolutionary conservation of biogenesis of β-barrel membrane proteins', *Nature*, 426(6968), pp. 862–866. doi: 10.1038/nature02208.
Paul, B. D., Snyder, S. H. and Kashfi, K. (2021) 'Effects of hydrogen sulfide on mitochondrial function and cellular bioenergetics', *Redox Biology*. doi: 10.1016/j.redox.2020.101772.
Peker, E. *et al.* (2021) 'Erv1 and Cytochrome c Mediate Rapid Electron Transfer via A Collision-Type Interaction', *Journal of Molecular Biology*, 433(15). doi: 10.1016/j.jmb.2021.167045.
Peleh, V., Cordat, E. and Herrmann, J. M. (2016) 'Mia40 is a trans-site receptor that drives protein import into the mitochondrial intermembrane space by hydrophobic substrate binding', *eLife*, 5(JUN2016). doi: 10.7554/eLife.16177.
Perkins, A. *et al.* (2015) 'Peroxiredoxins: Guardians against oxidative stress and modulators of peroxide signaling', *Trends in Biochemical Sciences*, pp. 435–445. doi: 10.1016/j.tibs.2015.05.001.
Petrungaro, C. *et al.* (2015) 'The Ca2+-dependent release of the Mia40-induced MICU1-MICU2 dimer from MCU regulates mitochondrial Ca2+ uptake', *Cell Metabolism*, 22(4), pp. 721–733. doi: 10.1016/j.cmet.2015.08.019.
Pfanner, N. *et al.* (1987) 'Mitochondrial protein import: involvement of the mature part of a cleavable precursor protein in the binding to receptor sites.', *The EMBO journal*, 6(11), pp. 3449–3454. doi: 10.1002/j.1460-2075.1987.tb02668.x.
Prakash, A. and Doublié, S. (2015) 'Base Excision Repair in the Mitochondria', *Journal of Cellular Biochemistry*, 116(8), pp. 1490–1499. doi: 10.1002/jcb.25103.
Qiu, J. *et al.* (2013) 'XCoupling of mitochondrial import and export translocases by receptor-mediated supercomplex formation', *Cell*, 154(3). doi: 10.1016/j.cell.2013.06.033.
Rak, M. *et al.* (2016) 'Mitochondrial cytochrome c oxidase deficiency', *Clinical Science*, 130(6). doi: 10.1042/CS20150707.
Rath, S. *et al.* (2021) 'MitoCarta3.0: An updated mitochondrial proteome now with sub-organelle localization and pathway annotations', *Nucleic Acids Research*, 49(D1), pp. D1541–D1547. doi: 10.1093/nar/gkaa1011.
Rathore, S. *et al.* (2019) 'Cryo-EM structure of the yeast respiratory supercomplex', *Nature Structural and Molecular Biology*, 26(1), pp. 50–57. doi: 10.1038/s41594-018-0169-7.
Reczek, C. R. and Chandel, N. S. (2015) 'ROS-dependent signal transduction', *Current Opinion in Cell Biology*, pp. 8–13. doi: 10.1016/j.ceb.2014.09.010.
Reinders, J. *et al.* (2006) 'Toward the complete yeast mitochondrial proteome: Multidimensional separation techniques for mitochondrial proteomics', *Journal of Proteome*

*Research*, 5(7), pp. 1543–1554. doi: 10.1021/pr050477f.
Reinhardt, C. *et al.* (2020) 'AIF meets the CHCHD4/Mia40-dependent mitochondrial import pathway', *Biochimica et Biophysica Acta - Molecular Basis of Disease*, 1866(6). doi: 10.1016/j.bbadis.2020.165746.
Roise, D. *et al.* (1988) 'Amphiphilicity is essential for mitochondrial presequence function.', *The EMBO journal*, 7(3), pp. 649–653. doi: 10.1002/j.1460-2075.1988.tb02859.x.
Schägger, H. and Pfeiffer, K. (2000) 'Supercomplexes in the respiratory chains of yeast and mammalian mitochondria', *EMBO Journal*, 19(8), pp. 1777–1783. doi: 10.1093/emboj/19.8.1777.
Schendzielorz, A. B. *et al.* (2018) 'Motor recruitment to the TIM23 channel's lateral gate restricts polypeptide release into the inner membrane', *Nature Communications*, 9(1). doi: 10.1038/s41467-018-06492-8.
Schiller, D. *et al.* (2008) 'Residues of Tim44 Involved in both Association with the Translocon of the Inner Mitochondrial Membrane and Regulation of Mitochondrial Hsp70 Tethering', *Molecular and Cellular Biology*, 28(13), pp. 4424–4433. doi: 10.1128/mcb.00007-08.
Schulz, T. J. *et al.* (2007) 'Glucose Restriction Extends Caenorhabditis elegans Life Span by Inducing Mitochondrial Respiration and Increasing Oxidative Stress', *Cell Metabolism*, 6(4), pp. 280–293. doi: 10.1016/j.cmet.2007.08.011.
Scialò, F., Fernández-Ayala, D. J. and Sanz, A. (2017) 'Role of mitochondrial reverse electron transport in ROS signaling: Potential roles in health and disease', *Frontiers in Physiology*. doi: 10.3389/fphys.2017.00428.
Sharma, S. *et al.* (2018) 'Cavitating Leukoencephalopathy With Posterior Predominance Caused by a Deletion in the APOPT1 Gene in an Indian Boy', *Journal of Child Neurology*, 33(6), pp. 428–431. doi: 10.1177/0883073818760875.
SHERMAN, F. (1964) 'Mutants of Yeast Deficient in Cytochrome C.', *Genetics*, 49, pp. 39–48. doi: 10.1093/genetics/49.1.39.
Shiota, T. *et al.* (2015) 'Molecular architecture of the active mitochondrial protein gate', *Science*, 349(6255), pp. 1544–1548. doi: 10.1126/science.aac6428.
Sickmann, A. *et al.* (2003) 'The proteome of Saccharomyces cerevisiae mitochondria', *Proceedings of the National Academy of Sciences of the United States of America*, 100(23), pp. 13207–13212. doi: 10.1073/pnas.2135385100.
Sideris, D. P. *et al.* (2009) 'A novel intermembrane space-targeting signal docks cysteines onto Mia40 during mitochondrial oxidative folding', *Journal of Cell Biology*, 187(7), pp. 1007–1022. doi: 10.1083/jcb.200905134.
Sideris, D. P. and Tokatlidis, K. (2007) 'Oxidative folding of small Tims is mediated by site-specific docking onto Mia40 in the mitochondrial intermembrane space', *Molecular Microbiology*, 65(5), pp. 1360–1373. doi: 10.1111/j.1365-2958.2007.05880.x.
Sideris, D. P. and Tokatlidis, K. (2010) 'Trapping oxidative folding intermediates during translocation to the intermembrane space of mitochondria: in vivo and in vitro studies.', *Methods in molecular biology (Clifton, N.J.)*, 619, pp. 411–423. doi: 10.1007/978-1-60327-412-8_25.
Signes, A. *et al.* (2019) ' APOPT 1/ COA 8 assists COX assembly and is oppositely regulated by UPS and ROS ', *EMBO Molecular Medicine*, 11(1). doi: 10.15252/emmm.201809582.
Signes, A. and Fernandez-Vizarra, E. (2018) 'Assembly of mammalian oxidative phosphorylation complexes I–V and supercomplexes', *Essays in Biochemistry*, pp. 255–270. doi: 10.1042/EBC20170098.
Sirrenberg, C. *et al.* (1996) 'Import of carrier proteins into the mitochondrial inner membrane

mediated by Tim22', *Nature*, 384(6609), pp. 582–585. doi: 10.1038/384582a0.
Stadtman, E. R. and Levine, R. L. (2003) 'Free radical-mediated oxidation of free amino acids and amino acid residues in proteins', *Amino Acids*, pp. 207–218. doi: 10.1007/s00726-003-0011-2.
Stojanovski, D., Pfanner, N. and Wiedemann, N. (2007) 'Import of Proteins into Mitochondria', *Methods in Cell Biology*, pp. 783–806. doi: 10.1016/S0091-679X(06)80036-1.
Suzuki, Y. *et al.* (2013) 'Human copper chaperone for superoxide dismutase 1 mediates its own oxidation-dependent import into mitochondria', *Nature Communications*, 4. doi: 10.1038/ncomms3430.
Takeda, H. *et al.* (2021) 'Mitochondrial sorting and assembly machinery operates by β-barrel switching', *Nature*, 590(7844), pp. 163–169. doi: 10.1038/s41586-020-03113-7.
Tarrago, L. *et al.* (2012) 'Methionine sulfoxide reductases preferentially reduce unfolded oxidized proteins and protect cells from oxidative protein unfolding', *Journal of Biological Chemistry*, 287(29), pp. 24448–24459. doi: 10.1074/jbc.M112.374520.
Terziyska, N. *et al.* (2005) 'Mia40, a novel factor for protein import into the intermembrane space of mitochondria is able to bind metal ions', *FEBS Letters*, 579(1), pp. 179–184. doi: 10.1016/j.febslet.2004.11.072.
Terziyska, N. *et al.* (2007) 'The sulfhydryl oxidase Erv1 is a substrate of the Mia40-dependent protein translocation pathway', *FEBS Letters*, 581(6), pp. 1098–1102. doi: 10.1016/j.febslet.2007.02.014.
Timón-Gómez, A. *et al.* (2018) 'Mitochondrial cytochrome c oxidase biogenesis: Recent developments', *Seminars in Cell and Developmental Biology*, pp. 163–178. doi: 10.1016/j.semcdb.2017.08.055.
Timón-Gómez, A. *et al.* (2020) 'Protocol for the Analysis of Yeast and Human Mitochondrial Respiratory Chain Complexes and Supercomplexes by Blue Native Electrophoresis', *STAR Protocols*, 1(2). doi: 10.1016/j.xpro.2020.100089.
Tranebjærg, L. *et al.* (1995) 'A new X linked recessive deafness syndrome with blindness, dystonia, fractures, and mental deficiency is linked to Xq22', *Journal of Medical Genetics*, 32(4), pp. 257–263. doi: 10.1136/jmg.32.4.257.
Vitali, D. G. *et al.* (2020) 'The Biogenesis of Mitochondrial Outer Membrane Proteins Show Variable Dependence on Import Factors', *iScience*, 23(1). doi: 10.1016/j.isci.2019.100779.
Vögtle, F. N. *et al.* (2009) 'Global Analysis of the Mitochondrial N-Proteome Identifies a Processing Peptidase Critical for Protein Stability', *Cell*, 139(2), pp. 428–439. doi: 10.1016/j.cell.2009.07.045.
Vögtle, F. N. *et al.* (2012) 'Intermembrane space proteome of yeast mitochondria', *Molecular and Cellular Proteomics*, 11(12), pp. 1840–1852. doi: 10.1074/mcp.M112.021105.
Webb, C. T. *et al.* (2006) 'Crystal structure of the mitochondrial chaperone TIM9•10 reveals a six-bladed α-propeller', *Molecular Cell*, 21(1), pp. 123–133. doi: 10.1016/j.molcel.2005.11.010.
Weckbecker, D. *et al.* (2012) 'Atp23 biogenesis reveals a chaperone-like folding activity of Mia40 in the IMS of mitochondria', *EMBO Journal*, 31(22), pp. 4348–4358. doi: 10.1038/emboj.2012.263.
Weinhäupl, K. *et al.* (2018) 'Structural Basis of Membrane Protein Chaperoning through the Mitochondrial Intermembrane Space', *Cell*, 175(5), pp. 1365-1379.e25. doi: 10.1016/j.cell.2018.10.039.
Weissbach, H., Resnick, L. and Brot, N. (2005) 'Methionine sulfoxide reductases: History and cellular role in protecting against oxidative damage', *Biochimica et Biophysica Acta - Proteins*

*and Proteomics*, pp. 203–212. doi: 10.1016/j.bbapap.2004.10.004.
Wenz, L. S. *et al.* (2015) 'Sam37 is crucial for formation of the mitochondrial TOM-SAM supercomplex, thereby promoting ß-barrel biogenesis', *Journal of Cell Biology*, 210(7), pp. 1047–1054. doi: 10.1083/jcb.201504119.
Wikström, M. *et al.* (2015) 'New perspectives on proton pumping in cellular respiration', *Chemical Reviews*, pp. 2196–2221. doi: 10.1021/cr500448t.
Van Wilpe, S. *et al.* (1999) 'Tom22 is a multifunctional organizer of the mitochondrial preprotein translocase', *Nature*, 401(6752), pp. 485–489. doi: 10.1038/46802.
Yamamoto, H. *et al.* (2009) 'Roles of Tom70 in import of presequence-containing mitochondrial proteins', *Journal of Biological Chemistry*, 284(46), pp. 31635–31646. doi: 10.1074/jbc.M109.041756.
Yamamoto, H. *et al.* (2011) 'Dual role of the receptor Tom20 in specificity and efficiency of protein import into mitochondria', *Proceedings of the National Academy of Sciences of the United States of America*, 108(1), pp. 91–96. doi: 10.1073/pnas.1014918108.
Yamano, K. *et al.* (2008) 'Tom20 and Tom22 share the common signal recognition pathway in mitochondrial protein import', *Journal of Biological Chemistry*, 283(7), pp. 3799–3807. doi: 10.1074/jbc.M708339200.
Yamano, K., Tanaka-Yamano, S. and Endo, T. (2010) 'Tom7 regulates Mdm10-mediated assembly of the mitochondrial import channel protein TOM40', *Journal of Biological Chemistry*, 285(53), pp. 41222–41231. doi: 10.1074/jbc.M110.163238.
Zara, V., Conte, L. and Trumpower, B. L. (2009) 'Biogenesis of the yeast cytochrome bc1 complex', *Biochimica et Biophysica Acta - Molecular Cell Research*, pp. 89–96. doi: 10.1016/j.bbamcr.2008.04.011.
Zhuang, J. *et al.* (2013) 'Mitochondrial disulfide relay mediates translocation of p53 and partitions its subcellular activity', *Proceedings of the National Academy of Sciences of the United States of America*, 110(43), pp. 17356–17361. doi: 10.1073/pnas.1310908110.
Zöller, E. *et al.* (2020) 'The intermembrane space protein Mix23 is a novel stress-induced mitochondrial import factor', *Journal of Biological Chemistry*, 295(43), pp. 14686–14697. doi: 10.1074/jbc.RA120.014247.